Article

Evaluation of amides, carbamates, sulfonamides and ureas of 4-prop-2-ynylidenecycloalkylamine as potent, selective, and bioavailable negative allosteric modulators of metabotropic glutamate receptor 5.

Davide Graziani, Silvia Caligari, Elisa Callegari, Carlo De Toma, Matteo Longhi, Fabio Frigerio, Roberto Dilernia, Sergio Menegon, Luca Pinzi, Lorenza Pirona, Valerio Tazzari, Anna Elisa Valsecchi, Giulio Vistoli, Giulio Rastelli, and Carlo Riva

J. Med. Chem., **Just Accepted Manuscript** • DOI: 10.1021/acs.jmedchem.8b01226 • Publication Date (Web): 09 Jan 2019

Evaluation of amides, carbamates, sulfonamides and ureas of 4-prop-2-ynylidenecycloalkylamine as potent, selective, and bioavailable negative allosteric modulators of metabotropic glutamate receptor 5.

Davide Graziani[a], Silvia Caligari[a], Elisa Callegari[a], Carlo De Toma[a], Matteo Longhi[a], Fabio Frigerio[a], Roberto Dilernia[a], Sergio Menegon[a], Luca Pinzi [b], Lorenza Pirona[a], Valerio Tazzari[a], Anna Elisa Valsecchi[a], Giulio Vistoli[c], Giulio Rastelli[b] and Carlo Riva[a].*

[a] Drug Discovery Department, Recordati S.p.A. Via M. Civitali 1, 20148 Milan (Italy).

[b] Department of Life Sciences, University of Modena and Reggio Emilia, Via Campi 103, 41125 Modena (Italy).

[c] Department of Pharmaceutical Sciences, Università degli Studi di Milano, Via Mangiagalli 25, 20133 Milan, Italy.

Keywords

Metabotropic glutamate receptor 5, negative allosteric modulators, metabolism, docking, solubility.

Abstract

Negative allosteric modulators (NAMs) of the metabotropic glutamate receptor 5 ($mGlu_5$) hold great promise for the treatment of a variety of central nervous system disorders. We recently reported that prop-2-ynylidenecycloalkylamine derivatives are potent and selective NAMs of the $mGlu_5$ receptor. In this work, we explored the amide, carbamate, sulfonamide and urea derivatives of prop-2-ynylidenecycloalkylamine

compounds with the aim of improving solubility and metabolic stability. *In silico* and experimental analyses were performed on the synthesized series of compounds to investigate structure-activity relationships. Compounds **12**, **32** and **49** of the carbamate, urea, and amide classes, respectively, showed the most suitable cytochrome inhibition and metabolic stability profiles. Among them, compound **12** showed excellent selectivity, solubility and stability profiles as well as suitable *in vitro* and *in vivo* pharmacokinetic properties. **12** was highly absorbed in rats and dogs and was active in anxiety, neuropathic pain and lower urinary tract models.

Introduction

The metabotropic glutamate 5 ($mGlu_5$) receptor is a G protein-coupled receptor that is highly expressed in the central nervous system (CNS). Indeed, it is mainly present in the postsynaptic cortex, hippocampus, striatum, caudate nucleus, and nucleus accumbens, usually colocalized with adenosine A_{2A}, dopamine D_2, and it modulates the activity of NMDA and AMPA ionotropic glutamate receptors.[1-5] Considering its distribution in the central nervous system, the $mGlu_5$ receptor has recently received

noteworthy attention as a promising drug target for a range of neurological disorders, including anxiety, chronic pain, schizophrenia, levodopa-induced dyskinesia in Parkinson's disease, epilepsy and Fragile X syndrome.[6-8]

The $mGlu_5$ receptor, which belongs to class C of the G protein-coupled receptor family, is characterized by a large extracellular N-terminal domain, named the "Venus flytrap domain" (VFT), where the endogenous substrate (glutamate) interacts with the orthosteric binding site. The allosteric binding site is located in the domain containing the seven-transmembrane helices[9,10], whose crystal structures (4OO9, 5CGD, 6FFH and 6FFI), in complex with the negative allosteric modulators mavoglurant, HTL14242, fenobam and M-MPEP, have recently been solved.[11,12,13] A cysteine-rich region, which links the VFT to the heptahelical transmembrane domains, is crucial for the intramolecular conformational rearrangements induced by the $mGlu_5$-glutamate interaction and hence for the enzymatic activity of the protein.[14]

Upon the interaction of glutamate with the orthosteric binding site, the $mGlu_5$ receptor mediates a plethora of important signaling pathways, such as inositol-1,4,5-

triphosphate (IP_3) and DAG messengers coupled with $G_{q/11}$ proteins and ERK 1/2, cAMP and mTOR/PI3K signaling.[15]

Ligands that interact with the $mGlu_5$ allosteric binding site are able to modulate the activity and efficacy of the endogenous orthosteric ligand. The concomitant binding of ligands at both the orthosteric and the allosteric binding sites may result in different outcomes. More specifically, allosteric ligands that promote potentiation of the endogenous signal (positive cooperativity) are classified as “positive allosteric modulators” (PAMs), whereas ligands that lead to the attenuation or complete block of the signal (negative cooperativity) are classified as “negative allosteric modulators” (NAMs). In this context, it is also possible to identify a third class of ligands, known as “neutral allosteric modulators” (NALs) or “silent allosteric modulators” (SAMs), which bind to the allosteric site and show neutral cooperativity with the orthosteric agonist.[16]

A notable number of companies and institutions have been involved in the research on new $mGlu_5$ receptor ligands. Ligands that interact with the $mGlu_5$ allosteric pocket can be classified based on their structure into alkyne-based or non-alkyne-based chemotypes. The presence and reactivity of the alkyne group has been associated

with the depletion of cellular glutathione (GSH) and consequent hepatotoxicity,[17] while some non-alkyne-based chemotypes, such as PF-06297470 and PF-06462894, were reported to induce specific adverse events associated with delayed type IV skin hypersensitivity.[18] Despite several alkyne-based (ADX-48621, AFQ056, RO-4917523)[19] and non-alkyne-based (fenobam, RGH-618,[20] VU0424238[21]) candidates (Chart 1) progressing to clinical studies, no $mGlu_5$ NAM is currently available for clinical use. In particular, based on a consistent preclinical disease model, mavoglurant (AFQ056) at Novartis and basimglurant (RO-4917523) at Roche were both under development in clinical phase 2/3 for Fragile X syndrome treatment. Unfortunately, both studies failed to meet the primary endpoints.[22,23]

In patients affected by Parkinson's disease, mavoglurant was investigated in phase 2 clinical trials for the attenuation of levodopa-induced dyskinesia, with inconclusive or conflicting results.[24,25] Basimglurant was studied at Roche in phase 2 clinical studies as an adjunctive therapy for the treatment of major depression in patients with an inadequate response to selective serotonin reuptake inhibitors (SSRIs) or serotonin-norepinephrine reuptake inhibitors (SNRIs). Despite some positive secondary

endpoints, basimglurant did not meet the primary endpoint on the Montgomery-Åsberg Depression Rating Scale (MADRS).[26] The analysis of previous failed clinical trials in Autistic Spectral Disorder (ASD) is ongoing and suggests an improved paradigm for translational research in neurodevelopmental disorders, such as the preclinical use of 1) more than one genetic background, 2) additional knock-out animal models for diseases and 3) results reported from at least two independent laboratories.[27] Moreover, the discovery of biased negative allosteric modulators[28] that preferentially target the ERK cellular pathway could represent an opportunity to reduce adverse events and offer advantages over the first generation of $mGlu_5$ modulators, which may be useful for the treatment of Fragile X syndrome.[29]

In a previous study,[30] we reported several 3-nitropyridin-2-yl derivatives of 4-(3-arylprop-2-ynylidene)piperidines to be potent NAMs of the $mGlu_5$ receptor, including, for example, compound **4**. Moreover, we investigated whether substitutions on the aromatic ring portion linked to the triple bond in the molecules can affect the binding and the interaction of the molecule with the $mGlu_5$ receptor. Compound **4** showed a high binding affinity and functional activity but was affected by a potent interaction with

cytochrome isoforms CYP1A2 (IC_{50} < 0.74 μM) and CYP3A4 (IC_{50} = 4.5 μM), and these characteristics and potential drug-drug interaction issues were common among the entire class of 4-(3-arylprop-2-ynylidene)piperidines that were directly substituted with aromatic derivatives. In this paper, we have explored the possibility of replacing the nitro-substituted heteroaryl ring that interacts with the extracellular subpocket of the allosteric site with different groups. To this aim, a series of carbonyl derivatives, such as amides, carbamates and ureas, and sulfonamide derivatives of prop-2-ynylidenecycloalkylamine, was investigated. Here, the synthesis, physicochemical properties, *in vitro* pharmacological activity, pharmacokinetic and metabolic stability data are reported. Ligand binding modes for the human $mGlu_5$ receptor and human CYP450 3A4 isoform are described. Potent and selective negative allosteric modulators of the $mGlu_5$ receptor, endowed with increased $mGlu_1$ selectivity and ameliorated drug-like properties, were obtained and compared with previously described molecules. In particular, the (3*E*)-3-prop-2-ynylidenepyrrolidine derivatives of the various investigated chemical classes (**12**, **32** and **49**) were the compounds endowed with high activity, drug-like *in vitro* profiles and were selected for preclinical

investigations. Compound **12** was further studied and shown to be clean in preclinical toxicological studies.

Results and Discussion

Chemical synthesis

MPEP (**1**), MTEP (**2**) and fenobam (**3**) (Chart 1) were purchased from Tocris Bioscience. Compound **4** (Chart 1) and the key intermediates 2-methyl-6-[3-(piperidin-4-ylidene)prop-1-yn-1-yl]pyridine (**14a**, Scheme 2) and compound **17** (Chart 2) were prepared as described by Anighoro *et al.*[30] The majority of the compounds described in this paper belong to four different chemical classes: amides, carbamates, sulfonamides and ureas.[31] These are derivatives of either 4-(3-arylprop-2-ynylidene)piperidine or 3-(3-arylprop-2-ynylidene)pyrrolidine. A small number of molecules are N-alkyl derivatives of 4-(6-methylpyrid-2-ylprop-2-ynylidene)piperidine.

Compound **10** was synthesized (Scheme **1**) from commercially available *tert*-butyl 3-oxoazetidine-1-carboxylate, which was reacted with the ylide generated from diethyl [3-(trimethylsilyl)prop-2-ynyl]phosphonate[32] to obtain the intermediate **10a**. The latter was converted into **10b** by carrying out a Sonogashira-Heck cross-coupling reaction

with 2-bromo-6-methylpyridine with concurrent removal of the trimethylsilyl group. Afterwards, the BOC deprotection of **10b** using TFA in chloroform resulted in **10c**, and then acylation of **10c** with ethyl chloroformate afforded compound **10**. Beginning with *tert*-butyl 6-oxo-2-azaspiro[3.3]heptane-2-carboxylate and using an analogous synthetic pathway, compound **11** was prepared. N-*tert*-Butoxycarbonyl-3-pyrrolidinone was submitted to the same Horner-Wadsworth-Emmons (HWE) procedure used to synthesize **10a** and **11a** after chromatographic separation of the *E*:*Z* isomers (obtained with 2:1 ratio) *tert*-butyl-(3*E*)-3-[3-(trimethylsilyl)prop-2-yn-1-ylidene]pyrrolidine-1-carboxylate (**12a)** and *tert*-butyl-(3*Z*)-3-[3-(trimethylsilyl)prop-2-yn-1-ylidene]pyrrolidine-1-carboxylate (**13a**). The structure of the isomers was elucidated by NOESY experiments (Supporting Information Figure S1). Afterwards, alkynyl Heck coupling of **12a** and **13a** with 2-bromo-6-methylpyridine afforded the compounds **12b** and **13b,** respectively, which, after the removal of the BOC protecting group (**12c** and **13c**), were acylated with ethyl chloroformate to give compounds **12** and **13.** Compounds **14** and **16** were prepared (Scheme 2) by acylating the key intermediate **14a** with either methyl chloroformate or ethyl chloroformate. Ethyl-4-[3-(trimethylsilyl)prop-2-yn-1-ylidene]piperidine-1-carboxylate (**15a**), an additional key

intermediate, was prepared from 1-ethoxycarbonyl-4-oxopiperidine by the standard HWE procedure with diethyl-[3-(trimethylsilyl)prop-2-ynyl]phosphonate. Then, a Sonogashira-Heck coupling was carried out on **15a** using the appropriate aryl or heteroaryl halogenide to obtain compounds **15** and **21–24**. The ureas **25–33**, amides **34–49** and sulfonamides **50–57** were synthesized from the key intermediates **14a**, **12c** and **47b** according to the procedures shown in Scheme 3. The ureas **25–27** were synthesized from **14a** by reaction with the appropriate commercial isocyanate. **28–31** and **33** were prepared by the use of triphosgene, which was previously reacted with the appropriate secondary amine in the presence of DIEA and then with **14a** or **12c**. **32** was prepared by a reaction between commercially available 3-methyl-1-[methyl(propan-2-yl)carbamoyl]-1H-imidazol-3-ium iodide and **12c**. Amides **34**, **40**, **48** and **49** were synthesized by acylating **14a** or **12c** with the appropriate aroyl or acyl chloride in the presence of TEA. **35**, **36**, **39**, **41–43**, and **46** were prepared from **14a** by condensation with the given carboxylic acid in the presence of EDCI and HOBt, while **37**, **38**, **44**, **45** and **47** were prepared from **14a** or **47b** by condensation with PS-DCC in DCM. The intermediate **47b** was synthesized (Scheme 2) by the standard HWE procedure with diethyl [3-(trimethylsilyl)prop-2-ynyl]phosphonate led on *tert*-

butyl-4-[3-(trimethylsilyl)prop-2-yn-1-ylidene]piperidine-1-carboxylate to give the N-BOC derivative **47a**, which then underwent BOC removal to give **47b**. Sulfonamides **50–57** were obtained by condensing **14a** with the proper sulfonyl chloride using TEA as the base. The $NaB(OAc)_3H$ reductive amination of **14a** with either butyraldehyde or benzaldehyde led to **58** or **59**, respectively. **60** was obtained from **14a** by reaction of 2-chlorocyclopentanone and DIPEA in DMA. A two-step one-pot synthesis of **61** was carried out by N-alkylation of **14a** with 2-bromoacetic acid and TEA, followed by amidification with pyrrolidine and polymer-supported by dicyclohexylcarbodiimide as the condensing agent. The full analytical characterization of compound **12** and its mesylate salt **12s** is available in the Supporting Information (Figures S10–S16).

Biological results

Binding and functional results

The newly synthesized compounds were evaluated for their ability to displace the allosteric antagonist [^{3}H]MPEP from the binding site and for their binding affinity for the membranes of CHO T-REx cells that were stably transfected with human $mGlu_5$ receptors. The binding affinities, expressed as inhibition constants (Ki), were obtained

by three independent experiments performed in triplicate and are reported in Tables 1-4. Specifically, Tables 1 to 4 report the biological data of the carbamate, urea, amide and sulfonamide derivatives, respectively. Table S5 (Supporting Information) reports the biological data of the alkyl derivatives. The displacement curves of [^{3}H]MPEP induced by compounds **12**, **32**, **49** and **55**, which were considered to be the prototypical compounds of each class of molecules, are shown in Figure 1. The Ki values of compounds **12**, **32**, **49** and **55** are 3.5 nM, 8.6 nM, 7.9 nM, and 2.7 nM, respectively.

Moreover, Tables 1-4 and T5 show the results of the functional Ca^{2+} mobilization assay measured in the CHO T-REx cells with cloned human $mGlu_5$ receptors, which was determined only for compounds with a Ki affinity for the $mGlu_5$ receptor of less than 20 nM. Figure 2 shows the ability of compounds **12**, **32**, **49** and **55** to inhibit the quisqualate-induced intracellular calcium concentration $[Ca^{2+}]_i$ response of the human $mGlu_5$ receptor. Under these experimental conditions, compounds **12**, **32**, **49** and **55** displayed the following IC_{50} values: 4.1 nM, 15.1 nM, 6.4 nM, and 43.8 nM, respectively.

The rat $mGlu_1$ binding affinity was measured using CHO T-REx cell membranes with $mGlu_1$ receptor stably transfected and as the [^{3}H]R214127 radiolabel.[33] The functional Ca^{2+} activity of the rat $mGlu_1$ receptor using the same cell line was determined for compounds that showed an $mGlu_1/mGlu_5$ binding ratio lower than 50-fold and for compounds endowed with an attractive overall *in vitro* profile. Despite the difference of only four residues between the $mGlu_5$ and $mGlu_1$ binding pockets,[34] none of the molecules discussed in this article showed an $mGlu_1/mGlu_5$ binding ratio lower than 50-fold. These results are in agreement with the interaction of the ligands in the lower intracellular subpocket (Figure 5), which is specific to the $mGlu_5$ receptor.[34]

While the "ene-yne portion" was described in the previous article[30] as one of the most suitable spacers for high-affinity $mGlu_5$ ligands, in this article, we have (i) investigated the effects of modulating the size of the ring condensed to the terminal double bond, (ii) explored the substituents on the nitrogen atom of the condensed ring, and (iii) studied the substitution on the triple bond. The substituents at the meta position of the aryl group linked to the triple bond have been reported to enhance the $mGlu_5$ affinity and activity of most $mGlu_5$ NAMs.[35] Consistently, we kept the 6-methylpyridine ring or

a meta-substituted phenyl ring as established substituents of the triple bond. Our work was focused on exploring the substitution of the nitrogen in the heterocyclic ring via derivatization with a variety of carbonyl group derivatives, i.e., carbamates (**10–24,** Chart 2), ureas (**25–33,** Chart 3) and amides (**34–49,** Chart 4), instead of the previously described 3-nitropyridine ring (compound **4**). The carbonyl group was proposed to be a putative hydrogen bond acceptor (HBA) replacement of the nitro group, which was previously suggested to take part in hydrogen bonding interactions with Asn747.[30] Furthermore, a series of sulfonamide derivatives (**50–57,** Chart 5) were synthesized as bioisosteres of the carbonyl group. The first aim of our work was to define the most suitable ring bonded to the -ene moiety; consequently, different sized rings containing nitrogen, including pyrrolidine, piperidine and the more tensioned 4-membered ring azetidine, were considered. The $mGlu_5$ affinities of the N-ethoxycarbonyl compounds **10** (azetidine), **12** (*E*-pyrrolidine) and **16** (piperidine) were 38.3 nM, 3.5 nM and 2.5 nM, respectively. The *Z*-pyrrolidine geometric isomer **13** was 69 times less active than the *E* isomer **12**. The affinities lower in the 4-membered rings than in the 5-membered and 6-membered rings. These affinities could be related to the distance between the pyridine ring centroid and the carbonyl HBA group, which is lower in compound **10**

than in compounds **12** (approximately 1.5 Å) and **16** (approximately 0.5-1.0 Å depending on chair or twisted piperidine conformation), where the latter appears to be optimal for establishing interactions with the binding pocket. Compound **11**, obtained from 2-azaspiro[3.3]heptan-6-one, showed a binding affinity comparable to **16** (3.6 nM and 2.5 nM, respectively). The replacement of the ethyl group with *tert*-butyl (**17**, Ki = 11.9 nM), benzyl (**19**, Ki = 4.8) or phenylethyl (**20**, Ki = 2.5 nM) groups resulted in NAMs that exhibited high $mGlu_5$ affinity. The only relevant exception was the cyclobutylmethyl analogue **18**, which was inactive or poorly active (Ki > 1000 nM). Molecules belonging to the carbamate series showed remarkable agreement between binding affinity and functional quisqualate-induced Ca^{2+} activity in the human $mGlu_5$ receptors. The ratio of functional vs binding activity was lower in small O-substituents of carbamates (methyl (**14**), ratio = 1.5; ethyl (**16**), ratio = 1.3; ethyl (**21**), ratio = 2.5 folds) and increased with bulkier substituents (benzyl (**19**), ratio = 51; phenylethyl (**20**), ratio = 20). Ethyl carbamates **21–24**, each carrying different meta-substituted phenyl rings at the alkyne moiety, were all potent nanomolar ligands.

The urea analogues were less potent than the carbamates. A direct comparison between the *tert*-butyl carbamate **17** (Ki = 11.9 nM) and the *tert*-butyl urea **25** (ki = 399

nM) suggests that the presence of an HBD in ureas is detrimental to binding affinity. This finding suggests that there may be repulsion between the HBD moieties of ligands and Asn747 and further reinforces the requirement of an HBA for potent affinity. N-Methylation restored the binding affinity, as shown by the comparisons of **26** (Ki = 92 nM) with **29** (Ki = 20.4 nM) and of **27** (Ki = 276 nM) with **30** (Ki = 4.3 nM). The best affinity value was obtained by modulating the bulkiness of the alkyl substituents (**31** vs. **25** and **28**); the isopropylethylamino derivative (**31**) showed a Ki of 2.9 nM. The pyrrolidino-analogues isopropylmethylamino **32** and isopropylethylamino **33** showed high binding affinity (8.6 nM and 5.8 nM, respectively) together with promising *in vitro* profile characterized by no interaction with the investigated cytochrome isoforms (see Table 2).

The $mGlu_5$ functional/binding activity ratios of **32** and **33** (1.7- and 5-fold, respectively) were less than that of **31** (45.8-fold). Although the two compounds displayed binding affinities less than **31,** they were significantly more active in the Ca^{2+} functional assay (15 and 29 nM).

Alkyl amides **34–39** showed moderate affinity (Ki > 20 nM); therefore, they were not profiled further. Specifically, the 2-methoxyacetyl and the 2-pyrrolidinacetyl groups of

36 and **37** were detrimental to affinity. The 2-phenacetamide and 3,5-difluorophenylacetamide derivatives **38** and **39** were less potent (83 nM and 194 nM), while the benzamide analogue **40** exhibited high binding affinity (18.4 nM). The presence of an aromatic ring directly bonded to the carbonyl group in compounds **40–49** resulted in nanomolar affinity. A meta substitution on the phenyl ring (**42**, **44–48**) showed similar or further increased affinity for the $mGlu_5$ receptor (**46**, Ki = 0.7 nM). From the limited set of data, it seems that the ortho and especially para methoxy substituents of amides (**41** and **43**) negatively affected binding affinity. Compounds **44** and **46** showed greater functional/binding activity ratios (122- and 70-fold, respectively) because of their different binding affinities (Ki = 11.3 nM and 0.7 nM, respectively) and Ca^{2+} functional assay results (IC_{50} = 1383 nM and 49.2 nM, respectively). Sulfonamides were synthesized as bioisosteres of the carbonyl groups that potentially interact with the Asn747 residue of the binding pocket. The presence of additional oxygen and the different hybridization states of the carbonyl vs. sulfonyl groups could play a role in the hypothesized bioisosteric effect.[36] In general, sulfonamides should have an H-bonding basicity (pK_{BHX} value ranging from 1.1 to 1.4) capable of establishing a strong H bond with Asn747. Considering that carbamates,

amides and ureas have higher pK_{BHX} values than sulfonamides (1.5–3.0) depending on substitution and cyclization,[37] the rank of affinities and activities obtained are in agreement with pK_{BHX} values. The secondary alkyl sulfonamides (**50–52**) exhibited weak activity. The aromatic sulfonamides **53–57** showed a higher binding affinity, even though we found the highest affinity with para substitution and not with meta substitution, as was found for the amide derivatives (**55**, **56** and **57** versus **54**). Regarding structure-activity relationships (SAR), it is interesting to observe the different behavior of amides and sulfonamides. With sulfonamides, the strongest affinity was obtained with para-substituted compounds; however, for amides, the strongest affinity was obtained with meta-substituted compounds. This could be due to the different dihedral angles imposed by the sulfonamide (approximately 103 degrees) versus amide (approximately 120 degrees) groups. The last series of molecules synthesized included several N-alkyl derivatives (Chart 6). The presence of the carbonyl group of carbamates, ureas or amides was essential for affinity. Compounds lacking the carbonyl group (Supporting Information Table S5) (see **58** and **59** vs **34** and **40**) proved completely inactive, confirming the importance of an HBA to interact with Asn747 for high binding affinity. Compound **60**, in which the carbonyl

group was separated by an additional sp^2 carbon compared to that of the amides, showed high binding affinity (25.7 nM). On the other hand, **61**, in which the carbonyl group is not directly bonded to the piperidine nitrogen but instead is separated by an additional sp3 carbon atom, resulted in a completely inactive class of compounds.

Cytochrome inhibition

1 (MPEP) and **2** (MTEP), even though they are very selective for the $mGlu_1$ receptors, CYP2D6 and CYP3A4 (see Table 1), were described as moderate competitive inhibitors of recombinant human CYP1A2 (Ki, 0.5–1 μM).[38] The 3-nitropyridine derivative **4** inhibited both the CYP1A2 and the CYP3A4 isoforms. Carbamates **10–24** were generally affected by the same problem, displaying a micromolar inhibition of CYP1A2 sometimes coupled with more relevant micromolar inhibition of CYP3A4. The replacement of the 3-nitropyridine ring of **4** with small alkyl carbamates (**14** and **16**) led to a clean CYP3A4 profile (IC_{50} > 20 μM), while the compounds bearing bulkier alkyl groups, such as benzyl (**19**) and phenylethyl (**20**), moderately inhibited cytochrome CYP3A4 (IC_{50} 7.7 μM and 3.7 μM, respectively). Lipophilicity was reported

to correlate with the P450 binding affinity of inhibitors and substrates of CYP3A4.[39] The replacement of the pyridine moiety bonded to the alkyne with a meta-substituted phenyl ring (**21**–**23**) increased lipophilicity, lowered solubility and negatively affected the CYP3A4 inhibition profile. The polar 3-cyano substituent (**24**) was beneficial for the CYP3A4 interaction and for solubility (CYP3A4 IC_{50} >20 μM and solubility = 544 μM). For generally small and planar lipophilic substrates and inhibitors, the interaction with CYP1A2 was unaffected by these latter changes.[40]

Although, in general, moderately bulky alkyl ureas generated active compounds, this substitution inhibited cytochromes and overall *in vitro* profiles. Compounds **29**, **30** and **31** were weak inhibitors of the CYP3A4 isoform, showing a IC_{50} values of 13.4, 4.0 and 15.4 μM, respectively. Again, a more favorable cytochrome inhibition profile could be attributed to the pyrrolidine ring derivatives (**32** and **33**). Benzamide **40** and the meta halo-substituted benzamides (**45** and **46**) were characterized by a clean profile versus the three cytochrome isoforms. The aromatic sulfonamides **55**–**57** were devoid of interaction with CYP1A2 (IC_{50} > 20 μM), while they retained moderate inhibition of CYP3A4.

None of the molecules described and investigated in the current article showed relevant inhibition of CYP2D6. CYP3A4 inhibition can be modulated by introducing the pyridine ring or the cyano group on the phenyl ring bonded to alkyne or by modulating the lipophilicity of the alkyl substituents of carbamates or ureas. The pyrrolidine moiety had a favorable impact on cytochrome inhibition, and compounds **12**, **32** and **49** al exhibited good pharmacokinetic *in vitro* profiles.

Metabolic stability results

Tables 1–4 show that most compounds display very limited *in vitro* metabolic stability in rat microsomes, while they exhibit acceptable stability in human microsomes. Although some of these compounds have a clean CYP inhibition profile and high human microsome stability, the rat microsome instability prevents *in vivo* testing in rodent models. With the aim of identifying possible metabolites and elucidating metabolic pathways to design stable molecules to be tested *in vivo*, metabolite generation in rat microsomes and identification by HPLC-MS/MS were carried out on three selected compounds (**16**, **31** and **46**) belonging to different chemical classes

(carbamates, ureas and amides, respectively). The results are shown in the Supporting Information (Figure S2). Compounds **16** and **31,** in rat microsomes, undergo primary and fast metabolic attack on the methyl pyridine ring. Two different metabolites were identified for **16**. The fragment with *m/z* 255 is specific to the 2-methyl-6-[3-(4-piperidylidene)prop-1-ynyl]pyridine portion. Both metabolites of compound **16** have the same mass spectrometric transition *m/z* 301.2/255.1, corresponding to the N-oxide formation or to the hydroxylation at two different positions on the same portion of the molecule (e.g., on pyridine and at its methyl substituent). Urea **31** first undergoes oxidation of the pyridine portion with transition *m/z* 342.3/255.1 and then undergoes a further transition (*m/z* 314.3/255.1) compatible with urea de-ethylation. Compound **46**, in rat microsomes, undergoes fast oxidative metabolic attack and exhibits metabolites with different mass transitions (*m/z* 367.2/139.3), which are compatible with a metabolic oxidation attack of the 2-methyl-6-[3-(4-piperidylidene)prop-1-ynyl]pyridine scaffold. Further fragmentations produced the 3-chloro-N,N-diethyl-benzamide oxidized ($[M]^+$ = 228.2), 3-chloro-N,N-diethyl-benzamide ($[M]^+$ = 212.2) and chlorobenzoyl ($[M]^+$ = 139.3) fragments. The fragments $[M]^+$ = 228.2 and $[M]^+$ = 212.2 are not present in the mass spectrum of compound **46**

without metabolism and are probably due to the initial oxidation at an unknown position of the scaffold followed by nuclear decomposition. Reported *in vitro* stability studies were performed to direct the synthesis of metabolically stable compounds, and no further investigations were conducted to further characterize the nature of metabolites. The results of the structure and stability relationships and the metabolite studies by HPLC-MS/MS of the investigated compounds are substantially in agreement. The metabolic attack for most of the molecules is directed on the 6-[3-(4-piperidylidene)prop-1-ynyl]pyridine scaffold, which was subjected to quick oxidation, and when the pyridine was substituted with a phenyl ring, the metabolic stability increased for carbamates (**21–24**, 29-64% versus **16**, 2.1%) and amides (**47**, 64% versus **46** <1%). Further indications could be derived by comparing equipotent compounds **11** and **16**. Compound **16** shows low metabolic stability in rats, while compound **11** is stable in both rat and human microsomes (80% and >95%, respectively). The carbonyl groups of both molecules tend to be coplanar to one of the two C-N bonds of the ring, and higher dihedral angles showed a net increase of energy. Minima conformation and dihedral contour plots of amide bond rotation are reported in the Supporting Information (Figures S3–S6). While the double bond and

carbonyl group of **11** lie on two different orthogonal planes, in **16** they are on two parallel planes. Therefore, the spiralization and the carbonyl orientation do not affect $mGlu_5$ activity but instead impair rat microsome metabolism. 2-Azaspiro[3.3]heptane exhibits good structural overlap with piperidine and can be used as a bioisostere to protect piperidine from metabolic attack. The *E*-pyrrolidine analogue **12** showed increased metabolic stability in both rat and human microsomes in comparison to the piperidine derivative **16**. The higher stability of pyrrolidine versus piperidine analogues in rat microsomes was also confirmed in the other synthesized chemical classes. In fact, pyrrolidine compounds **32** and **33** were significantly more stable (57 and 20%, respectively) than **31** (<1%). Moreover, compound **31**, according to the HPLC-MS studies, undergoes two fast and concurrent oxidations, the first being on the pyridine ring and the other on the ethyl chain of the urea, leading to de-ethylation. The latter degradation is also possible for compound **33.** The methyl-substituted urea **32** showed a slower N-oxidative dealkylation, proving a more stable compound. Pyrrolidine exhibited higher stability than piperidine, which was also corroborated by the amide analogues. Pyrrolidine derivative **48** shows 55% remaining, while the stability of piperidine analogue **46** is almost zero.

The aromatic amides are potent ligands for the $mGlu_5$ receptor (**42**, **45**, **46**). Unfortunately, these compounds, even while showing an acceptable profile, were clearly unstable in rat and human microsomes (e.g., **46**) because of oxidative attack. Substitution of the pyridine ring with a meta-chlorophenyl ring leads to compound **47**, which was particularly stable in both rat and human species but displayed cytochrome interactions. As previously discussed, the five-membered pyrrolidine ring derivatives (**48** and **49**) were stable in both human and rat microsomes. In particular, **49** showed a very appealing overall profile consisting of high solubility, high binding affinity (7.9 nM), well-correlated functional activity in the calcium assay (6.4 nM) and a clean profile for the most important cytochromes.

The last group of molecules investigated here was the piperidine sulfonamides, which demonstrated instability in rat and human microsomes (**55–57**). Alkyl piperidine derivatives (**58–61**) were almost inactive, with the exception of ketone **60**, which showed high stability in both rat and human microsomes. The direct comparison of **34** (rat % rem. 1%) and **58** (rat % rem. 22%) suggests that the carbonyl group is necessary to obtain ligands with high $mGlu_5$ affinity and that it affects the rate of rat metabolism.

In conclusion, we observed that the main metabolic attack to these classes of molecules is on the pyridine ring, and the rate of metabolism is affected by HBA (e.g., carbonyl moiety belonging to carbamate or ureas groups) and by its torsion angles in the constrained rings present on the opposite side of the molecule. Further support for these findings can be confirmed by exchanging the pyridine rings of derivatives with phenyl rings (**21–24** versus **16** and **47** versus **46**). In fact, the phenyl derivatives **21–24** and **47** possess metabolic stability in rats ranging from 29% to 64% and are invariably more metabolically stable than the pyridine derivatives **16** and **46** in the same species. The percent of a group of selected molecules (**16**, **31**, **32**, **41** and **47**) remaining after 30 minutes in the human CYP3A4 isoform was determined, and the results are in substantial agreement with the obtained percent remaining in the human microsomes (Table 5). Although the measured metabolism is likely due to an extended set of metabolizing enzymes, including hydrolytic enzymes the act on labile groups such as carbamates and amides, the metabolic stability of the reported compounds was further investigated by performing human CYP3A4 docking simulations. In fact, this cytochrome plays a particularly relevant role; this is confirmed in Table 5, in which an encouraging agreement between the extent of metabolism exerted by human

microsomes and by the CYP3A4 enzyme alone is reported. Moreover, it should be noted that the resolved structures of the rat CYP3A isoforms are not yet available, and thus, this docking analysis is focused on human CYP3A4 only and is aimed at rationalizing the different metabolic stabilities of each proposed class that was observed in the human microsomes. As detailed in Supporting Information Experiment E1 (Docking simulations of molecules as possible substrates of the human CYP3A4 isoform), the obtained docking results are in satisfactory agreement with the reported metabolic data for both metabolic stability, which is related to the general propensity of a given substrate to approach the heme group, and for the detected metabolites, which are in line with the computed binding modes (Supporting Information Figures S8-S9). Indeed, and as observed in the monitored metabolic pathways, the pyridine ring is the moiety that often contacts the heme group, and the computed complexes appear to be largely influenced by few polar interactions stabilized by the carbamate/urea functions. Compounds **12, 32**, and **49,** which were characterized by high rat and human stability, were selected for further investigation.

Analysis of compound solubility

Carbamates **10–14** and **16** were significantly more soluble (600-939 μM) than the 3-nitropyridine derivative **4** (28 μM). The bulky and lipophilic carbamates **18** and **20** had increased cLogP by approximately 1 unit compared to ethyl carbamates (see Table S1), and their solubilities were comparable to that of compound **4** (12 and 31 μM). The introduction of a phenyl ring in **21–24** caused a decrease in solubility in comparison with the solubility of pyridine derivatives. In particular, the *m*-Me (**21**) and *m*-Cl phenyl (**23**) groups were detrimental for solubility (4 and 15 μM, respectively), while the small *m*-F phenyl (**22**) and the polar *m*-CN phenyl (**24**) groups were able to restore high solubility. The two urea compounds **32** and **33** were very soluble (962 μM and 927 μM, respectively). The solubility of the aromatic amide derivatives was influenced by the ring substituent position. Ortho (**41**) and meta (**42**) methoxy derivatives showed high solubility (468 and 386 μM, respectively). Pyrrolidine and piperidine *m*-Cl benzoyl derivatives **46** and **48** were sufficiently soluble (58 μM and 157 μM, respectively). The furoyl substituent (**49**) was one of the most suitable aromatic fragments, lowering the cLogP value ($LogP_{GALAS}$ 2.4) and conferring high aqueous solubility (420 μM). Aromatic sulfonamides were insoluble (**52**, **54** and **57**), while the cyclohexylmethyl derivative **51** maintained high solubility (49 μM). The solubility of most of the

carbamates and ureas was optimal to obtain a candidate with high aqueous and plasma solubility, and the low cLogP values (e.g., compound **12** $LogP_{GALAS}$ 2.8) were compatible with optimal brain barrier penetration[41], indicating the ability to elicit the desirable biological response.

Binding mode and structure-activity relationships analysis

The compounds presented in this study were docked to both 4OO9 and 5CGD $mGlu_5$ crystal structures as described in the experimental section.[11,12] The two crystal structures mainly differ in the position of the Trp785 and Ser809 side chains, which determine the different binding site accessibilities for the ligands (Figure 4). Therefore, induced-fit docking calculations were performed for both crystal structures, and the predicted binding modes were used to discuss structure-activity relationships (SAR). Figure 5 exemplifies the binding mode of a representative high-affinity compound (**46**) in two alternate conformations that differ mainly in the position of the Trp785 side chain. The amino acid numbers refer to the 4OO9 crystal structure.

By analyzing the predicted binding modes, the phenyl and pyridine ring derivatives were found to bind in the lower intracellular subpocket of $mGlu_5$ that is lined by the Ile625, Ser654, Ser658, Tyr659, Ser809 and Ala810 residues, which is in agreement with previous observations.[12,30] The nitrogen atom of the pyridine analogs forms hydrogen bonds with Ser809. Such an interaction, which was already discussed for compounds of this series by Anighoro *et al.*[30] and observed in 5CGD and 5CGC crystal structures, is of high interest for negative allosteric modulator activity. In fact, previously reported mutational studies showed that the mutation of Ser809 and Tyr659 with valine greatly affected the binding of $mGlu_5$ NAMs,[42] such as MPEP, which binds the lower chamber of the allosteric pocket, similar to the compounds we investigated. Moreover, the methyl-substituted phenyl ring compounds such as **21** can also fit into the lower pocket and can be substituted with a cyano group (**24**) or halogen atom (**22**, **23**), retaining similar affinity and almost identical binding mode. In such cases, Ser809 is engaged in an H-bond network with WAT4126, Thr781 and Tyr659, as observed in the 5CGC and 5CGD crystal structures.[12]

The substitution of the 4-methylene piperidine or 3-methylene pyrrolidine rings with small alkyl groups was tolerated and provided favorable hydrophobic interactions with

the side chain of Pro655, a residue that plays a key role in the binding of NAMs into $mGlu_5$.[42,43] Interestingly, the induced fit docking calculations we performed converged on similar results in the two crystal structures. In fact, while sterically hindered substituted compounds docked preferentially to receptors with Trp785 in the "out" conformation (4OO9 crystal structure), the induced fit docking of such compounds in the Trp785 "in" receptor conformation (5CGD crystal structure) restored the Trp "out" conformation and resulted in very similar binding modes. Moreover, unsubstituted compounds perfectly docked in both structures with similar binding modes (Figure 5). This convergence of the induced-fit docking results increases the reliability of the predicted binding modes and suggests a key role of the Pro655 and Trp785 residues in ligand binding. Remarkably, these findings are consistent with previously reported mutational studies on the binding of allosteric ligands into mGlu receptors.[44,45] The carbonyl oxygens of the carbamate, amide and urea groups and the sulfonyl oxygens of sulfonamide groups of the active compounds formed a hydrogen bond with Asn747, which is important for binding affinity.[42-44] This finding is consistent with the Asn747 hydrogen bonds observed in the structure of mavoglurant in complex with $mGlu_5$ (4OO9) as well as with previous modeling studies.[11,12,30] Interestingly, the obtained

docking results suggest that the hydrogen bonding with Asn747 could be formed in the presence of different linkers (e.g., **11** vs **16**). Compounds unable to form such hydrogen bonds (e.g., **58**, **59** and **61**) were inactive or significantly less active. Finally, the aliphatic or aromatic substituents attached to the carbamate, amide, urea and sulfonamide groups docked in a receptor pocket lined by Ile651, Gly652, Ile708, Val740, Pro743, Tyr792 and Met802, which is directed toward the extracellular side of the receptor. Different substitutions in this area are well tolerated.

Analysis of ligand and lipophilic efficiency

Ligand efficiency (LE) and lipophilic efficiency (LipE) values[46] were calculated for the investigated compounds using the formula LE = − RT(ln Ki)/N (where N is the number of heavy atoms). The number of heavy atoms was calculated by MOE (CCG). Optimal LE and LipE ranges, based on average values reported for different datasets of oral drugs (0.45-0.52 and 4.43-5.02, respectively), were used as a reference.[46] The LE values are listed in the last columns of Tables 1-4 and T5 (Supporting Information), while the LipE values are reported in the Supporting Information (Table S1). Most

compounds showed favorable LE values. The LEs of carbamates were higher than 0.50 for compounds **12–16** and **21–24**, confirming that carbamates are the most efficient class of $mGlu_5$ NAMs. Urea **31**, and amides **34**, **46** and **49** showed an LE > 0.49, while sulfonamide efficiency was lower. LipE was calculated using the pKi of binding affinity on the human $mGlu_5$ receptor and the calculated LogP based on the GALAS algorithm by ACD/Percepta (ACD Labs).[47] In Figure 3, LipE integer values are represented as diagonal lines in the pKi-cLogP scatter plot. Each compound is colored according to the investigated scaffold. Compounds with low LipE values are more likely to suffer from attrition, while compounds with high LipE values are associated with improved ADMET and increased specificity for the target.[46] Both standards **1** (MPEP) and **2** (MTEP) are characterized by a small chemical skeleton (15 and 14 heavy atoms, respectively) mainly composed of lipophilic aromatic carbons (3.6 and 2.2 $LogP_{GALAS}$) coupled with nanomolar binding affinities. The standard compounds **1** and **2** show a stunning ligand efficiency (LE > 0.7), but the LipE value of compound **1** (4.38) is reduced by a high clogP (3.6). Among the studied clinical candidates, **9**, **3**, and **5** exhibited high LipE values (6.56, 5.79 and 5.08, respectively), confirming the high-quality metric characteristics of these molecules. The pool of carbamates with

LipE > 5 (**12**, **14**, **15**, **16** and **24**) consists of high-quality ligands in terms of activity and *in vitro* properties (solubility, cytochrome profile and metabolic stability). On the scatter plot graph (Figure 3), on the edge line of value 5, a group of high-quality ureas are found (**31**, **32** and **33**). The only amide showing a LipE value higher than 5 was compound **49**, owing to the cLogP contribution given by the 2-furyl group.

In conclusion, the LE and LipE analysis highlights compounds **12**, **14**, **15**, **16**, **24**, **32** and **49** as the best-performing compounds.

In vitro characterization of compound 12

Among all the synthesized derivatives described in this paper, compound **12** emerged with an overall *in vitro* profile as a quality lead and was selected for further investigation (Table 6). **12** was characterized by high water solubility (768 μM in buffer at pH 7.4), equipotent binding affinity and functional activity in the human $mGlu_5$ receptor (3.5 nM and 4.1 nM, respectively). **12** was found to be selective versus rat $mGlu_1$ receptor (binding inhibition 1.36% at 1 μM), which is the subtype that shares the highest structural homology with $mGlu_5$. Selectivity was confirmed by a functional assay in the

human $mGlu_1$ receptor, where **12** did not induce agonist or antagonist activity (Euroscreen; EC_{50} > 30 μM and IC_{50} > 20 μM, respectively) (Supporting Information Figures **S17** and **S18**). Compound **12** did not inhibit the most relevant CYP human isoforms (3A4, 2D6, 2B6, 2C8, 2C9, 2C19 and 2E1, IC_{50} > 20 μM) and moderately inhibited CYP1A2 (IC_{50} 4.52 μM).

A number of triple bond-containing drugs are available on the market and are systemically administered (e.g., the muscarinic receptor antagonist oxybutynin), and a number of negative allosteric modulators containing triple bonds have been described in some reports[17] as depleting glutathione storages and producing potential reactive GSH adducts. To investigate potential side effects of the systemic administration of **12**, a predictive methodology based on the *in vitro* formation of glutathione conjugates was used.[48] Compound **12** was incubated in the mouse S9 fraction with NADPH and GSH for 120 minutes, and following HPLC-MS investigation, no GSH adduct was detected. A preliminary assessment of lead quality was based on an *in vitro* package designed to avoid potential poly-pharmacological, cytotoxic, cardiotoxic and genotoxic effects. Compound **12** was evaluated for selectivity against

a panel of 75 receptors (Cerep) (Supporting Information Table S2). The binding inhibition was expressed as percent inhibition of radioligands at a 1 μM concentration. No inhibition higher than 50% was found for the tested receptors, confirming the high selectivity of this molecule. Undesirable pharmacological prolongation of the QT interval of ECG may cause a delay in ventricular repolarization and a polymorphic ventricular tachycardia, named torsade de pointes (TdP), which is potentially lethal. To prevent this risk, candidates are currently evaluated against a cardiac *in vitro* safety panel of ion channels that have a fundamental and documented contribution to human arrhythmias.[49] **12** tested safe in these preliminary preclinical *in vitro* tests (Table 6). Drug-induced liver injury (DILI) is one of the most relevant reasons for attrition in drug development, and *in vitro* preclinical assays based on HepG2 cells have been developed to predict potential hepatotoxicity. **12** did not inhibit HepG2 cell viability at a 10 μM concentration (Table 6). The potential mutagenicity of **12** was tested. The compound was negative for the two strains (TA98 and TA100) investigated in the *Salmonella typhimurium* non-GLP AMES test. The overall *in vitro* and safety profile of **12** was encouraging and justified further *in vivo* studies.

In vivo pharmacokinetics of 12

The pharmacokinetic properties of **12** were determined in rats and dogs after intravenous administration of 1 mg/kg and oral administration of 3 mg/kg (Table 7). Administration of a single oral dose in rats (3 mg/kg suspension in 0.5% Methocel in water) resulted in high bioavailability (F = 51%). **12** was readily absorbed (Tmax = 1 hour), with a reasonable half-life ($t_{1/2}$ = 2.2 hours). The compound was able to enter into the brain with an almost equal brain/plasma concentration ratio (K_p = 0.7). The determined *in vitro* protein binding in rat plasma (94.8%) was in agreement with a suitable free fraction. The good pharmacokinetic profile of **12** was confirmed by single oral dose administration (3 mg/kg) in dogs (Table 7). The apparent absolute oral bioavailability of **12** in dogs is more than 100%, suggesting that the compound might be the substrate of transporters in the intestine of this species but not in rats (F = 51%).[50] In dogs, compound **12** was even more readily and significantly absorbed after oral administration (Tmax = 0.25 hours), while the half-life was unchanged ($t_{1/2}$ = 2.55 hours).

In vivo pharmacology of 12

Fenobam, a clinically validate anxiolytic, was the first agent discovered to exert its effects by $mGlu_5$ antagonist mechanisms.[51] Vogel's conflict test is a popular model of anxiety based on the fear of a painful stimulus received by rats during water administration and using benzodiazepines as a positive control.[52] Fenobam[51] and basimglurant[19] were reported to be effective in increasing drinking time at the spout at 30 and 0.03 mg/kg, respectively. Mavoglurant was tested on stress-induced hyperthermia, a comparable anxiety model. Mavoglurant efficacy was effective as a positive control at the oral dose of 10 mg/kg.[53] Compound **12** was tested in rats for anxiolytic activity in Vogel's conflict test[52] (Figure 6) at 0.3, 3 and 30 mg/kg and caused a significant increase in the number of electric shocks received (punishment drinking) by treated animals. The activity of compound **12** was dose-dependent and statistically significant ($P < 0.001$) compared with the vehicle controls at 3 and 30 mg/kg. The effect of $mGlu_5$ antagonists on acute nociception is controversial. Basimglurant was tested *per os* at the dose of 0.1–10.0 mg/kg on the Bennet model of cold allodynia,

where it dose-dependently increased the rate of inhibition with a minimal effective dose of 0.3 mg/kg. In a different model of neuropathic pain, the Chung model based on spinal nerve ligature, basimglurant had no statistically significant effect on the pain induced by thermal stimulation.[54] Conversely, in neuropathic pain model induced by chronic constriction injury (Bennett model),[55] the intraperitoneal administration of 10 mg/kg compound **12** in rats 60 minutes before testing moderately reduced thermal hyperalgesia (Figure 7) but it was not effective at reducing mechanical allodynia, as reported for other $mGlu_5$ NAMs.[56] The $mGlu_5$ receptor subtype is involved in the afferent processing of reflex micturition. The standard MPEP showed a marked inhibitory effect on reflex micturition pathways and increased the bladder capacity in the rats at the oral dose of 10 mg/kg.[57] The activity of basimglurant on the lower urinary tract was characterized, and it dose-dependently increased the threshold of bladder-filling volume with a minimal effective dose of 0.03 mg/kg. Basimglurant was also tested for 1 hour on an isovolumetric bladder contraction model and was able to enlarge the interval between voiding contractions in comparison to the vehicle.[54] Compound **12** was similarly tested on lower urinary tract models at concentrations of 0.01, 0.03 and 0.1 mg/kg by iv administration in anaesthetized female rats on

isovolumic volume-induced voiding contractions (Figure 8). The compound showed an ED_{10} value of 0.015 mg/kg, based on the disappearance time (DT) expressed in minutes. In conscious male rats, the bladder volume capacity (BVC), defined as the volume (mL) of saline infused into the bladder and necessary to induce micturition contraction, was determined. The tested oral doses of **12** were 1 and 3 mg/kg in 0.5% Methocel solution, and **12** was able to statistically increase the BVC for more than 4 hours at 3 mg/kg (P = 0.001) compared to the BVC of vehicle (Figure 9).

Conclusions

The previously described aryl and heteroaryl derivatives of prop-2-ynylidenecycloalkylamine (e.g., **4**) are characterized as a class of compounds with high binding affinity and potent functional activity but are affected by issues that reduce the potential for drug development, such as low solubility and unwanted interaction with cytochrome isoforms (CYP1A2). In this paper, we describe and characterize new amide, carbamate, urea and sulfonamide derivatives of 4-prop-2-ynylidenecycloalkylamine as potent and selective NAMs of the $mGlu_5$ receptor, and

we further develop the most promising compounds. The amide, carbamate and urea derivatives substituted with large bulky lipophilic groups showed high binding affinity but impaired Ca^{2+} functional assay results on $mGlu_5$, increasing the functional/binding ratio. The optimal activity was obtained with an ethyl substituent on carbamates, an N-isobutyl-methyl substituent in ureas, and a furanyl group in amides. Moreover, docking studies in two $mGlu_5$ receptor crystal structures were performed to predict the ligand binding modes and to help to qualitatively interpret structure-activity relationships. The molecules were also tested for their ability to inhibit the most relevant CYP450 isoenzymes, and the ADME profiles of the amide, carbamate, sulfonamide and urea derivatives of 4-(3-arylprop-2-ynylidene)piperidine were optimized. None of the newly synthesized compounds potently inhibited the CYP2D6 isoform. An extensive SAR investigation was performed to decrease the interaction with CYP1A2 and CYP3A4 isoforms. Derivatives of 3-(3-arylprop-2-ynylidene)pyrrolidine were characterized by a reduced interaction with these isoforms. The metabolic stability of the compounds was widely investigated to optimize the half-life of the molecules in both rats and humans. Pyridine derivatives were subjected to extensive metabolism by rat and human microsomes. The docking simulations on the

human crystal structure of the CYP3A4 isoform revealed that the pyridine ring could interact with the prosthetic heme group, suggesting that these molecules are reasonable substrates of the CYP3A4 isoform. Accordingly, the SAR analysis suggests that metabolism may be influenced by the presence of the pyridine ring and the presence and orientation of the carbonyl group linked to the piperidine nitrogen. 3-(3-Arylprop-2-ynylidene)pyrrolidine derivatives **12**, **32** and **49** were the best lead compounds for drug development. Among the discussed compounds, compound **12** proved to be a soluble and selective $mGlu_5$ NAM with a suitable *in vitro* and *in vivo* pharmacokinetic profile. Based on the latter evidence, **12** is a candidate that has slightly lower functional activity in Ca^{2+} mobilization in human $mGlu_5$ than the previously described compound **4** (IC_{50} 4.1 nM vs 0.8 nM) but is characterized by a higher selectivity versus the $mGlu_1$ subtype, a cleaner cytochrome profile and improved stability in both rats and humans. **12** was profiled against a panel consisting of 75 receptors (CEREP) and showed an excellent selectivity profile. **12** was investigated in cell viability studies (hepatotoxicity), *in vitro* cardiac safety studies (hERG, Nav1.5 and Cav1.2 patch-clamps) and mini AMES tests. **12** was highly absorbed in rats and dogs following oral administration and crossed the brain barrier

(K_p = 0.7). Similar to the other mentioned $mGlu_5$ NAMs, **12** was discovered to be active in anxiety, neuropathic pain and lower urinary tract models.

Experimental section

Chemical synthesis and analytical procedures

All reactions were carried out employing standard chemical techniques. Unless otherwise noted, reactions were carried out in anhydrous solvents under N_2 atmosphere. The solvents used for extraction, washing, and chromatography were HPLC grade and were used without further purification.

Petroleum ether (PE) is a mixture of low boiling hydrocarbon (>90% between 40-60°C). All NMR spectra were recorded on 400 MHz Bruker Advance Spectrometers. ^{1}HNMR chemical shifts were reported as δ (ppm) relative to residual solvent peaks. Low-resolution mass spectra were obtained on 2795 Waters instruments. The flow was split at the exit of the column to a Waters 2996 PAD detector and to a Micromass ZQ detector fitted with an electrospray source and equipped with a Xterra MS C18 4.6 x 50 mm 3.5 µm, running a gradient of 20% - 100% acetonitrile in a buffer solution of 20 mM NH_4HCO_3 at pH 8. Analytical thin-layer chromatography was carried out on precoated silica gel 60 F254 Merck plates. Flash chromatography was performed using silica gel 60 (35-70 µm) purchased from Merck, using SP1® or Horizon® or

Isolera® flash purification systems from Biotage Inc. with prepacked silica gel cartridges. The purity of the biologically tested compounds was determined by analytical HPLC or the UPLC method. The purity of all compounds was 95% or higher, with the exception of compound **39**. The analytical HPLC was performed on a Waters instrument comprising a separation module (Waters 2695), an automatic injector, a photodiode array detector (Waters 2996), and a software system controller (Empower). The reverse-phase column Xterra C18 4.6 x 100 mm, 5 µm was used at a flow rate of 1.3 mL/min and UV detection at 220 nm, running a gradient of 20% - 100% acetonitrile in a buffer solution of 20 mM NH_4HCO_3 at pH 8 or alternatively by a Waters H-Class UPLC/PAD system running a gradient of 20% - 100% acetonitrile in a buffer solution of 20 mM NH_4HCO_3 at pH 8, using a Waters C18 BEH 100 x 2.1 mm, 1.7 µm column at a flow rate of 0.6 mL/min. IR spectra were recorded on a Perkin Elmer Spectrum One FT-IT spectrometer using KBr pellets. Reagents were purchased from commercial sources at the highest commercial quality. The compound R214127 was synthesized by the Recordati Drug Discovery Department following reported procedures.[33] [^{3}H]MPEP and [^{3}H]R214127 were obtained from American Radiolabeled Chemicals Inc. (Saint Louis, MO, USA). The newly synthesized

compounds (**10–61**) were examined for Pan Assay INterference compoundS (PAINS)[58] using the KNIME workflow in SMARTS format[59], and no substructural alert was found.

tert-Butyl 3-[3-(trimethylsilyl)prop-2-yn-1-ylidene]azetidine-1-carboxylate (10a)

To a yellowish solution of diethyl [3-(trimethylsilyl)prop-2-ynyl]phosphonate (815 mg, 2.85 mmol) in 7 mL of anhydrous THF stirred at –70°C under nitrogen atmosphere, was added dropwise a 1M THF solution of LHMDS (3.28 mL, 1.5 mmol). The so obtained brownish reaction mixture was stirred at –70°C for 15 min. Afterwards, a yellow solution of 1-*tert*-butoxycarbonyl-3-azetidinone (503 mg, 2.85 mmol) in 8 mL of THF was dripped over 15 min. The resulting pale orange solution was stirred at -70°C for 15 min, then at rt overnight. The reaction mixture was quenched with a saturated aqueous solution of NH_4Cl and extracted with EtOAc (3x). Evaporation of the solvent to dryness afforded a crude which was purified by silica gel chromatography (SP1® - Biotage) eluting with PE - EtOAc 95:5. 480 mg (63%) of compound **10a** were isolated as colorless oil. MS (ESI) *m/z* 266.7 $[M+H]^+$; **^{1}H-NMR** ($CDCl_3$) δ: 5.47 (s, 1H), 4.82-5.22 (m, 1H), 3.74-4.74 (m, 4H), 1.48 (s, 9H), 0.24 (s, 9H).

tert-Butyl 3-[3-(6-methylpyridin-2-yl)prop-2-yn-1-ylidene]azetidine-1-carboxylate (10b)

To a solution of compound **10a** (400 mg, 1.51 mmol) and 2-bromopyridine (172 µL, 1.51 mmol) in 10 mL of anhydrous DMF, previously degassed by bubbling nitrogen for 5 min, was quickly added *tetrakis*(triphenylphosphine)palladium(0) (87.2 mg, 0.08 mmol), tetrabutylammonium fluoride (395 mg, 1.51 mmol) and sodium acetate (248 mg, 3.02 mmol). Afterwards, the reaction mixture was heated at 120°C in a microwave oven (Personal Chemistry® - Biotage) for 10 min. The reaction mixture was then cooled to rt, poured into water and extracted with EtOAc (3x). The combined organic layers were dried over Na_2SO_4 and evaporated to dryness. The crude residue was purified by silica gel chromatography (SP1® - Biotage) eluting with a gradient of PE - EtOAc from 8:2 to 3:7. **10b** (429 mg, 72.2%) was isolated as yellowish solid. MS (ESI) *m/z* 285.5 $[M+H]^+$. **^{1}H-NMR** ($CDCl_3$) *δ*: 7.57 (dd, J=7.8, 7.8Hz, 1H), 7.26 (d, J=7.8 Hz, 1H), 7.12 (d, J=7.8 Hz, 1H), 5.72 (s, 1H), 4.70 (s, 2H), 4.60 (s, 2H), 2.59 (s, 3H), 1.48 (s, 9H). HPLC 96.0% (UV).

2-[3-(Azetidin-3-ylidene)prop-1-yn-1-yl]-6-methylpyridine (10c)

To a solution of compound **10b** (320 mg, 1.13 mmol) in 25 mL of $CHCl_3$ stirred at 0-5°C was added TFA (871 µL, 11.3 mmol). The reaction mixture was then heated at 60°C and stirred for 2h. After overnight stirring at rt, it was alkalinized by addition of 1N NaOH and extracted with $CHCl_3$ (3x). The combined organic extracts were dried over Na_2SO_4 and evaporated to dryness *in vacuo* to afford **10c (**208 mg, 96.1%, yellowish oil), used without further purification in the following step. MS (ESI) *m/z* 185.3 $[M+H]^+$; **^{1}H-NMR** ($CDCl_3$) *δ*: 7.39-7.63 (m, 1H), 7.23 (br d, J=8.0 Hz, 1H), 7.08 (br d, J=8.0 Hz, 1H), 5.59 (s, 1H), 3.66-4.32 (m, 4H), 2.36-2.81 (m, 3H).

Ethyl 3-[3-(6-methylpyridin-2-yl)prop-2-yn-1-ylidene]azetidine-1-carboxylate (10)

To a brownish solution of compound **10c** (48 mg, 0.26 mmol), triethylamine (75µL, 0.52 mmol) in 3 mL of DCM was added dropwise ethyl chloroformate (33.3 µL, 0.34 mmol) while stirring at rt. The reaction mixture was stirred at rt for 3 days, poured into water and extracted with DCM (3x). The combined extracts were dried over Na_2SO_4 and evaporated to dryness *in vacuo*. The crude residue (69 mg, brownish oil) was purified by silica gel chromatography (SP1® - Biotage) eluting with PE - EtOAc 6:4 giving 34.8 mg (52%) of **10** as white solid. MS (ESI) *m/z* 257.2 $[M+H]^+$. **^{1}H-NMR**

($CDCl_3$) *δ*: 7.57 (dd, J=7.8, 7.8 Hz, 1H), 7.25 (d, J=7.8 Hz, 1H), 7.12 (d, J=7.8 Hz, 1H), 5.70-5.77 (m, 1H), 4.73-4.80 (m, 2H), 4.63-4.69 (m, 2H), 4.17 (q, J=7.1 Hz, 2H), 2.59 (s, 3H), 1.29 (t, J=7.1 Hz, 3H). HPLC 99.3% (UV).

tert-Butyl 6-[3-(trimethylsilyl)prop-2-yn-1-ylidene]-2-azaspiro[3.3]heptane-2-carboxylate (11a)

To a solution of diethyl [3-(trimethylsilyl)prop-2-ynyl]phosphonate (3.07 g, 12.4 mmol) in anhydrous THF (25 mL) stirred at –60°C under a nitrogen atmosphere was added dropwise a 1M solution of LHMDS (10.5 mL, 10.5 mmol) in MTBE. The reaction mixture was then stirred for 30 min at the same temperature. Afterwards, a solution of 1,1-dimethylethyl 2-azaspiro[3.3]heptane-6-oxo-2-carboxylic acid (2 g, 9.47 mmol) in 15 mL of anhydrous THF was added stirring at –60°C for further 15 min, then warming at rt and stirring for 2 h at the same temperature. The reaction mixture was quenched with water and extracted with EtOAc (3x), which was washed with brine and dried over Na_2SO_4 evaporating the solvent to dryness. The crude residue was purified by silica gel chromatography (SP1® - Biotage) eluting with a gradient of PE - EtOAc from 95:5 to 8:2. Compound **11a** (2.75 g, 95%) was obtained as white solid. MS (ESI) *m/z* 306.5

[M+H]$^+$. **^{1}H-NMR** ($CDCl_3$) *δ*: 5.36 (quin, J=2.5 Hz, 1H), 3.98 (d, J=8.3 Hz, 2H), 3.95 (d, J=8.3 Hz, 2H), 3.00 (d, J=2.5 Hz, 2H), 2.94 (d, J=2.5 Hz, 2H), 1.46 (s, 9H), 0.20 ppm (s, 9H).

tert-Butyl 6-[3-(6-methylpyridin-2-yl)prop-2-yn-1-ylidene]-2-azaspiro[3.3]heptane-2-carboxylate (11b)

To a solution of compound **11a** (400 mg, 1.51 mmol) and 2-bromopyridine (448 µL, 3.93 mmol) in 16 mL of DMF, previously degassed bubbling nitrogen for 5 min, was quickly added *tetrakis*(triphenylphosphine)palladium(0) (227 mg, 0.20 mmmol), tetrabutylammonium fluoride (1.03 g, 3.93 mmol) and sodium acetate (644 mg, 7.84 mmol). Afterwards, the reaction mixture was heated at 120°C in a microwave oven (Personal Chemistry® Biotage) for 10 min. The reaction mixture was then cooled, poured into water and extracted with Et_2O, which was dried over Na_2SO_4 and evaporated to dryness. The crude residue was purified by silica gel chromatography (SP1® - Biotage) eluting with a gradient of PE - EtOAc from 9:1 to 4:6. **11b** was isolated as yellowish solid (270 mg, 55.2%). MS (ESI) *m/z* 325.2 [M+H]$^+$. **^{1}H-NMR** ($CDCl_3$) *δ*: 7.56 (dd, J=7.8, 7.6 Hz 1 H) 7.24 (d, J=7.6 Hz, 1 H) 7.09 (d, J=7.8 Hz, 1 H) 5.58 (t,

J=2.3 Hz, 1 H) 3.94 - 4.05 (m, 4 H) 3.12 (br. s., 2 H) 3.01 (s, 2 H) 2.59 (br. s., 3 H) 1.46 (s, 9 H). HPLC 93.7% (UV).

6-[3-(6-Methylpyridin-2-yl)prop-2-yn-1-ylidene]-2-azaspiro[3.3]heptane (11c)

Compound **11b** (120 mg, 0.37 mmol) was dissolved in a 4.4 M hydrogen chloride solution in *i*-PrOH (8 mL) and stirred at rt for 2 h. Solvent evaporation afforded 79.5 mg (96%) of **11c** as brownish oil, used in the next step without further purification. MS (ESI) *m/z* 225.2 $[M+H]^+$. **^{1}H-NMR** ($CDCl_3$) *δ*: 7.53 (dd, J=7.8, 7.8 Hz, 1H), 7.23 (d, J=7.8 Hz, 1H), 7.07 (d, J=7.8 Hz, 1H), 5.55 (quin, J=2.4 Hz, 1H), 3.77 (d, J=8.3 Hz, 2H), 3.72 (d, J=8.3 Hz, 2H), 3.08 (d, J=2.4 Hz, 2H), 3.01 (d, J=2.4 Hz, 2H), 2.56 (s, 3H).

Ethyl 6-[3-(6-methylpyridin-2-yl)prop-2-yn-1-ylidene]-2-azaspiro[3.3]heptane-2-carboxylate (11)

To a solution of compound **11c** (120 mg, 0.54 mmol) in DCM stirred at rt was added TEA (112 µL, 0.80 mmol) and ethyl chloroformate (80 µL, 0.80 mmol). Stirring was continued for 2 h. Afterwards, the solvent was evaporated and the crude purified by silica gel chromatography (SP1® - Biotage) eluting with a gradient of PE - EtOAc from

7:3 to 3:7, affording 90 mg (57%) of **11** as clear oil. MS (ESI) *m/z* 297.4 $[M+H]^+$. **^{1}H-NMR** ($CDCl_3$) *δ*: 7.54 (dd, J=7.8, 7.8 Hz, 1H), 7.23 (d, J=7.8 Hz, 1H), 7.08 (d, J=7.8 Hz, 1H), 5.55-5.61 (m, 1H), 4.13 (q, J=7.1 Hz, 2H), 4.00-4.09 (m, 4H), 3.12 (br. s., 2H), 3.02 (s, 2H), 2.57 (s, 3H), 1.26 (t, J=7.1 Hz, 3H). HPLC 99.1% (UV).

tert-Butyl (3*E*)-3-(3-trimethylsilylprop-2-ynylidene)pyrrolidine-1-carboxylate (12a) and _tert_-butyl (3*Z*)-3-(3-trimethylsilylprop-2-ynylidene)pyrrolidine-1-carboxylate (13a)

To a yellowish solution of diethyl [3-(trimethylsilyl)prop-2-ynyl]phosphonate (2.96 g, 11.9 mmol) in 10 mL of anhydrous THF stirred at -60°C under a nitrogen atmosphere, was added a 1 M solution of LHMDS in THF (11.9 mL, 11.9 mmol). The resulting orange reaction mixture was stirred at -60°C°C for 10 min. A solution of N-*tert*-butoxycarbonyl-3-pyrrolidinone (2 g, 10.8 mmol) in 20 mL of THF was then added dropwise over 10 min and stirring was continued at -60°C for further 15 min. Afterwards, the reaction mixture was warmed to rt and stirred for 2 h; then it was quenched with a saturated solution of NH_4Cl and extracted with EtOAc (3x). The combined organic extracts were washed with brine, dried over Na_2SO_4 and evaporated to dryness. The crude orange oily residue was purified by silica gel chromatography

(Horizon® - Biotage) eluting with PE - EtOAc 85:15, affording 1.28 g (42.4%) of the less polar *E* isomer (**12a**) and 640 mg (21.2%) of the more polar *Z* isomer (**13a**), both as colorless oils.

12a: MS (ESI) *m/z* 280.6 $[M+H]^+$. **^{1}H NMR** ($CDCl_3$) δ: 5.46-5.54 (m, 1H), 4.05 (s, 2H), 3.54 (t, J=7.4 Hz, 2H), 2.79 (t, J=7.4 Hz, 2H), 1.49 (s, 9H), 0.22 (s, 9H).

13a: MS (ESI) *m/z* 280.5 $[M+H]^+$. **^{1}H NMR** ($CDCl_3$) δ: 5.42-5.61 (m, 1H), 4.14 (s, 2H), 3.52 (br t, J=7.4 Hz, 2H), 2.66 (br t, J=7.4 Hz, 2H), 1.50 (s, 9H), 0.21 (s, 9H).

***tert*-Butyl (3*E*)-3-[3-(6-methylpyridin-2-yl)prop-2-yn-1-ylidene]pyrrolidine-1-carboxylate (12b)**

To a solution of compound **12a** (0.9 g, 3.25 mmol) and 2-bromo-6-methylpyridine (3.93 mL, 3.39 mmol) in 12 mL of DMF, previously degassed bubbling nitrogen for 5 min, was quickly added *tetrakis*(triphenylphosphine)palladium(0) (186 mg, 0.16 mmol), tetrabutylammonium fluoride (0.9 g, 3.25 mmol) and sodium acetate trihydrate (0.528 mg, 6.43 mmol). Afterwards, the reaction mixture was heated at 120°C in a microwave oven (Personal Chemistry® Biotage) for 10 min. The reaction mixture was cooled to rt, poured into water and extracted with EtOAc (3x), which was dried over

Na_2SO_4 and evaporated to dryness *in vacuo*. The crude was purified via silica gel chromatography (Isolera® - Biotage) eluting with a gradient of PE - EtOAc from 9:1 to 6:4. **12b** (0.68 g, 70.8%) was isolated as yellowish solid. MS (ESI) *m/z* 299.3 $[M+H]^+$. **^{1}H NMR** ($CDCl_3$) δ: 7.57 (dd, J=7.8 Hz, 1 H), 7.27 (d, J=7.8 Hz, 1 H), 7.11 (d, J=7.8 Hz, 1 H), 5.72 (br s, 1 H), 4.12 (s, 2 H), 3.57 (br s, 2 H), 2.92 (br t, J=8.1 Hz, 2 H), 2.60 (s, 3 H), 1.50 (s, 9 H).

Methyl-6-[(3*E*)-3-pyrrolidin-3-ylideneprop-1-ynyl]pyridine (12c)

To a solution of compound **12b** (250 mg, 0.84.28 mmol), in 10 mL of $CHCl_3$, cooled at 0-5°C, was added TFA (0.97 µL, 12.6 mmol) under stirring; then the reaction mixture was heated at reflux for 4 h. Afterwards, it was cooled to rt, alkalinized by addition of 1N NaOH and extracted with $CHCl_3$ (4x). The extraction solvent was dried over Na_2SO_4 and evaporated to dryness affording 166 mg (100%) of **12c** as a brownish oil, used in the following step without further purification. MS (ESI) *m/z* 199.6 $[M+H]^+$

Ethyl (3*E*)-3-[3-(6-methylpyridin-2-yl)prop-2-yn-1-ylidene]pyrrolidine-1-carboxylate (12)

To a solution of compound **12c** (160 mg, 0.81 mmol) in DCM (8 mL) stirred at rt was added TEA (232 µL, 1.61 mmol) and ethyl chloroformate (103 □L, 1.05 mmol). After overnight stirring, the solvent was evaporated to dryness and the crude residue purified by silica gel chromatography (Isolera® - Biotage) eluting with a gradient of PE – EtOAc from 95:5 to 6:4, affording 125 mg (57%) of **12** as a pale white solid.

^{1}H-NMR ($CDCl_3$) *δ*: 7.55 (dd, J=7.8, 7.8 Hz, 1H), 7.26 (d, J=7.8 Hz, 1H), 7.10 (d, J=7.8 Hz, 1H), 5.73 (br. s., 1H), 4.18 (br. s, 2H), 4.18 (q, J=7.1 Hz, 2H), 3.62 (br. s., 2H), 2.93 (br. s., 2H), 2.58 (s, 3H), 1.29 (t, J=7.1 Hz, 3H).**^{13}C-NMR** (101 MHz, $CDCl_3$) *δ*: 158.96, 154.95, (153.82 and 153.06), 142.73, 136.29, 124.02, 122.43, 101.80, 93.15, 85.63, 61.17, (50.80 and 50.52), (45.26), (31.04 and 30.35), 24.53, 14.78. The NMR signals of pyrrolidine ring carbon, in brackets, were split due to the chemical shielding anisotropy of the carbamate carbonyl group. UPLC 99.5% (UV), MS (ESI) *m/z* 271.3 $[M+H]^+$.

Ethyl (3*E*)-3-[3-(6-methylpyridin-2-yl)prop-2-yn-1-ylidene]pyrrolidine-1-carboxylate mesylate salt (12s)

Compound **12** (150 mg, 0.56mmol) was dissolved in 2.5 mL of acetone at rt and 0.6 mL (0.56 mmol) of methansulphonic acid solution, freshly prepared with 120µL of methansulphonic acid in 2 mL of acetone, were added. After solid precipitation, the suspension was kept for 4 hours at room temperature and then stored at 4°C during the night. This precipitate was filtered under vacuum and was suspended in 6 mL of acetone and 0.5 mL of EtOH and stirred at 40°C to obtain a clear solution. The solution was stirred 6 h at rt and stored overnight at 4°C. The obtained precipitate was filtered under vacuum and dried under vacuum at 40°C to obtain 105.5 mg of mesylate salt. Yield 51.7%. **^{1}H-NMR** (DMSO-d6) δ ppm 10.67 (br s, 1 H), 8.22 (dd, J=7.9, 7.9 Hz 1 H), 7.79 (d, J=7.9 Hz, 1 H), 7.68 (d, J=7.9 Hz, 1 H), 5.99 - 6.05 (m, 1 H), 4.15 (br s, 2 H), 4.06 (q, J=7.1 Hz, 2 H), 3.54 (br t, J=7.4 Hz, 2 H), 2.84 - 3.00 (m, 2 H), 2.65 (s, 3 H), 2.41 (s, 3 H), 1.20 (t, J=7.1 Hz, 3 H); **^{13}C-NMR** (101 MHz, DMSO-d6) *δ* ppm: 158.99 and 159.65 (d*, 1 C), 156.85, 154.49, 143.35, 136.86, 126.86, 126.03, 100.41, 94.03, 87.81, 61.02, 50.90 and 51.31 (d*, 1 C), 45.29 and 45.56 (d*, 1 C), 40.20, 30.69 and 31.51 (d*, 1 C), 21.38, 15.16. d* = split signal due to magnetic shielding anisotropy of carbonyl group of carbamate residue. **^{13}C-NMR** (101 MHz, 333 K, DMSO-d6) *δ* ppm:

158.49, 157.21, 154.56, 142.26, 137.93, 126.46, 125.50, 100.59, 92.77, 88.83, 60.98, 51.13, 45.48, 40.18, 31.10, 21.88, 15.11.

***tert*-Butyl (3*Z*)-3-[3-(6-methylpyridin-2-yl)prop-2-yn-1-ylidene]pyrrolidine-1-carboxylate (13b)**

To a solution of compound **13a** (0.6 g, 2.15 mmol), obtained along with the *E* isomer and described in the first step of compound **12**, and 2-bromo-6-methylpyridine (2.62 µL, 2.26 mmol) in 8 mL of DMF, previously degassed by bubbling nitrogen for 5 min, was quickly added *tetrakis*(triphenylphosphine)palladium(0) (124 mg, 0.107 mmol), tetrabutylammonium fluoride (0.6 g, 2.15 mmol) and sodium acetate trihydrate (0.352 mg, 4.29 mmol). Afterwards, the reaction mixture was heated at 120°C in a microwave oven (Personal Chemistry® Biotage) for 10 min, then it was cooled to rt, poured into water and extracted with EtOAc (3x), which was dried over Na_2SO_4 and evaporated to dryness. The crude residue was purified via silica gel chromatography (Isolera® - Biotage) eluting with a gradient of PE - EtOAc from 9:1 to 6:4. **13b** (0.43 g, 67%) was isolated as yellowish solid. MS (ESI) *m/z* 299.3 $[M+H]^+$. **^{1}H-NMR** ($CDCl_3$) *δ*: 7.48-7.68 (m, 1 H) 7.28 (d, J=7.6 Hz, 1 H) 7.14 (d, J=7.6 Hz, 1 H) 5.73 (br. s., 1 H) 4.14 - 4.42

(m, 2 H) 3.56 (br. s., 2 H) 2.74 (br. s., 2 H) 2.63 (br. s., 3 H) 1.51 (s, 9 H). HPLC 93.1% (UV).

(3*Z*)-3-[3-(6-Methyl-2-pyridyl)-prop-2-ynylidene]pyrrolidine (13c)

To a solution of compound **13b** (250 mg, 0.67 mmol) in 9.6 mL of $CHCl_3$, stirred at 0-5°C, was added TFA (774 µL, 10 mmol), then the reaction mixture was heated at reflux for 4 h. After cooling to rt and addition of 1N NaOH to alkaline pH, the mixture was extracted with $CHCl_3$ (4x). The combined extracts were dried over Na_2SO_4 and evaporated to dryness affording **13c** as brownish oil (130 mg, 100%), used without further purification in the following step. MS (ESI) *m/z* 199.6 $[M+H]^+$; **^{1}H-NMR** ($CDCl_3$) *δ*: 7.55 (dd, J=7.8, 7.8 Hz, 1H), 7.26 (d, J=7.8 Hz, 1H), 7.09 (d, J=7.8 Hz, 1H), 5.68-5.78 (m, 1H), 3.76 (s, 2H), 3.23 (t, J=7.1 Hz, 2H), 2.74-2.87 (m, 2H), 2.58 (s, 3H).

Ethyl (3*Z*)-3-[3-(6-methylpyridin-2-yl)prop-2-yn-1-ylidene]pyrrolidine-1-carboxylate (13)

To a solution of compound **13c** (120 mg, 0.61 mmol) in DCM (6 mL) stirred at rt was added TEA (174 µL, 1.21 mmol) and ethyl chloroformate (174 □L, 1.21 mmol). After overnight stirring, the solvent was evaporated to dryness and the crude residue

purified by silica gel chromatography (Isolera® - Biotage) eluting with a gradient of PE – EtOAc from 9:1 to 6:4, affording 107 mg (65%) of **13** as yellow oil. MS (ESI) *m/z* 271.5 $[M+H]^+$. **^{1}H-NMR** ($CDCl_3$) *δ*: 7.58 (dd, J=7.8, 7.8 Hz, 1H), 7.29 (d, J=7.8 Hz, 1H), 7.12 (d, J=7.8 Hz, 1H), 5.74 (s, 1H), 4.25-4.38 (m, 2H), 4.19 (q, J=7.1 Hz, 2H), 3.61 (br. s., 2H), 2.75 (br. s., 2H), 2.60 (s, 3H), 1.30 (t, J=7.1 Hz, 3H). HPLC 95.0% (UV).

Methyl 4-[3-(6-methylpyridin-2-yl)prop-2-yn-1-ylidene]piperidine-1-carboxylate (14)

To a solution of 2-methyl-6-[3-(piperidin-4-ylidene)prop-1-yn-1-yl]pyridine (**14a,**[30] 60 mg, 0.28mmol) in DCM (3.5 mL) stirred at 0°C- rt was added TEA (48.6 µL, 0.34 mmol) and methyl chloroformate (26.2 µL, 0.34 mmol). After overnight stirring at rt, the solvent was evaporated to dryness and the crude extracted with Et_2O (3x). The combined organic extracts were washed with water, dried over Na_2SO_4 and evaporated to dryness to afford **14** (72.5 mg, 95%, brownish solid). MS (ESI) *m/z* 271.4 $[M+H]^+$. **^{1}H-NMR** ($CDCl_3$) *δ*: 7.54 (dd, J=7.8, 7.8 Hz, 1H), 7.25 (d, J=7.8 Hz, 1H), 7.09 (d, J=7.8 Hz, 1H), 5.61 (s, 1H), 3.75 (s, 3H), 3.47-3.63 (m, 4H), 2.60-2.67 (m, 2H), 2.58 (s, 3H), 2.30-2.39 (m, 2H). HPLC 95.4% (UV).

Ethyl 4-[3-(trimethylsilyl)prop-2-yn-1-ylidene]piperidine-1-carboxylate (15a)

15a was prepared following the procedure reported above for **12a** by reacting diethyl [3-(trimethylsilyl)prop-2-ynyl]phosphonate with 1-ethoxycarbonyl-4-oxopiperidine instead of N-*tert*-butoxycarbonyl-3-pyrrolidinone. Purification of the crude by silica gel chromatography (SP1® – Biotage) eluting with PE - EtOAc 93:7 afforded the title product as colorless oil (76%). MS (ESI) *m/z* 226.3 $[M+H]^+$. **^{1}H-NMR** (DMSO-d6) *δ*: 5.48 (s, 1H), 4.05 (q, J = 7.1 Hz, 2H), 3.33-3.47 (m, 4H), 2.35-2.45 (m, 2H), 2.13-2.26 (m, 2H), 1.19 (t, J = 7.1 Hz, 3H), 0.14-0.22 (m, 9H)

Ethyl 4-[3-(pyridin-2-yl)prop-2-yn-1-ylidene]piperidine-1-carboxylate (15)

Prepared by reacting **15a** and 2-iodopyridine (instead of 2-bromo-6-methylpyridine) following the procedure reported above for **12b**. Purification of the crude by silica gel chromatography (SP1® – Biotage) eluting with PE - EtOAc 65:35 afforded **15** as brownish oil (60.2%). MS (ESI) *m/z* 271.2 $[M+H]^+$. **^{1}H-NMR** ($CDCl_3$) *δ*: 8.59 (dd, J=4.8, 1.7 Hz, 1H), 7.64 (ddd, J=7.8, 7.5, 1.7 Hz, 1H), 7.42 (dd, J=7.8, 0.9 Hz, 1H), 7.20 (ddd, J=7.5, 4.8, 0.9 Hz, 1H), 5.60 (s, 1H), 4.17 (q, J=7.1 Hz, 2H), 3.45-3.61 (m, 4H), 2.57-2.68 (m, 2H), 2.28-2.37 (m, 2H), 1.29 (t, J=7.1 Hz, 3H). HPLC 96.3% (UV).

Ethyl 4-[3-(6-methylpyridin-2-yl)prop-2-yn-1-ylidene]piperidine-1-carboxylate (16)

Prepared as described for compound **9** but using ethyl chloroformate in place of methyl chloroformate. Purification of the crude by silica gel chromatography (Isolera® – Biotage) eluting with a gradient of PE - EtOAc from 100:0 to 20:80 afforded **16** (65%) as a dense oil. MS (ESI) *m/z* 285.6 $[M+H]^+$. **^{1}H-NMR** ($CDCl_3$) *δ*: 7.57 (dd, J=7.8, 7.8 Hz, 1H), 7.26 (d, J=7.8 Hz, 1H), 7.10 (d, J=7.8 Hz, 1H), 5.61 (s, 1H), 4.17 (q, J=7.1 Hz, 2H), 3.46-3.65 (m, 4H), 2.61-2.73 (m, 2H), 2.59 (s, 3H), 2.23-2.40 (m, 2H), 1.29 (t, J=7.1 Hz, 3H). HPLC 97.5% (UV).

Cyclobutylmethyl 4-[3-(6-methylpyridin-2-yl)prop-2-yn-1-ylidene]piperidine-1-carboxylate (18)

To a solution of cyclobutanemethanol (29.3 mg, 0.34 mmol) and triphosgene (37.2 mg, 0.13 mmol) in DCM (1.5 mL) stirred at r.t., was added dropwise a solution of diisopropylethylamine (DIEA, 70 µL, 0.407 mmol) in 1.5 mL of DCM over 30 min. After 2 h stirring at rt, to the reaction mixture was added a solution of 2-methyl-6-[3-(piperidin-4-ylidene)prop-1-yn-1-yl]pyridine(**14a**)[30] (60 mg, 0.28 mmol) and 70 µL of DIEA in 0.8 mL of DCM. After 24h at rt, the reaction mixture was evaporated to dryness *in vacuo* and the residue was purified by silica gel chromatography (Horizon® –

Biotage) eluting with a DCM - EtOAc gradient from 97:3 to 90:10 to afford 65.2 mg (71%) of **18** as grey solid. MS (ESI) *m/z* 325.7 $[M+H]^+$. **^{1}H-NMR** ($CDCl_3$) *δ*: 7.66 (dd, J=7.8, 7.8 Hz, 1H), 7.32 (d, J=7.8 Hz, 1H), 7.16 (d, J=7.8 Hz, 1H), 5.63 (s, 1H), 4.10 (d, J=6.6 Hz, 2H), 3.49-3.63 (m, 4H), 2.55-2.80 (m, 6H), 2.29-2.42 (m, 2H), 2.03-2.17 (m, 2H), 1.72-2.02 (m, 4H). HPLC 95.5% (UV).

Benzyl 4-[3-(6-methylpyridin-2-yl)prop-2-yn-1-ylidene]piperidine-1-carboxylate (19)

Compound **19** was prepared following the procedure reported above for compound **18** replacing cyclobutanemethanol with benzyl alcohol. The crude was purified by silica gel chromatography (Horizon® - Biotage) eluting with a PE – EtOAc gradient from 85:15 to 8:2 to afford **19** (57%) as yellow oil. MS (ESI) *m/z* 346.09 $[M+H]^+$. **^{1}H-NMR** ($CDCl_3$) *δ*: 7.58 (dd, J=7.8, 7.8 Hz, 1H), 7.30-7.44 (m, 5H), 7.28 (d, J=7.8 Hz, 1H), 7.12 (d, J=7.8 Hz, 1H), 5.62 (s, 1H), 5.18 (s, 2H), 3.49-3.68 (m, 4H), 2.64-2.79 (m, 2H), 2.61 (s, 3H), 2.25-2.44 (m, 2H). HPLC 96.5% (UV).

2-Phenylethyl 4-[3-(6-methylpyridin-2-yl)prop-2-yn-1-ylidene]piperidine-1-carboxylate (20)

Compound **20** was prepared following the procedure reported above for compound **18** replacing cyclobutanemethanol with 2-phenylethanol. The crude was purified by silica gel chromatography (Horizon® – Biotage) eluting with a PE – EtOAc gradient from 8:2 to 7:3 to afford **20** (53.1%) as beige oil. MS (ESI) *m/z* 361.6 $[M+H]^+$. **^{1}H-NMR** ($CDCl_3$) *δ*: 7.55 (dd, J=7.7, 7.7 Hz, 1H), 7.18-7.38 (m, 6H), 7.09 (d, J=7.7 Hz, 1H), 5.60 (s, 1H), 4.34 (t, J=6.9 Hz, 2H), 3.37-3.68 (m, 4H), 2.99 (t, J=6.9 Hz, 2H), 2.50-2.68 (m, 2H), 2.58 (s, 3H), 2.16-2.39 (m, 2H). HPLC 95.7% (UV).

Ethyl 4-[3-(3-methylphenyl)prop-2-yn-1-ylidene]piperidine-1-carboxylate (21)

Compound **21** was prepared following the procedure reported above for compound **15** replacing 2-iodopyridine with 3-iodotoluene. The crude was purified by silica gel chromatography (SP1® – Biotage) eluting with PE - EtOAc 9:1 to afford **21** (72%) as yellow oil. MS (ESI) *m/z* 284.6 $[M+H]^+$. **^{1}H-NMR** (DMSO-d6) *δ*: 7.15-7.31 (m, 4H), 5.67 (s, 1H), 4.07 (m, 2H), 3.37-3.53 (m, 4H), 2.45-2.55 (m, 2H), 2.24-2.34 (m, 2H), 2.30 (s, 3H), 1.20 (m, 3H). HPLC 95.4% (UV).

Ethyl 4-[3-(3-fluorophenyl)prop-2-yn-1-ylidene]piperidine-1-carboxylate (22)

Compound **22** was prepared following the procedure reported above for compound **15** replacing 2-iodopyridine with 3-fluoroiodobenzene. The crude was purified by silica gel chromatography (SP1® – Biotage) eluting with a gradient of PE – EtOAc from 95:5 to 9:1 to afford **22** (82%) as orange oil. MS (ESI) *m/z* 288.8 $[M+H]^+$. **^{1}H-NMR** (DMSO-d6) *δ*: 7.39-7.46 (m, 1H), 7.26-7.34 (m, 2H), 7.22 (m, 1H), 5.69 (s, 1H), 4.07 (m, 2H), 3.39-3.52 (m, 4H), 2.48-2.57 (m, 2H), 2.30 (m, 2H), 1.20 (m, 3H). HPLC 97.3% (UV).

Ethyl 4-[3-(3-chlorophenyl)prop-2-yn-1-ylidene]piperidine-1-carboxylate (23)

Compound **23** was prepared following the procedure reported above for compound **15** replacing 2-iodopyridine with 3-chloroiodobenzene. The crude was purified by silica gel chromatography (SP1® – Biotage) eluting with a gradient of PE – Et_2O from 6:4 to 5:5 to afford **23** (79%) as brownish oil. MS (ESI) *m/z* 304.7 $[M+H]^+$. **^{1}H-NMR** (DMSO-d6) *δ*: 7.48-7.56 (m, 1H), 7.37-7.47 (m, 3H), 5.69 (s, 1H), 4.07 (m, 2H), 3.40-3.51 (m, 4H), 2.49-2.54 (m, 2H), 2.30 (m, 2H), 1.20 (m, 3H). HPLC 99.0% (UV).

Ethyl 4-[3-(3-cyanophenyl)prop-2-yn-1-ylidene]piperidine-1-carboxylate (24)

Compound **24** was prepared following the procedure reported above for compound **15** replacing 2-iodopyridine with 3-iodobenzonitrile. The crude was purified by silica gel

chromatography (SP1® – Biotage) eluting with a PE – Et_2O 8:2 to afford **24** (82%) as yellowish oil. MS (ESI) *m/z* 295.5 $[M+H]^+$. **^{1}H-NMR** (DMSO-d6) *δ*: 7.96 (m, 1H), 7.82 (m, 1H), 7.77 (m, 1H), 7.59 (m, 1H), 5.71 (s, 1H), 4.07 (m, 2H), 3.38-3.50 (m, 4H), 2.46-2.58 (m, 2H), 2.31 (m, 2H), 1.20 (m, 3H). HPLC 98.5% (UV).

N-*tert*-Butyl-4-[3-(6-methylpyridin-2-yl)prop-2-yn-1-ylidene]piperidine-1-carboxamide (25)

Compound **25** was prepared as described above for compound **9**, replacing *tert*-butylisocyanate for methyl chloroformate. The crude was purified by silica gel chromatography (SP1® - Biotage) eluting with a gradient of PE - EtOAc from 1:0 to 2:8, affording **25**, which was further purified by preparative HPLC, using MS-C18 XTerra column 30x50 mm and eluting with ammonium bicarbonate 20 mM buffer at pH 8 – acetonitrile gradient. Yield: 49%. MS (ESI) *m/z* 312.5 $[M+H]^+$. **^{1}H-NMR** ($CDCl_3$) *δ*: 7.62 (dd, J=7.8, 7.8 Hz, 1H), 7.29 (d, J=7.8 Hz, 1H), 7.13 (d, J=7.8 Hz, 1H), 5.61 (s, 1H), 4.38 (br. s., 1H), 3.36-3.50 (m, 4H), 2.66-2.81 (m, 2H), 2.64 (s, 3H), 2.31-2.42 (m, 2H), 1.38 (s, 9H). HPLC 95.8% (UV).

N-Butyl-4-[3-(6-methylpyridin-2-yl)prop-2-yn-1-ylidene]piperidine-1-carboxamide (26)

Compound **26** was prepared as described for compound **14**, replacing butyl isocyanate for methyl chloroformate. After the usual work-up, **26** was obtained as a brownish solid (91.5%). MS (ESI) *m/z* 312.6 $[M+H]^+$. **^{1}H-NMR** ($CDCl_3$) δ: 7.52-7.86 (m, 1H), 7.33 (d, J=7.8 Hz, 1H), 7.18 (d, J=7.8 Hz, 1H), 5.62 (s, 1H), 4.52 (t, J=6.1 Hz, 1H), 3.42-3.60 (m, 4H), 3.20-3.36 (m, 2H), 2.72-2.85 (m, 2H), 2.69 (s, 3H), 2.30-2.45 (m, 2H), 1.48-1.62 (m, 2H), 1.29-1.45 (m, 2H), 0.95 (t, J=7.2 Hz, 3H). HPLC 95.6% (UV).

4-[3-(6-Methylpyridin-2-yl)prop-2-yn-1-ylidene]-N-[(1S)-1-phenylethyl]piperidine-1-carboxamide (27)

Compound **27** was prepared as described above for compound **14**, replacing (1S)-1-phenylethylisocyanate for methyl chloroformate. The crude was purified by silica gel chromatography (SP1® - Biotage) eluting with a gradient of PE - EtOAc from 1:0 to 2:8, affording **27 (**78%). MS (ESI) *m/z* 360.3 $[M+H]^+$. **^{1}H-NMR** ($CDCl_3$) *δ*: 7.56 (dd, J=7.8, 7.8 Hz, 1H), 7.31-7.40 (m, 4H), 7.20-7.30 (m, 2H), 7.09 (d, J=7.8 Hz, 1H), 5.60 (s, 1H), 5.05 (dq, J=7.0, 7.1 Hz, 1H), 4.76 (d, J=7.0 Hz, 1H), 3.39-3.54 (m, 4H), 2.63-

2.71 (m, 2H), 2.58 (s, 3H), 2.29-2.41 (m, 2H), 1.52 ppm (d, J=7.1 Hz, 3H). HPLC 97.3% (UV).

N-*tert*-Butyl-N-methyl-4-[3-(6-methylpyridin-2-yl)prop-2-yn-1-ylidene]piperidine-1-carboxamide (28)

Compound **28** was synthesized following the procedure reported above for compound **18** replacing N-*tert*-butyl-N-methylamine for cyclobutanemethanol. The crude was purified by silica gel chromatography (Horizon® - Biotage) eluting with a gradient of PE - EtOAc from 7:3 to 4:6, affording **28** (58.7%). MS (ESI) *m/z* 326.2 $[M+H]^+$. **^{1}H-NMR** ($CDCl_3$) δ: 7.56 (dd, J=7.8, 7.8 Hz, 1H), 7.27 (d, J=7.8 Hz, 1H), 7.09 (d, J=7.8 Hz, 1H), 5.59 (s, 1H), 3.27-3.51 (m, 4H), 2.79 (s, 3H), 2.61-2.69 (m, 2H), 2.59 (s, 3H), 2.30-2.41 (m, 2H), 1.34 (s, 9H). HPLC 96.2% (UV).

N-Butyl-N-methyl-4-[3-(6-methylpyridin-2-yl)prop-2-yn-1-ylidene]piperidine-1-carboxamide (29)

Compound **29** was synthesized following the procedure reported above for compound **18** replacing N-butyl-N-methylamine for cyclobutanemethanol. The crude was purified by silica gel chromatography (Horizon® - Biotage) eluting with a gradient of PE - EtOAc

from 5:5 to 4:6, affording **29** (28%). MS (ESI) *m/z* 326.2 $[M+H]^+$. **^{1}H-NMR** ($CDCl_3$) *δ*: 7.65 (dd, J=7.8, 7.8 Hz, 1H), 7.32 (d, J=7.8 Hz, 1H), 7.15 (d, J=7.8 Hz, 1H), 5.60 (s, 1H), 3.26-3.36 (m, 4H), 3.16-3.24 (m, 2H), 2.86 (s, 3H), 2.68-2.73 (m, 2H), 2.67 (s, 3H), 2.35-2.41 (m, 2H), 1.50-1.62 (m, 2H), 1.25-1.40 (m, 2H), 0.95 (t, J=7.3 Hz, 3H). HPLC 95.4% (UV).

N-Methyl-4-[3-(6-methylpyridin-2-yl)prop-2-yn-1-ylidene]-N-(1-phenylethyl)piperidine-1-carboxamide (30)

Compound **30** was synthesized following the procedure reported above for compound **18** replacing N-(1-phenylethyl)-N-methylamine for cyclobutanemethanol. The crude was purified by silica gel chromatography (Horizon® - Biotage) eluting with PE - EtOAc 6:4, affording **30** as white solid (66%). MS (ESI) *m/z* 374.2 $[M+H]^+$. **^{1}H-NMR** ($CDCl_3$) *δ*: 7.74 (dd, J=7.8, 7.8 Hz, 1H), 7.32-7.41 (m, 5H), 7.25-7.31 (m, 1H), 7.21 (d, J=7.8 Hz, 1H), 5.63 (s, 1H), 5.30 (q, J=7.2 Hz, 1H), 3.27-3.42 (m, 4H), 2.70-2.83 (m, 5H), 2.62 (s, 3H), 2.38-2.47 (m, 2H), 1.58 (d, J=7.2 Hz, 3H). HPLC 95.3% (UV).

N-Ethyl-4-[3-(6-methylpyridin-2-yl)prop-2-yn-1-ylidene]-N-(propan-2-yl)piperidine-1-carboxamide (31)

Compound **31** was synthesized following the procedure reported above for compound **18** replacing N-isopropyl-N-ethylamine for cyclobutanemethanol. The crude was purified by silica gel chromatography (Horizon® - Biotage) eluting with PE - EtOAc 4:6, affording **31** as brownish dense oil (63%). MS (ESI) *m/z* 391.6 $[M+H]^+$. **^{1}H-NMR** ($CDCl_3$) *δ*: 7.54 (dd, J=7.8 Hz, 1H), 7.26 (d, J=7.8, 7.8 Hz, 1H), 7.08 (d, J=7.8 Hz, 1H), 5.58 (s, 1H), 3.84 (spt, J=6.7 Hz, 1H), 3.24-3.36 (m, 4H), 3.14 (q, J=7.1 Hz, 2H), 2.63-2.72 (m, 2H), 2.58 (s, 3H), 2.33-2.41 (m, 2H), 1.19 (d, J=6.7 Hz, 6H), 1.11 (t, J=7.1 Hz, 3H). HPLC 97.1% (UV).

(3*E*)-N-Methyl-3-[3-(6-methylpyridin-2-yl)prop-2-yn-1-ylidene]-N-(propan-2-yl)pyrrolidine-1-carboxamide (32)

To a solution of compound **12c** (93 mg, 0.469 mmol) and TEA (150 mL, 1.08 mmol) in DCM (8 mL) was added 3-methyl-1-[methyl(propan-2-yl)carbamoyl]-1H-imidazol-3-ium iodide (218 mg, 0.704 mmol). The reaction mixture was kept under stirring at rt for 16 h. Afterwards, water was added and the mixture was extracted with DCM (3x). The combined organic layers were washed with water and dried over Na_2SO_4. Silica gel chromatography (Isolera® - Biotage, SNAP 25 column) eluting with a gradient of DCM

- EtOAc from 6:4 to 0:1 afforded 74 mg (53%)of **32**. MS (ESI) *m/z* 298.1 $[M+H]^+$. **^{1}H-NMR** ($CDCl_3$) *δ*: 7.56 (dd, J=7.8, 7.8 Hz, 1H), 7.27 (d, J=7.8 Hz, 1H), 7.10 (d, J=7.8 Hz, 1H), 5.71 (quin, J=2.2 Hz, 1H), 4.08-4.20 (m, 3H), 3.52-3.60 (m, 2H), 2.84-2.91 (m, 2H), 2.72 (s, 3H), 2.59 (s, 3H), 1.17 (d, J=6.6 Hz, 6H). HPLC 95.4% (UV).

(3*E*)-N-Ethyl-3-[3-(6-methylpyridin-2-yl)prop-2-yn-1-ylidene]-N-(propan-2-yl)pyrrolidine-1-carboxamide (33)

Compound **33** was synthesized following the procedure reported above for compound **18** replacing N-ethyl-N-isopropylamine for cyclobutanemethanol and **12c** for **14a**. The crude was purified by silica gel chromatography (Isolera HP® - Biotage) eluting with a gradient of PE - EtOAc from 8:2 to 4:6, affording **33** (50%) as yellow-white solid. MS (ESI) *m/z* 312.3 $[M+H]^+$. **^{1}H-NMR** ($CDCl_3$) *δ*: 7.58 (dd, J=7.8, 7.8 Hz, 1H), 7.28 (d, J=7.8 Hz, 1H), 7.11 (d, J=7.8 Hz, 1H), 5.72 (s, 1H), 4.15 (s, 2H), 3.95 (spt, J=6.8 Hz, 1H), 3.52-3.61 (m, 2H), 3.15 (q, J=7.0 Hz, 2H), 2.84-2.91 (m, 2.60 (s, 3H), 1.19 (d, J=6.8 Hz, 6H), 1.12 (t, J=7.0 Hz, 3H). HPLC 95.4% (UV).

1-{4-[3-(6-Methylpyridin-2-yl)prop-2-yn-1-ylidene]piperidin-1-yl}butan-1-one (34)

To a solution of 2-methyl-6-[3-(piperidin-4-ylidene)prop-1-yn-1-yl]pyridine (**14a**) (220 mg, 1.04 mmol) and TEA (164 µL, 1.14 mmol) in 10 mL of DCM was added dropwise under stirring butyryl chloride (119 µL, 1.12 mmol). After 30 min. the reaction mixture was poured into water and extracted with DCM (3x), drying the combined organic layers with Na_2SO_4. Evaporation gave a crude residue that was purified by silica gel chromatography (Isolera® - Biotage) eluting with a gradient of PE - EtOAc from 9:1 to 1.5:8.5 affording 240 mg (82%) of **34**. MS (ESI) *m/z* 383.17 $[M+H]^+$. **^{1}H-NMR** ($CDCl_3$) *δ*: 7.55 (dd, J=7.8, 7.8 Hz, 1H), 7.22-7.27 (m, 1H), 7.09 (d, J=7.8 Hz, 1H), 5.62 (s, 1H), 3.63-3.77 (m, 2H), 3.44-3.59 (m, 2H), 2.59-2.71 (m, 2H), 2.57 (s, 3H), 2.25-2.45 (m, 4H), 1.68-1.74 (m, 2H), 1.00 (t, J=7.3 Hz, 3H). HPLC 98.2% (UV).

3,3-Dimethyl-1-{4-[3-(6-methylpyridin-2-yl)prop-2-yn-1-ylidene]piperidin-1-yl}butan-1-one (35)

To a solution of 3,3-dimethylbutyric acid (47.4 mg, 0.4 mmol) in 5 mL of DCM - DMF (4:1) stirred at a 0-5°C was added 1-hydroxybenzotriazole (80.8 mg, 0.52 mmol) and, after 30 min, EDC (100 mg, 0.52 mmol). After further 30 min stirring, was added 2-methyl-6-[3-(piperidin-4-ylidene)prop-1-yn-1-yl]pyridine(**14a**) (84.9 mg, 0.4 mmol).

The reaction mixture was stirred for further 2 h, then kept overnight resting. Water was then added and the pH made alkaline by addition of 1N NaOH. The organic layer was separated, washed with brine and dried over Na_2SO_4. Evaporation gave a crude residue that was purified by silica gel chromatography (Isolera® - Biotage) eluting with $CHCl_3$ - 1.8 N methanolic ammonia 100:0.02 affording **35** (93 mg, 75%) as ivory solid. MS (ESI) *m/z* 311.2 $[M+H]^+$. **^{1}H-NMR** ($CDCl_3$) *δ*: 7.55 (dd, J=7.8, 7.8 Hz, 1H), 7.25 (d, J=7.8 Hz, 1H), 7.10 (d, J=7.8 Hz, 1H), 5.63 (s, 1H), 3.64-3.76 (m, 2H), 3.53-3.63 (m, 2H), 2.60-2.72 (m, 2H), 2.58 (s, 3H), 2.27-2.40 (m, 4H), 1.09 (s, 9H). HPLC 98.3% (UV).

2-Methoxy-1-{4-[3-(6-methylpyridin-2-yl)prop-2-yn-1-ylidene]piperidin-1-yl}ethanone (36)

Compound **36** was synthesized following the procedure reported above for compound **35** replacing 2-methoxyacetic acid for 3,3-dimethylbutyric acid. The crude was purified by silica gel chromatography (Isolera® - Biotage) eluting with $CHCl_3$ - 1.8 N methanolic ammonia 100:0.05 affording **36** (70%)as yellowish-green oil. MS (ESI) *m/z* 285.2 $[M+H]^+$. **^{1}H-NMR** ($CDCl_3$) *δ*: 7.56 (dd, J=7.8, 7.8 Hz, 1H), 7.26 (d, J=7.8 Hz, 1H), 7.10

(d, J=7.8 Hz, 1H), 5.64 (s, 1H), 4.16 (s, 2H), 3.63-3.74 (m, 2H), 3.49-3.59 (m, 2H), 3.46 (s, 3H), 2.62-2.74 (m, 2H), 2.58 (s, 3H), 2.32-2.43 (m, 2H). HPLC 99.0% (UV).

1-{4-[3-(6-Methylpyridin-2-yl)prop-2-yn-1-ylidene]piperidin-1-yl}-2-(pyrrolidin-1-yl)ethanone (37)

To a solution of 1-pyrrolidineacetic acid (136 mg, 1.05 mmol) in 15 mL of DCM was added PS-carbodiimide (980 mg, 1.39 mmol) stirring at rt for 20 min. A solution of 2-methyl-6-[3-(piperidin-4-ylidene)prop-1-yn-1-yl]pyridine (149 mg, 0.7 mmol) in 10 mL of DCM was the added. Stirring was continued for 16 h at rt. The resin was filtered on paper, washed with DCM, which was evaporated to dryness *in vacuo*. The crude residue was purified by silica gel chromatography (Isolera® -Biotage) eluting with $CHCl_3$ - 1.8 N methanolic ammonia 100:1 to 100:3 to afford **37** (66 mg, 30%, yellowish oil). MS (ESI) *m/z* 324.4 $[M+H]^+$. **^{1}H-NMR** ($CDCl_3$) δ: 7.55 (dd, J=7.8, 7.8 Hz, 1H), 7.26 (d, J=7.8 Hz, 1H), 7.10 (d, J=7.8 Hz, 1H), 5.63 (s, 1H), 3.55-3.73 (m, 4H), 3.44 (s, 2H), 2.60-2.78 (m, 6H), 2.58 (s, 3H), 2.29-2.41 (m, 2H), 1.79-1.91 (m, 4H). HPLC 95.4% (UV).

1-{4-[3-(6-Methylpyridin-2-yl)prop-2-yn-1-ylidene]piperidin-1-yl}-2-phenylethanone (38)

Compound **38** was synthesized following the procedure reported above for compound **37** replacing 2-phenylacetic acid for 1-pyrrolidineacetic acid. The crude was purified by silica gel chromatography (Isolera® - Biotage) eluting with $CHCl_3$ - 1.8 N methanolic ammonia 100:0.2 affording **38** (80.4%, ivory solid). MS (ESI) *m/z* 331.2 $[M+H]^+$. **^{1}H-NMR** ($CDCl_3$) *δ*: 7.68 (dd, J=7.8, 7.8 Hz, 1H), 7.24-7.43 (m, 6H), 7.20 (d, J=7.8 Hz, 1H), 5.60 (s, 1H), 3.80 (s, 2H), 3.65-3.76 (m, 2H), 3.41-3.61 (m, 2H), 2.46-2.82 (m, 5H), 1.93-2.40 (m, 2H). HPLC 98.3% (UV).

2-(3,5-Difluorophenyl)-1-{4-[3-(6-methylpyridin-2-yl)prop-2-yn-1-ylidene]piperidin-1-yl}ethanone (39)

Compound **39** was synthesized following the procedure reported above for compound **35** replacing 3,5-difluorophenylacetic acid for 3,3-dimethylbutyric acid. The crude was purified by silica gel chromatography (Isolera® - Biotage) eluting with $CHCl_3$ - 1.8 N methanolic ammonia 100:0.03 to afford **39** (79.1%, ivory solid). MS (ESI) *m/z* 367.23 $[M+H]^+$. **^{1}H-NMR** ($CDCl_3$) *δ*: 7.58 (dd, J=7.8, 7.8 Hz, 1H), 7.27 (d, J=7.8 Hz, 1H), 7.11

(d, J=7.8 Hz, 1H), 6.79-6.91 (m, 2H), 6.65-6.77 (m, 1H), 5.62 (s, 1H), 3.76 (s, 2H), 3.61-3.75 (m, 2H), 3.46-3.61 (m, 2H), 2.49-2.79 (m, 5H), 2.09-2.41 (m, 2H). HPLC 91.9% (UV).

{4-[3-(6-Methylpyridin-2-yl)prop-2-yn-1-ylidene]piperidin-1-yl}(phenyl)methanone (40)

Compound **40** was synthesized following the procedure reported above for compound **34** replacing benzoyl chloride for butyryl chloride. The crude was purified by silica gel chromatography (Isolera® - Biotage) eluting with a gradient of PE - EtOAc from 1:0 to 2:8, to afford **40** (72%, oil). MS (ESI) *m/z* 317.6 $[M+H]^+$. **^{1}H-NMR** ($CDCl_3$) *δ*: 7.66-7.57 (m, 1H), 7.47-7.40 (m, 5H), 7.33-7.25 (m, 1H), 7.17-7.11 (m, 1H), 5.66 (s, 1H), 3.86-3.38 (m, 4H), 2.82-2.65 (m, 2H), 2.63 (s, 3H), 2.54-2.25 (m, 2H). HPLC 96.5% (UV).

(2-Methoxyphenyl){4-[3-(6-methylpyridin-2-yl)prop-2-yn-1-ylidene]piperidin-1-yl}methanone (41)

Compound **41** was synthesized following the procedure reported above for compound **35** replacing 2-methoxybenzoic acid for 3,3-dimethylbutyric acid. The crude was purified by silica gel chromatography (Isolera® - Biotage) eluting with $CHCl_3$ - 1.8 N methanolic ammonia 100:0.03 affording **41** (90.4%, oil). MS (ESI) *m/z* 347 $[M+H]^+$. **^{1}H-**

NMR ($CDCl_3$) *δ*: 7.71 (dd, J=7.8, 7.8 Hz, 1H), 7.31-7.46 (m, 2H), 7.27 (d, J=7.8 Hz, 1H), 7.20 (d, J=7.8 Hz, 1H), 6.98-7.06 (m, 1H), 6.89-6.97 (m, 1H), 5.66 (s, 1H), 3.86 (s, 3H), 3.72-4.02 (m, 2H), 3.19-3.53 (m, 2H), 2.64-2.86 (m, 5H), 2.12-2.56 (m, 2H). HPLC 95.7% (UV).

(3-Methoxyphenyl){4-[3-(6-methylpyridin-2-yl)prop-2-yn-1-ylidene]piperidin-1-yl}methanone (42)

Compound **42** was synthesized following the procedure reported above for compound **35** replacing 3-methoxybenzoic acid for 3,3-dimethylbutyric acid. The crude was purified by silica gel chromatography (Isolera® - Biotage) eluting with $CHCl_3$ - 1.8 N methanolic ammonia 100:0.03, affording **42** (55.8%, oil). MS (ESI) *m/z* 347.18 $[M+H]^+$. **^{1}H-NMR** ($CDCl_3$) *δ*: 7.65-7.88 (m, 1H), 7.30-7.41 (m, 2H), 7.22 (d, J=7.8 Hz, 1H), 6.92-7.03 (m, 3H), 5.68 (s, 1H), 3.85 (s, 3H), 3.30-3.89 (m, 4H), 2.75 (s, 3H), 2.17-2.85 (m, 4H). HPLC 95.4% (UV).

(4-Methoxyphenyl){4-[3-(6-methylpyridin-2-yl)prop-2-yn-1-ylidene]piperidin-1-yl}methanone (43)

Compound **43** was synthesized following the procedure reported above for compound **35** replacing 4-methoxybenzoic acid for 3,3-dimethylbutyric acid. The crude was purified by silica gel chromatography (Isolera® - Biotage) eluting with $CHCl_3$ - 1.8 N methanolic ammonia 100:0.05 to afford **43** (91.4%) as clear yellow oil. MS (ESI) *m/z* 347.1 $[M+H]^+$. **^{1}H-NMR** ($CDCl_3$) *δ*: 7.55 (dd, J=7.8, 7.8 Hz, 1H), 7.38-7.48 (m, 2H), 7.25 (d, J=7.8 Hz, 1H), 7.09 (d, J=7.8 Hz, 1H), 6.89-6.99 (m, 2H), 5.64 (s, 1H), 3.86 (s, 3H), 3.51-3.83 (m, 4H), 2.60-2.78 (m, 2H), 2.58 (s, 3H), 2.28-2.48 (m, 2H). HPLC 96.9% (UV).

(3-Methylphenyl){4-[3-(6-methylpyridin-2-yl)prop-2-yn-1-ylidene]piperidin-1-yl}methanone (44)

Compound **44** was synthesized following the procedure reported above for compound **37** replacing 3-methylbenzoic acid for 1-pyrrolidineacetic acid. The crude was purified by silica gel chromatography (Isolera® - Biotage) eluting with $CHCl_3$ - 1.8 N methanolic ammonia 100:0.2 to afford **44** (70.4%, yellow solid). MS (ESI) *m/z* 331.42 $[M+H]^+$. **^{1}H-NMR** ($CDCl_3$) *δ*: 7.55 (dd, J=7.8, 7.8 Hz, 1H), 7.18-7.39 (m, 5H), 7.10 (d, J=7.8 Hz,

1H), 5.65 (s, 1H), 3.33-3.99 (m, 4H), 2.58 (br. s., 3H), 2.40 (s, 3H), 2.16-2.86 (m, 4H). HPLC 95.1% (UV).

(3-Fluorophenyl){4-[3-(6-methylpyridin-2-yl)prop-2-yn-1-ylidene]piperidin-1-yl}methanone (45)

Compound **45** was synthesized following the procedure reported above for compound **37** replacing 3-fluorobenzoic acid for 1-pyrrolidineacetic acid. The crude was purified by silica gel chromatography (Isolera® - Biotage) eluting with $CHCl_3$ - 1.8 N methanolic ammonia 100:0.2 to afford **45** (77.5%, pale yellow oil). MS (ESI) *m/z* 335.34 $[M+H]^+$. **^{1}H-NMR** ($CDCl_3$) δ: 7.74-7.86 (m, 2H), 7.56 (dd, J=7.8, 7.8 Hz, 1H), 7.36-7.45 (m, 1H), 7.28 (d, J=7.8 Hz, 1H), 7.14-7.21 (m, 1H), 7.11 (d, J=7.8 Hz, 1H), 5.66 (s, 1H), 3.29-4.00 (m, 4H), 2.59 (s, 3H), 2.25-2.83 (m, 4H). HPLC 95.6% (UV).

(3-Chlorophenyl){4-[3-(6-methylpyridin-2-yl)prop-2-yn-1-ylidene]piperidin-1-yl}methanone (46)

Compound **46** was synthesized following the procedure reported above for compound **35** replacing 3-chlorobenzoic acid for 3,3-dimethylbutyric acid. The crude was purified by silica gel chromatography (Isolera® - Biotage) eluting with $CHCl_3$ - 1.8 N methanolic

ammonia 100:0.3 to give **46** (80.8%) as a yellowish-green oil. MS (ESI) *m/z* 351.22 $[M+H]^+$. **^{1}H-NMR** ($CDCl_3$) *δ*: 7.59-7.85 (m, 1H), 7.30-7.47 (m, 5H), 7.19 (d, J=7.8 Hz, 1H), 5.68 (br. s., 1H), 3.24-4.04 (m, 4H), 2.69 (s, 3H), 2.69 (s, 4H). HPLC 95.3% (UV).

tert-Butyl 4-[3-(3-chlorophenyl)prop-2-yn-1-ylidene]piperidine-1-carboxylate (47a)

Prepared by reaction of *tert*-butyl 4-[3-(trimethylsilyl)prop-2-yn-1-ylidene]piperidine-1-carboxylate[30] and 3-chloroiodobenzene (instead of 2-bromo-6-methylpyridine) following the procedure reported above for Compound **13c**. Purification of the crude by silica gel chromatography (Horizon® – Biotage) eluting with a PE – EtOAc gradient from 95:5 to 85:15 afforded **47a** as brownish oil (80.2%) which was used in the next step without further purification.

4-[3-(3-chlorophenyl)prop-2-yn-1-ylidene]piperidine (47b)

Prepared following the procedure described above for Compound **10c** starting from compound **47a** and used without further purification in the next step. **^{1}H-NMR** ($CDCl_3$) *δ*: 7.41-7.46 (m, 1H), 7.18-7.36 (m, 3H), 5.50 (s, 1H), 2.89-3.06 (m, 4H), 2.53-2.64 (m, 2H), 2.28-2.37 (m, 2H).

(3-Chlorophenyl){4-[3-(3-chlorophenyl)prop-2-yn-1-ylidene]piperidin-1-yl}methanone (47)

Compound **47** was synthesized following the procedure reported above for compound **37** replacing 3-methylbenzoic acid for pyrrolidineacetic acid. The crude was purified by automated flash chromatography (Isolera® - Biotage) eluting with PE - EtOAc 8:2. The collected fractions containing the title compound were further purified eluting with a PE - *tert*-Butyl methyl ether gradient from 65:35 to 50:50 to give **47** (12.7%). MS (ESI) *m/z* 371.2 $[M+H]^+$. **^{1}H-NMR** ($CDCl_3$) *δ*: 7.21-7.49 (m, 8H), 5.63 (br. s., 1H), 3.36-4.00 (m, 4H), 2.24-2.82 (m, 4H). HPLC 95.2% (UV).

(3-Chlorophenyl){(3*E*)-3-[3-(6-methylpyridin-2-yl)prop-2-yn-1-ylidene]pyrrolidin-1-yl}methanone (48)

Compound **48** was prepared following the procedure reported above for compound **11** starting from compound **12c** instead of compound **11c** and replacing 3-chlorobenzoyl chloride for ethyl chloroformate. The reaction crude was purified by silica gel chromatography (SP1® - Biotage) eluting with EtOAc to yield **48** (82%, yellowish solid). MS (ESI) *m/z* 337.9 $[M+H]^+$. **^{1}H-NMR** (DMSO-d6) *δ*: 7.67 (dd, J=7.8, 7.8 Hz, 1H), 7.41-

7.61 (m, 4H), 7.31 (d, J=7.8 Hz, 1H), 7.22 (d, J=7.8 Hz, 1H), 5.88 (s, 1H), 4.12-4.46 (m, 2H), 3.48-3.86 (m, 2H), 2.81-2.90 (m, 2H), 2.46 (s, 3H). HPLC 95.9% (UV).

Furan-2-yl{(3*E*)-3-[3-(6-methylpyridin-2-yl)prop-2-yn-1-ylidene]pyrrolidin-1-yl}methanone (49)

Compound **49** was prepared following the procedure reported above for compound **11** starting from compound **12c** instead of compound **11c** and replacing 2-furoyl chloride for ethyl chloroformate. The reaction crude was purified by RP flash chromatography (Isolera® - Biotage) eluting with MeCN – ammonium formate buffer 40:60, affording **49** (62%) as yellowish dense oil. MS (ESI) *m/z* 293.1 $[M+H]^+$. **^{1}H-NMR** ($CDCl_3$) *δ*: 7.52-7.64 (m, 2H), 7.25-7.34 (m, 1H), 7.07-7.18 (m, 2H), 6.49-6.58 (m, 1H), 5.82 (br. s, 1H), 4.36-4.77 (m, 2H), 3.81-4.21 (m, 2H), 2.90-3.18 (m, 2H), 2.59 (s, 3H). HPLC 95.5% (UV).

2-{3-[1-(Ethylsulfonyl)piperidin-4-ylidene]prop-1-yn-1-yl}-6-methylpyridine (50)

A solution of compound **14a** (89 mg, 0.42 mmol) and ethanesulfonyl chloride (90 µL, 0.95 mmol) in chloroform (5 mL) was stirred at rt for 1 h. Afterwards, the reaction mixture was washed with 0.1 N NaOH, then with water, drying the organic layer over

Na_2SO_4 and evaporating to dryness *in vacuo*. The crude residue was purified by silica gel chromatography (Isolera® - Biotage) eluting with PE - EtOAc 1:1 giving 58 mg (37.5%) of **50**. MS (ESI) *m/z* 305.22 $[M+H]^+$. **^{1}H-NMR** ($CDCl_3$) *δ*: 7.65 (dd, J=7.8, 7.8 Hz, 1H), 7.30 (d, J=7.8 Hz, 1H), 7.16 (d, J=7.8 Hz, 1H), 5.65 (s, 1H), 3.32-3.51 (m, 4H), 3.00 (q, J=7.5 Hz, 2H), 2.75-2.89 (m, 2H), 2.66 (s, 3H), 2.39-2.52 (m, 2H), 1.39 (t, J=7.5 Hz, 3H). HPLC 95.1% (UV).

2-(3-{1-[(Cyclohexylmethyl)sulfonyl]piperidin-4-ylidene}prop-1-yn-1-yl)-6-methylpyridine (51)

Compound **51** was obtained (51%) following the procedure reported above for compound **50**, replacing ethanesulfonyl chloride with cyclohexylmethanesulfonyl chloride and purifying the crude residue by silica gel chromatography (Isolera® - Biotage) eluting with PE - EtOAc 7:3. MS (ESI) *m/z* 373.28 $[M+H]^+$. **^{1}H-NMR** ($CDCl_3$) *δ*: 7.72 (dd, J=7.8, 7.8 Hz, 1H), 7.36 (d, J=7.8 Hz, 1H), 7.21 (d, J=7.8 Hz, 1H), 5.66 (s, 1H), 3.29-3.50 (m, 4H), 2.82-2.93 (m, 2H), 2.75-2.8 (m, 2H), 2.72 (s, 3H), 2.41-2.54 (m, 2H), 1.61-2.02 (m, 5H), 0.98-1.42 (m, 6H). HPLC 95.6% (UV).

2-{3-[1-(Benzylsulfonyl)piperidin-4-ylidene]prop-1-yn-1-yl}-6-methylpyridine (52)

Compound **52** was obtained (59.3%) following the procedure reported above for compound **50**, replacing ethanesulfonyl chloride with benzylsulfonyl chloride and purifying the crude residue by silica gel chromatography (Isolera® - Biotage) eluting with PE - EtOAc 6:4. MS (ESI) *m/z* 367.7 $[M+H]^+$. **^{1}H-NMR** ($CDCl_3$) *δ*: 7.57 (dd, J=7.8, 7.8 Hz, 1H), 7.36-7.46 (m, 5H), 7.25 (d, J=7.8 Hz, 1H), 7.12 (d, J=7.8 Hz, 1H), 5.57 (s, 1H), 4.25 (s, 2H), 3.07-3.30 (m, 4H), 2.61 (s, 3H), 2.54-2.72 (m, 2H), 2.25-2.38 (m, 2H). HPLC 97.7% (UV).

2-Methyl-6-{3-[1-(phenylsulfonyl)piperidin-4-ylidene]prop-1-yn-1-yl}pyridine (53)

Compound **53** was obtained (46.6%) following the procedure reported above for compound **50**, replacing ethanesulfonyl chloride with phenylsulfonyl chloride and purifying the crude residue by silica gel chromatography (Isolera® - Biotage) eluting with PE - EtOAc. MS (ESI) *m/z* 353.2 $[M+H]^+$. **^{1}H-NMR** ($CDCl_3$) *δ*: 7.76-7.88 (m, 2H), 7.71 (dd, J=7.8 Hz, 1H), 7.59-7.66 (m, 1H), 7.48-7.58 (m, 2H), 7.32 (d, J=7.8 Hz, 1H), 7.20 (d, J=7.8 Hz, 1H), 5.57 (s, 1H), 3.09-3.28 (m, 4H), 2.77-2.89 (m, 2H), 2.71 (s, 3H), 2.37-2.55 (m, 2H). HPLC 95.9% (UV).

2-(3-{1-[(3-Bromophenyl)sulfonyl]piperidin-4-ylidene}prop-1-yn-1-yl)-6-methylpyridine (54)

Compound **54** was obtained (64.4%) following the procedure reported above for compound **50** replacing ethanesulfonyl chloride with 3-bromobenzenesulfonyl chloride and purifying the crude residue by silica gel chromatography (Isolera® - Biotage) eluting with PE - EtOAc 6:4. MS (ESI) *m/z* 433.03 $[M+H]^+$. **^{1}H-NMR** ($CDCl_3$) *δ*: 7.93 (s, 1H), 7.66-7.81 (m, 2H), 7.54 (dd, J=7.8, 7.8 Hz, 1H), 7.38-7.47 (m, 1H), 7.23 (d, J=7.8 Hz, 1H), 7.09 (d, J=7.8 Hz, 1H), 5.57 (s, 1H), 3.11-3.28 (m, 4H), 2.71-2.81 (m, 2H), 2.57 (s, 3H), 2.37-2.51 (m, 2H). HPLC 99.2% (UV).

2-(3-{1-[(4-Methylphenyl)sulfonyl]piperidin-4-ylidene}prop-1-yn-1-yl)-6-methylpyridine (55)

Compound **55** was obtained (71%) following the procedure reported above for compound **50**, replacing ethanesulfonyl chloride with 4-methylphenylsulfonyl chloride and purifying the crude residue by silica gel chromatography (Isolera® - Biotage) eluting with PE-EtOAc 1:1. MS (ESI) *m/z* 367.13 $[M+H]^+$. **^{1}H-NMR** ($CDCl_3$) *δ*: 7.60-7.73 (m, 3H), 7.30-7.39 (m, 2H), 7.25-7.30 (m, 1H), 7.10-7.23 (m, 1H), 5.55 (s, 1H),

3.07-3.25 (m, 4H), 2.74-2.87 (m, 2H), 2.67 (s, 3H), 2.44 (s, 3H), 2.39-2.50 (m, 2H). HPLC 96.6% (UV).

2-(3-{1-[(4-Methoxyphenyl)sulfonyl]piperidin-4-ylidene}prop-1-yn-1-yl)-6-methylpyridine (56)

Compound **56** was obtained (36%) following the procedure reported above for compound **50**, replacing ethanesulfonyl chloride with 4-methoxybenzenesulfonyl chloride and purifying the crude residue by silica gel chromatography (Isolera® - Biotage) eluting with PE-EtOAc 1:1. MS (ESI) *m/z* 383.15 $[M+H]^+$. **^{1}H-NMR** ($CDCl_3$) δ: 7.69-7.78 (m, 2H), 7.66 (dd, J=7.8, 7.8 Hz, 1H), 7.29 (d, J=7.8 Hz, 1H), 7.16 (d, J=7.8 Hz, 1H), 6.96-7.06 (m, 2H), 5.55 (s, 1H), 3.89 (s, 3H), 3.06-3.21 (m, 4H), 2.74-2.83 (m, 2H), 2.66 (s, 3H), 2.39-2.49 (m, 2H). HPLC 97.0% (UV).

4-({4-[3-(6-Methylpyridin-2-yl)prop-2-yn-1-ylidene]piperidin-1-yl}sulfonyl)benzonitrile (57)

Compound **57** was obtained (59.6%) following the procedure reported above for compound **50**, replacing ethanesulfonyl chloride with 4-cyanobenzenesulfonyl chloride and purifying the crude residue by silica gel chromatography (Isolera® -

Biotage) eluting with PE - EtOAc 1:1. MS (ESI) *m/z* 378 $[M+H]^+$. **^{1}H-NMR** ($CDCl_3$) *δ*: 7.88-7.95 (m, 2H), 7.81-7.88 (m, 2H), 7.71 (dd, J=7.8, 7.8 Hz, 1H), 7.33 (d, J=7.8 Hz, 1H), 7.22 (d, J=7.8 Hz, 1H), 5.59 (s, 1H), 3.13-3.31 (m, 4H), 2.81-2.94 (m, 2H), 2.72 (s, 3H), 2.41-2.54 (m, 2H). HPLC 95.0% (UV).

2-[3-(1-Butylpiperidin-4-ylidene)prop-1-yn-1-yl]-6-methylpyridine (58)

A suspension of compound **14a** (220 mg, 1.04 mmol), butyraldehyde (127 µl, 1.41mmol), sodium triacetoxyborohydride (331 mg, 1.56 mmol) in 15 mL of DCM was stirred at rt for 1.5 h. The reaction mixture was diluted with brine, extracted with DCM, which was dried over Na_2SO_4 and evaporated to dryness *in vacuo*. The crude residue was purified by silica gel chromatography (Isolera® - Biotage) eluting with a gradient of PE - EtOAc containing 10% of 1.8N methanolic ammonia from 9:1 to 3:7 to give 279 mg (33.3%) of **58**. MS (ESI) *m/z* 269.3 $[M+H]^+$. **^{1}H-NMR** ($CDCl_3$) *δ*: 7.54 (dd, *J*=7.8, 7.8 Hz, 1 H), 7.25 (d, *J*=7.8 Hz, 1 H), 7.08 (d, *J*=7.8 Hz, 1 H), 5.56 (s, 1 H), 2.57 (s, 3 H), 2.26 - 2.93 (m, 10 H), 1.51 - 1.75 (m, 2 H), 1.29 - 1.44 (m, 2 H), 0.96 (t, *J*=7.3 Hz, 3 H). HPLC 95.4% (UV).

2-[3-(1-Benzylpiperidin-4-ylidene)prop-1-yn-1-yl]-6-methylpyridine (59)

Compound **59** was synthesized (33%)following the procedure reported above for compound **58**, replacing butyraldehyde with benzaldehyde and purifying the crude residue by silica gel chromatography (Isolera® - Biotage) eluting with PE - EtOAc 1:1. MS (ESI) *m/z* 303.2 $[M+H]^+$. **^{1}H-NMR** ($CDCl_3$) *δ*: 7.53 (dd, J=7.8, 7.8 Hz, 1 H), 7.27 - 7.46 (m, 5 H), 7.23 (d, J=7.8 Hz, 1 H), 7.07 (d, J=7.8 Hz, 1 H), 5.53 (s, 1 H), 3.64 (s, 2 H), 2.56 (s, 3 H), 2.29 - 2.81 (m, 8 H). HPLC 97.8% (UV).

2-{4-[3-(6-Methylpyridin-2-yl)prop-2-yn-1-ylidene]piperidin-1-yl}cyclopent-2-en-1-one (60)

To a suspension of compound **14a** (737 mg, 3.48 mmol) in DMA (10 mL) stirred at rt was added DIEA (0.790 mL, 4.52 mmol) then 2-chlorocyclopentanone (0.383 mL, 3.83 mmol). The reaction mixture was stirred at rt for 2 days, then was poured into water, extracted with EtOAc (3x), which was washed with brine, dried over Na_2SO_4 and evaporated to dryness: The crude was purified by silica gel liquid chromatography (Horizon® – Biotage) eluting with EtOAc and 1.8 N methanolic ammonia 1:0.01. Re-purification eluting with DCM – MeOH 10:0.15 afforded 155 mg (15.1%) of **60**. MS (ESI) *m/z* 293.3 $[M+H]^+$. **^{1}H-NMR** ($CDCl_3$) *δ*: 7.55 (dd, J=7.8, 7.8 Hz, 1H), 7.26 (d,

J=7.8 Hz, 1H), 7.09 (d, J=7.8 Hz, 1H), 6.43 (s, 1H), 5.57 (s, 1H), 3.13-3.25 (m, 4H), 2.69-2.78 (m, 2H), 2.58 (s, 3H), 2.50-2.56 (m, 2H), 2.44-2.49 (m, 2H), 2.38-2.44 (m, 2H). HPLC 95.9% (UV).

2-{4-[3-(6-Methylpyridin-2-yl)prop-2-yn-1-ylidene]piperidin-1-yl}-1-(pyrrolidin-1-yl)ethanone (61)

To an orange solution of compound **14a** (106 mg, 0.5 mmol) and TEA (0.718 mL, 0.5 mmol) in DMA (5 mL) stirred at rt, was added 2-bromoacetic acid (91 mg, 0.648 mmol).

To the so obtained solution in DCM containing was added 465 mg (0.66 mmol) of PS-carbodimide (1.42 M) and the mixture was stirred at room temperature for 15 minutes. Pyrrolidine (42 µL, 0.5 mmol) was dripped and the mixtures was stirred 48h at room temperature. The resin was filtered off, washed with DCM. The solution was dried over Na_2SO_4 and evaporated to dryness in vacuo. The crude oil was purified by silica gel chromatography (Isolera®- Biotage) eluting with a gradient of $CHCl_3$ – MeOH from 97:3 to 85:15 affording 28 mg (17.3%) of **61** as yellowish oil. MS (ESI) *m/z* 324.4 $[M+H]^+$. **^{1}H-NMR** ($CDCl_3$) *δ*: 7.53 (dd, J=7.8, 7.8 Hz, 1H), 7.24 (d, J=7.8 Hz, 1H), 7.08 (d, J=7.8 Hz, 1H), 5.54 (s, 1H), 3.48-3.54 (m, 4H), 3.18-3.29 (m, 2H), 2.63-2.85 (m, 6H), 2.57

(s, 3H), 2.38-2.53 (m, 2H), 1.98 (quin, J=6.8 Hz, 2H), 1.88 (quin, J=6.8 Hz, 2H). HPLC 96.8% (UV).

Protein and ligand preparation and binding site analysis

Three crystal structures of $mGlu_5$ (4OO9, 5CGC and 5CGD) were available in the Protein Data Bank (accessed in September 2016).[11,12] While 5CGC and 5CGD structures are very similar, they differ from 4OO9 for the conformation of the Trp785 and Ser809 side chains. In fact, Trp785 was found to adopt an “out” (4OO9) or “in” (5CGC and 5CGD) orientation that affects binding site accessibility and shape. The Ser809 residue provides different hydrogen bond networks in the 4OO9 and 5CGD/5CGC binding sites. Therefore, docking was performed on both 4OO9 and 5CGD, *i.e.* the structure with better resolution between 5CGC and 5CGD. Structures were prepared for docking using the *Protein Preparation Wizard* utility available in Maestro 10.3 of Schrödinger suite.[60,61] First, structures were preprocessed to assign bond orders and to add hydrogen atoms. Then, geometries were optimized applying a threshold of 0.3 Å during the restrained minimization step. All the co-crystallized

ions, solvent and water molecules were removed from the structures except for the water 4126 in the 4OO9 crystal structure and the water molecule 4116 in the 5CGD crystal structure, which participate to a hydrogen bond network in the respective binding sites. Ligands were prepared using *MacroModel* (version 10.9) and *LigPrep* (version 3.5) utilities available in Maestro 10.3 of Schrödinger suite.[62,63] Five conformations per ligand were initially generated, and appropriate ionization state and tautomers evaluated for each conformation at physiological pH. Afterwards, ligand conformations were minimized with the OPLS2005 force field.[64]

Docking calculations for $mGlu_5$ receptor

Docking calculations were performed with the *Induced Fit Docking* (*Glide* version 6.8, *Prime* version 4.1) protocol available in Maestro 10.3 of the Schrödinger suite.[65,66] Receptor grids were centered on the co-crystallized ligands of 4OO9 (mavoglurant) and 5CGD (HTL14242). Receptor grids were generated with default parameters. Induced Fit Docking calculations were performed using default parameters except for the receptor and ligand van der Waals scaling, which were set to 0.8, and the refinement of the top 30 structures within 100 kcal/mol of the best pose. Prime

refinement was performed only by letting residues Asn747, the Trp785 and the Ser809 free to move. Binding modes were selected after visual inspection.

LogP calculations

LogP calculations were performed using the GALAS algorithm of Percepta (ACDlabs). GALAS calculates the LogP predicted value and the Reliability Index value (RI). RI estimate the reliability of the LogP prediction in base to the similarity of the test molecule to the training set molecules. RI was larger than 0,5 for the most of compounds. The only compound with a low RI was compound **11** (RI = 0.19). LE, LipE and LELP, reported in Table S1 (Supporting Information) were calculated according to the formulas reported by Hopkins.[46]

Kinetic solubility determination protocol

Solubility was determined using the following methodology. Test compounds were accurately weighted and dissolved in DMSO to obtain a 100 mM concentration of stock solution. 20 µL of stock solution were diluted to 2000 µL using TRIS HCl buffer at pH 7.4 to obtain a final concentration 1mM of the tested compounds. The samples, in duplicate, were shaken for 4 hours at 36°C. 600 µL of mixture were centrifuged at

9000 rpm for 3 min using Polyvinylidene fluoride (PVDF) spin filter 0.2 µm. 500 µL of filtered solution were diluted to 1mL with HPLC mobile phase (80% acetonitrile in a buffer solution of 20 mM NH_4HCO_3 at pH 8). The concentration of the sample was determined by Waters H-Class UPLC/PAD system running a gradient of 20% - 100% acetonitrile in a buffer solution of 20 mM NH_4HCO_3 at pH 8. Determination of solubility was extrapolated by a regression curve based on successive dilutions prepared at 0.5 mM, 0.05 mM and 0.005 mM from stock solution (100 mM). Solubility results were expressed as µM concentration of the test molecules at pH 7.4 in buffer of TRIS HCl.

Biology

CHO T-REx h-mGlu$_5$ and CHO T-REx r-mGlu$_1$.

Cell lines stably transfected were generated using inducible expression vectors encoding human mGlu$_5$ and rat mGlu$_1$ receptor using the Tetracycline-Regulated Expression system (T-REx^{TM} system, Invitrogen, Life Technologies). Human mGlu$_5$ and rat mGlu$_1$ open reading frame (ORF), comprehensive of the stop codon, were cloned into the pcDNA4/TO/myc-HisTM A vector, carrying the TetO2. The insertion site was respectively HindIII-PstI for mGlu$_5$ and BamH1-XhoI for mGlu$_1$ receptors. The

obtained constructs were then transfected into the T-REx CHO™ cell line using the FuGENE protocol (Roche); the CHO T-REx™ cell line stably expresses the Tet repressor (from the pcDNA6/TR plasmid) under the selection of blasticidin 10 μg/mL. Stable clones were obtained selecting with zeocine 1 mg/mL and maintaining in ULTRA CHO medium (LONZA) supplemented with dialyzed FBS, zeocin, blasticidin, at 37°C, in an atmosphere of 5 % CO_2. The expression of h-$mGlu_5$ and r-$mGlu_1$ receptors was derepressed with 1 μg/mL tetracycline 18 h before binding experiment, while the expression of h-$mGlu_5$ and r-$mGlu_1$ receptors was derepressed respectively with 3 ng/mland 10 ng/mL tetracycline 18h before calcium fluorescence experiment.

Radioligand binding assay at native $mGlu_5$ and cloned $mGlu_1$ and $mGlu_5$ receptor subtypes.

Male Sprague Dawley rats (Crl:CD(SD)BR, 200-300 g bw) from Charles River Italy were used. Animals were housed with free access to food and water and maintained on a forced 12 h light-dark cycle at 22-24°C for at least one week before experiments were carried out. The animals were handled according to internationally accepted principles for care of laboratory animals (E.E.C. Council Directive 86/609, O. J. no

L358, 18/12/86). Affinity at transmembrane glutamate metabotropic $mGlu_1$ and $mGlu_5$ receptor subtypes was evaluated according to the methods of Lavreysen[33] and Anderson[67] respectively, with some modifications. Briefly, male Sprague Dawley rats were killed by cervical dislocation and their brain rapidly removed. Forebrain (cortex, striatum and hippocampus) and cerebellum were dissected and homogenized (2x20 sec) in 50 volumes of cold 50 mM Tris buffer pH 7.4, using a Politron homogenizer (Kinematica). Homogenates were centrifuged at 48000xg for 15 min, resuspended in 50 volumes of the same buffer, incubated at 37°C for 15 min and centrifuged and resuspended two more times. The final pellets were frozen and stored at -80°C until use.

Native $mGlu_5$ membranes from rat forebrain were resuspended in 100 volumes of 20mM HEPES, 2 mM $MgCl_2$, 2mM $CaCl_2$, pH 7.4, then were incubated in a final volume of 1 mL for 60 min at 25°C with 4 nM [^{3}H]MPEP in absence or presence of competing drugs. Non-specific binding was determined in the presence of 10 μM MPEP. Cloned $mGlu_1$ were obtained resuspending CHO T-REx r-$mGlu_1$cells (60 μg/well) in 50 mM Tris, 1.2 mM $MgCl_2$, 2mM $CaCl_2$, pH 7.4, that then were incubated

in a final volume of 1 mL for 30 min at 0°C with 2 nM [^{3}H]R214127 in absence or presence of competing drugs. Non-specific binding was determined in the presence of 1 μM R214127. Cloned $mGlu_5$ was obtained resuspending CHO T-REx h-$mGlu_5$ cells (50 μg/well) in 20 mM HEPES, 2 mM $MgCl_2$, 2mM $CaCl_2$, pH 7.4, that then were incubated in a final volume of 1 mL for 60 min at 25°C with 4 nM [^{3}H]MPEP in absence or presence of competing drugs. Non-specific binding was determined in the presence of 10 μM MPEP. The incubation was stopped by addition of cold Tris buffer pH 7.4 and rapid filtration through 0.2% polyethyleneimine pretreated Filtermat 1204-401 (Perkin Elmer) filters. The filters were then washed with cold buffer and the radioactivity retained on the filters was counted by liquid scintillation spectrometry (Betaplate 1204 BS-Wallac).

Calcium Fluorescence Measurements.

Cells were seeded into black-walled, clear-bottom, 96-well plates at a density of 80000 cell/well, in RPMI (without Phenol Red, without L-glutamine; Gibco LifeTechnologies, CA) supplemented with 10% dialyzed FBS. Following 18 h incubation with tetracycline, the cells were loaded with 2 μM Ca^{2+}- sensitive fluorescent dye Fluo-4/AM (Molecular

Probes) in Hanks' balanced saline solution (HBSS, Gibco LifeTechnologies, CA) with 20 mM HEPES (Sigma) and 2.5mM probenecid (Sigma), for 1h at 37°C. The cells were washed three times with HBSS to remove extracellular dye. Fluorescence signals were measured by using the fluorescence microplate reader Flexstation III (Molecular Devices) at sampling intervals of 1.5 s for 60 s. The antagonist potency was determined by three independent experiments performed in triplicate and using EC_{80} of the agonist quisqualate determined the same day of the experiment. The NAMs were applied 10 min before the application of the agonist. For binding and calcium assay studies, the compounds were dissolved in DMSO or demineralized water according to their solubility. All the reported doses were those of the corresponding salts or bases.

Statistical analysis.

Binding and functional results were obtained by three independent experiments and each assay point was determined at least as duplicate. The inhibition curves of the tested compounds at native and cloned $mGlu_1$ and $mGlu_5$ subtypes were determined by nonlinear regression analysis using software Prism 4.0 (Graphpad, San Diego,

CA). The IC_{50} values and pseudo-Hill slope coefficients were estimated by the software. The values for the inhibition constant, K_i, were calculated according to the equation $K_i = IC_{50}/(1 + [L]/K_d)$, where [L] is the concentration of radioligand and K_d is the equilibrium dissociation constant of the radioligand-receptor complex. The dissociation constants used for calculation were Kd = 3.04 nM for [^{3}H]MPEP and Kd = 1.72 nM for [^{3}H] R214127.

Pharmacokinetics *in vitro*

All experiments were carried out in duplicate in standards 96 plates. Selective and sensitive LC/MS/MS method was developed for the determination of tested compounds in the samples. Compounds were detected by mass spectrometry in the multiple ion reaction monitoring mode (MRM). The peak area ratios, between the analyte and the internal standard, were the responses used for quantification.

Cytochromes inhibition determination (IC_{50})

Materials standard, reagents and buffers

Recombinant human cytochromes CYP1A2 (lot n° 65938), CYP2D6*1 (lot n° 39596) and CYP3A4 (lot n° 44677) high throughput inhibitor screening kits were supplied by GenTest™ (BD Biosciences).

Test molecules were dissolved in acetonitrile at 1 mM concentration. Prototypical inhibitors for CYP1A2 (furafylline, 1 mM solution), CYP2D6 (quinidine, 25 µM solution) and CYP3A4 (ketoconazole, 0.25 mM solution) were dissolved in acetonitrile at the above concentration established on the basis of inhibitor Ki.

Three Buffer solutions were prepared according to indications reported in GenTest™ kit:

Buffer 1: NADPH-Cofactor Mix consists of water solution of cofactors (NAD+, $MgCl_2$ and glucose 6-phosphate), glucose 6-phosphate dehydrogenase and control insect cell membrane protein.

Buffer 2: NADPH-Cofactor Mix consists of water solution of cofactors (NAD+, $MgCl_2$ and glucose 6-phosphate), glucose 6-phosphate dehydrogenase and control insect cell membrane protein, supplemented with acetonitrile concentration of 4% (v/v).

Enzyme /Substrate Mix consists of phosphate buffer supplemented with specific recombinant P450 and respective fluorescence substrate.

Determination of test compound cytochrome inhibition (IC_{50})

Determination of test compound IC_{50} for CYP1A2

In a 96-well plate, test compound and furafylline were added to Buffer 1 to achieve for both the desired final concentrations of 20 µM at an acetonitrile maximum concentration of 4% (v/v). The samples were serially diluted, (dilution factor 1:3) in Buffer 2 to obtain a concentration range between 20 and 0.0091 µM of test compound. Plate was pre-incubated at ca. 37°C for 10 minutes. Enzyme/Substrate Mix (CYP1A2 diluted to achieve the concentration of 3.75 pmol/ml and 3-cyano-7-ethoxycoumarin (CEC) diluted to achieve 5 µM in total reaction volume) was added and the plate was incubated at ca. 37°C for 15 minutes. Reaction was terminated by adding 0.1 M Tris Base in acetonitrile. Plate was read at an excitation and emission wavelength suitable to detect the 3-cyano-7-hydroxycoumarin metabolite (CHC) (405 nm excitation and 460 nm emission) at Wallac 1420 multilabel counter (Perkin Elmer).

Determination of test compound IC_{50} for CYP2D6

In a 96-well plate, test compound and quinidine were added to Buffer 1 to achieve the desired final concentrations of 20 and 0.5 μM respectively at acetonitrile concentration of 4% (v/v). The samples were serially diluted (dilution factor 1:3) in Buffer 2 to obtain a concentration range between 20 and 0.0091 μM of test compound and between 0.5 and 0.00023 μM of quinidine. Plate was pre-incubated at ca. 37°C for 10 minutes. Then, Enzyme/Substrate Mix (CYP2D6 diluted to achieve the concentration of 7.5 pmol/ml and 3-[2-(N,N-diethylamino)ethyl]-7-methoxy-4-methylcoumarin (AMMC) diluted to achieve the concentration of 1.5 μM in total reaction volume) was added and the plate was incubated at ca. 37°C for 30 minutes. Reaction was terminated by adding 0.1 M Tris Base in acetonitrile. Plate was read at an excitation and emission wavelength suitable to detect the 3-[2-(N,N-diethylamino)ethyl]-7-hydroxy-4-methylcoumarin hydrochloride metabolite (AHMC) (390 nm excitation and 460 nm emission) at Wallac 1420 multilabel counter (Perkin Elmer).

Determination of test compound IC_{50} for CYP3A4

In a 96-well plate, test compound and ketoconazole were added to Buffer 1 to achieve the desired final concentrations of 20 and 5 μM respectively at acetonitrile

concentration of 4% (v/v). The samples were serially diluted (dilution factor 1:3) in Buffer 2 to obtain a concentration range between 20 and 0.0091 µM of test compound and between 5 and 0.00228 µM of ketoconazole. Plate was pre-incubated 10 minutes at ca. 37°C. Then, Enzyme/Substrate Mix (CYP3A4 diluted to achieve the concentration of 5 pmol/ml and 7-benzyloxy-trifluoromethylcoumarin (BFC) diluted to achieve the concentration of 50 µM in total reaction volume) was added (2% organic solvent (v/v) in total reaction volume) and the plate incubated at ca. 37°C for 30 minutes. Reaction was terminated by adding 0.1 M Tris Base in acetonitrile. Plate was read at an excitation and emission wavelength suitable to detect the 7-hydroxytrifluoromethylcoumarin metabolite (HFC) (405 nm excitation and 535 nm emission) at Wallac 1420 multilabel counter (Perkin Elmer).

***In vitro* metabolic stability - Determination of test compound percent remaining in microsome or CYP3A4 supersomes**

Pools of microsomes obtained from male human (lot n° 0510370) and male rat (lot n° 0610320) livers were supplied by Xenotech. Positive control substrates for human and

rat microsomes (verapamil and dextromethorphan respectively) were supplied by Sigma-Aldrich. Incubation buffer 1.15% KCl solution at pH of 7.4.

Human CYP3A4 + P450 reductase + cytochrome b5 supersomes (lot n° 456202) were supplied by GenTestTM (BD Biosciences). Positive control substrate, testosterone, was supplied by Sigma-Aldrich. Incubation buffer 1.15% KCl solution at pH of 7.4.

Determination of percent remaining

Test compound and positive control 1 mM stock solutions in acetonitrile were diluted in acetonitrile at final concentration of 0.2 mM. Microsomes of every species were prepared in incubation buffer to achieve the final concentration of cytochrome P450 of 2 nmol/mL (or alternatively supersomes were prepared in incubation buffer to achieve the final concentration of Cyp3A4 of 40 pmol/mL). After a pre-incubation for 5 minutes at ca. 37°C in thermostated bath, 2.5 µL of diluted test compound was added to incubation mixture to obtain a final substrate concentration of 2 µM, at acetonitrile concentration of 1% (v/v). Incubation was carried out with and without NADPH (2 mM) for 30 minutes under shaking. Total volume of reaction was 250 µL. The reaction was terminated by adding cold acetonitrile containing an internal standard. Samples were

centrifuged at 4000 rpm for 10 minutes, then the supernatant was transferred into 96 well plate for HPLC/MS/MS analysis. Metabolic stability of test compound or control substrate were measured using LC/MS/MS detection of parent compounds, and the results are reported as percent compound remaining at the end of the experiment.

Using microsomes the LC/MS/MS was performed on a API 2000 (Sciex) equipped with a column Zorbax SB C18 50x2.1mm, 3.5 µm at 30°C and using as mobile phase a gradient of 30–70% acetonitrile in a buffer solution of 2mM ammonium formate at pH=3.5 in electrospray positive ionization mode.

Using CYP3A4 supersomes the LC/MS/MS was performed on a API 4000-QTRAP (Sciex) equipped with a column Zorbax SB C18 50x2.1mm, 3.5 µm at 30°C using as mobile phase a gradient of 10–90% acetonitrile in a buffer solution of 2 mM ammonium formate at pH=3.5 in electrospray positive ionization mode.

In vitro GSH adduct formation

Materials standard, reagents and buffers

Test compound and positive control (ticlopidine) were diluted in acetonitrile at final concentration of 10 mM solutions. Mouse liver S9 fraction was prepared in incubation

buffer to achieve the final concentration of protein of 2 mg/mL. After a pre-incubation for 5 minutes at ca. 37°C in thermostated bath, 2.5 µL of diluted test compound was added to incubation mixture to obtain a final substrate concentration of 100 µM, at acetonitrile concentration of 1% (v/v). Incubation was carried out with GSH (5 mM) and with and without NADPH (2 mM) for 120 minutes under shaking. Total volume of reaction was 250 µL. The reaction was terminated by adding cold acetonitrile. Samples were centrifuged at 4000 rpm for 10 minutes, then the supernatant was transferred into 96 well plate for HPLC/MS/MS analysis.

Using microsomes the LC/MS/MS was performed on a API 2000 (Sciex) using a column Zorbax SB C18 50x2.1mm, 3.5µm at 30°C using as mobile phase a gradient of 30 – 70% acetonitrile in a buffer solution of 2mM ammonium formate at pH=3.5 in electrospray positive ionization mode. Determination of GSH conjugates, of test and control compounds (**12** and ticlopidine respectively), were studied using LC/MS/MS detection using the following experimental condition. The LC/MS/MS was performed on a API 2000 (Sciex) using a Zorbax SB C18 150x4.6mm, 5 µm at 30°C using an

isocratic mobile phase 80% acetonitrile in a buffer solution of 2 mM ammonium formate at pH=3.5 in electrospray positive ionization mode.

Metabolite generation and identification

Pools of microsomes obtained from male rat livers (lot n° 0710387) were supplied by Xenotech. The experimental procedure in rat microsomes was conducted as for *in vitro* stability determination, but the reaction was blocked adding cold acetonitrile at different times (5, 15, 30 minutes). Determination of parent compounds (**16**, **31** and **46**) and possible metabolite formation was studied using LC/MS/MS detection using the following experimental condition. The LC/MS/MS was performed on a API 2000 (Sciex) using a Zorbax SB C18 150x4.6mm, 5mm at 30°C using an isocratic mobile phase 80% acetonitrile in a buffer solution of 2mM ammonium formate at pH=3.5 in electrospray positive ionization mode.

In vivo pharmacology

Male Wistar Han rats from Charles River Italy were used in these experiments. Animals were housed with free access to food and water and maintained on a forced 12 hr light-dark cycle at 22-24°C for at least one week before the experiments were

carried out. The animals were handled according to internationally accepted principles for care of laboratory animals (E.E.C. Council Directive 86/609, O. J. n° L358, 18/12/86).

Neuropathic pain

CCI to the sciatic nerve of the left hind leg in rat (200-225 g bw) was performed under general anesthesia using the well characterized Bennett model.[55] Briefly, rats were anesthetized with equitensin for the duration of surgery. The left thigh was shaved and a small incision (1–1.5 cm in length) was made to expose the sciatic nerve. The right common sciatic nerve was exposed at the level of the mid-thigh and, proximal to the trifurcation of the nerve was loosely ligated around the entire diameter of the nerve at four distinct sites (spaced 1 mm apart) using silk sutures (3.0). The surgical site was closed with muscle and skin suture. The rats with sciatic nerve exposure without ligation served as the sham control group. Rats were randomly separated into several groups: sham control and vehicle and drug treated groups, and each group contained 10 rats. Pilot studies established that under our experimental conditions mechano-allodynia and thermal hyperalgesia peaks develop by D5–D7 following CCI; then the

pain thresholds were measured 7 days after surgery. Drugs were administrated intraperitoneally one hour before testing at the dose of 10 mg/5ml/kg. The vehicle used consisted of DMF (8%), Tween 80 (8%) and distilled water (84%).

Thermal hyperalgesia was tested according to the Hargreaves procedure,[68] using a Plantar Test Apparatus (Ugo Basile, Comerio, Italy). Briefly, mice were placed in smaller clear Plexiglas cubicles and allowed to acclimatize. A constant intensity radiant heat was aimed at the midplantar area of the hind paw. The time, in seconds (s), from initial heat source activation until paw withdrawal was recorded.

Mechanical allodynia was assessed using the Dynamic Plantar Aesthesiomether (Ugo Basile, Comerio, Italy). Animals were placed in a test cage with a wire mesh floor, and the rigid tip of a von Frey-filament (punctate stimulus) was applied to the skin of the midplantar area of the hind paw. The filament exerted an increasing force, starting below the threshold of detection and increasing until the animal removed its paw. Withdrawal threshold was expressed in grams.

Vogel conflict test

The method, using a conflict situation created by the simultaneous presence of attractive and aversive stimuli as a model of anxiety, follows that described by Vogel.[52]

Rat (175-200 g bw) was deprived of water for approximately 48 hours before testing and on the preceding day of the test, rats are placed into the test chambers equipped with a metal water spout mounted on the wall of the chamber and a metal grid floor for delivering electric shocks. The rat was left to explore until it found the water spout, then, every time it drank, it received a slight electric shock (1.7 mA, 1 s) 2 seconds after it started lapping. The number of punished drinks was counted during a 3-minute test. Number of licks and shocks delivered are recorded and stored. Anxiolytic or anxiogenic activity is reflected by increased or decreased number of accepted shocks, respectively.

Rats were randomly separated into several groups: vehicle- and drug-treated groups, and each group contained 10 rats. Drugs were administrated orally one hour before testing, at the dose of 0.3 mg, 3 mg and 30 mg/5ml/kg. The vehicle used consisted of distilled water.

Isovolumic volume induced voiding contractions

Female rats were anaesthetized with sc injection of urethane 1.25 g/kg (5 mL/kg), and the urinary bladder was catheterized via the urethra by use of polyethylene tubing (0.58 mm internal diameter, 0.96 mm outer diameter) filled with physiological saline. Intravesical pressure was measured by a pressure transducer and displayed continuously on a chart recorder. The bladder was filled via the recording catheter by 0.1–0.2 mL incremental volumes of saline until spontaneous and rhythmic bladder voiding contractions occurred (usually at 0.8–1.5 mL of filling) as a result of CNS activity. Frequency and amplitude of the rhythmic bladder voiding contractions was recorded and calculated for 15-min periods. After acquisition of basal values, a priming response with iv administration of vehicle through a polyethylene cannula inserted into the jugular vein was performed in each rat. Rats with no response to vehicle priming were then treated iv with the test compound and the effect was assessed by measuring the duration of bladder quiescence in terms of disappearance time (DT) of bladder contraction in minutes.

Cystometric studies

Male rats, anaesthetized with equithensin solution (3 mL/kg) i.p., were placed in a supine position and an about 10 mm midline incision was made in the shaved and cleaned abdominal wall. The urinary bladder was gently freed from adhering tissues, emptied and then cannulated, via an incision at the dome, with a polyethylene cannula (PE50: internal diameter 0.58 mm, outer diameter 0.96 mm), which was permanently sutured with silk thread. The cannula was exteriorized through a sc tunnel in the area of the sternum. For drug testing, rats were tested 1 day after catheter implantation. On the day of the experiment, the rats were placed in Bollman's cages; after a stabilization period of 20 min, the free tip of the cannula was connected by a T-shape tube to a pressure transducer and to a peristaltic for a continuous infusion of saline solution into the urinary bladder, at the constant rate of 0.1 mL/min. The urodynamic variables calculated from the cystometrogram acquired and analyzed by Power-Laboratory 8. The rats were treated orally with the test compound **12** under continuous infusion of the bladder with saline, and changes in BVC were evaluated for 5 h.

Statistical analysis for *in vivo* experiments

Data are expressed as mean ± SEM for n animals. Behavioral and urological data were analyzed by: one-way ANOVA with Tukey's post-test in neuropathic pain model, paired t-test analysis in induced voiding contractions. ED_{10} value, based on disappearance time (DT) expressed in minutes, was calculated by linear regression analysis. Vogel's conflict test and cystometric studies were analyzed by one-way ANOVA with Dunnett's post hoc comparison. Significant differences were defined at a $P < 0.05$. All statistical analysis was performed using GraphPad Prism (v5.03, GraphPad Software, Inc., San Diego, CA).

Supporting Information

Experiment S1, Table S1–S5 and Figure S1–S18. This material is available free of charge via the Internet at http://pubs.acs.org

Docking simulations of molecules as possible substrates of the human CYP3A4 isoform, ligand quality indicators, metabolic pathway, minima conformations and energy plots, cytochrome sequence alignment and molecules docking simulation into

the heme cavity. Analytical characterization, HTS profile study, functional assay and safety characterization of compound **12**.

Corresponding Author

Davide Graziani, Drug Discovery Department, Recordati S.p.A. Via M Civitali, 1, 20148 Milano, Italy. Tel +39 02 48787 214, Fax +39 02 48787 668 Email graziani.d@recordati.it

Author information

D.G. and C.R. directed and designed the chemistry. V.T. designed the chemistry. C.D.T., F.F and M.L. performed the medicinal chemistry. E.C. and L.P. directed and performed molecular pharmacology experiments. S.M. directed and performed the analytical work. R.D. performed the analytical work. S.C. designed and performed in vitro DMPK work. A.V. designed and performed in vivo experiments. G.R. directed the computational studies. L.P. performed the computational studies. G.V. directed and performed the computational metabolic studies.

Acknowledgment

We would like to acknowledge dr. Amedeo Leonardi and dr. Gianni Motta that directed the medicinal chemistry group at Recordati and dr. David Clarke for the helpful and effective discussions.

Notes

The authors declare no competing financial interest.

Abbreviations

bw, body weight; BVC, Bladder Volume Capacity; $[Ca^{2+}]_{i,}$ intracellular calcium concentration; CCI Chronic Constriction Injury, DIEA, N,N-Diisopropylethylamine; EDC, *N*-(3-Dimethylaminopropyl)-*N*-ethylcarbodiimide hydrochloride; DILI, Drug-Induced Liver Injury; DMF, N,N-dimethylformamide; DT, disappearance time; Good Laboratory Practice, GLP; GPCR, G-protein coupled receptor; HOBt, 1-hydroxybenzotriazole; HWE, Horner-Wadsworth-Emmons; K_p, total brain plasma ratio; (LHMDS, lithium bis(trimethylsilyl)amide; $mGluR_5$, metabotropic glutamate receptor subtype 5; NAM, negative allosteric modulator; PAD, Photodiode Array Detector; PS-DCC, polymer supported cyclohexylcarbodiimide; TEA, triethylamine;

TFA, trifluoroacetic acid; UPLC, ultra-performance liquid chromatography; VFT venus flytrap.

References

(1) Romano, C.; Sesma, M.A.; McDonald, C.T.; O'Malley K.; Van den Pol, A.N.; Olney, J.W. Distribution of metabotropic glutamate receptor $mGluR_5$ immunoreactivity in rat brain. *J. Comp. Neurol.* **1995,** *355*, 455–469.

(2) Nishi, A.; Liu, F.; Matsuyama, S.; Hamada, M.; Higashi, H.; Nairn, A.C.; Greengard, P. Metabotropic $mGlu_5$ receptors regulate adenosine A2A receptor signaling. *Proc. Natl. Acad. Sci. USA* **2003**, *100*,1322–1327.

(3) Cabello, N.; Gandia, J.; Bertarelli, D.C.; Watanabe, M.; Lluís, C.; Franco, R.; Ferré, S.; Luján, R.; Ciruela, F. Metabotropic glutamate type 5, dopamine D2 and adenosine A2a receptors form higher-order oligomers in living cells. *J. Neurochem*. **2009**, *109*, 1497–1507.

(4) Tebano, M.T.; Martire, A.; Rebola, N.; Pepponi, R.; Domenici, M.R.; Grò, M.C.; Schwarzschild, M.A.; Chen, J.F.; Cunha, R.A.; Popoli, P. Adenosine A2A receptors and metabotropic glutamate 5 receptors are colocalized and functionally interact in the hippocampus: a possible key mechanism in the modulation of N-methyl-D-aspartate effects. *J. Neurochem.* **2005**, *95*, 1188–1200.

(5) Nakamoto, M.; Nalavadi, V.; Epstein, M.P.; Narayanan, U.; Bassell, G.J.; Warren, S.T. Fragile X mental retardation protein deficiency leads to excessive $mGluR_5$-dependent internalization of AMPA receptors. *Proc. Natl. Acad. Sci. USA* **2007**, *104*, 15537–15542.

(6) Nicoletti, F.; Bockaert, J.; Collingridge, G.L.; Conn, P.J.; Ferraguti, F.; Schoepp, D.D.; Wroblewski, J.T.; Pin, J.P. Metabotropic glutamate receptors: from the workbench to the bedside. *Neuropharmacol.* **2011**, *60*, 1017–1041.

(7) Gregory, K.J.; Herman, E.J.; Ramsey, A.J.; Hammond, A.S.; Byun, N.E.; Stauffer, S.R.; Manka, J.T.; Jadhav, S.; Bridges, T.M.; Weaver, C.D.; Niswender, C.M.; Steckler, T.; Drinkenburg, W.H.; Ahnaou, A.; Lavreysen, H.; Macdonald, G.J.; Bartolomé, J.M.; Mackie, C.; Hrupka, B.J.; Caron, M.G.; Daigle, T.L.; Lindsley, C.W.; Conn, P.J.; Jones, C.K. N-aryl piperazine metabotropic glutamate receptor 5 positive allosteric modulators possess efficacy in preclinical models of NMDA hypofunction and cognitive enhancement. *J. Pharmacol. Exp. Ther.* **2013**, *347*, 438–457.

(8) Nickols, H.H.; Conn, P.J. Development of allosteric modulators of GPCRs for treatment of CNS disorders. *Neurobiol. Dis.* **2014**, *61*, 55–71.

(9) O'Hara, P. J.; Sheppard, P. O.; Thøgersen, H.; Venezia, D.; Haldeman, B. A.; McGrane, V.; Houamed, K. M.; Thomsen, C.; Gilbert, T. L.; Mulvihill, E. R. The ligand-binding domain in metabotropic glutamate receptors is related to bacterial periplasmic binding proteins. *Neuron* **1993**, *11*, 41–52.

(10) Conn, P. J.; Pin, J. P. Pharmacology and functions of metabotropic glutamate receptors. *Ann. Rev. Pharmacol. Toxicol.* **1997**, *37*, 205–237.

(11) Doré, A. S.; Okrasa, K.; Patel, J. C.; Serrano-Vega, M.; Bennett, K.; Cooke, R. M.; Errey, J. C.; Jazayeri, A.; Khan, S.; Tehan, B.; Weir, M.; Wiggin, G. R.; Marshall, F. H. Structure of class C GPCR metabotropic glutamate receptor 5 transmembrane domain. *Nature* **2014**, *511*, 557–562.

(12) Christopher, J. A.; Aves, S. J.; Bennett, K. A.; Doré, A. S.; Errey, J. C.; Jazayeri, A.; Marshall, F. H.; Okrasa, K.; Serrano-Vega, M. J.; Tehan, B. G.; Wiggin, G. R.; Congreve, M. Fragment and structure-based drug discovery for a class C GPCR: Discovery of the $mGlu_5$ negative allosteric modulator HTL14242 (3-Chloro-5-[6-(5-Fluoropyridin-2-yl)pyrimidin-4-yl]benzonitrile). *J. Med. Chem.* **2015**, *58*, 6653–6664.

(13) Christopher, J. A.; Orgován, Z.; Congreve, M.; Doré, A. S.; Errey, J. C.; Marshall, F. H.; Mason, J. S.; Okrasa, K.; Rucktooa, P.; Serrano-Vega, M. J.; Ferenczy, G. G. and Keserű, G. M. Structure-based optimization strategies for G protein-coupled receptor (GPCR) allosteric modulators: A case study from analyses of new metabotropic glutamate receptor 5 ($mGlu_5$) x-ray structures. *J. Med. Chem.* in press, doi: 10.1021/acs.jmedchem.7b01722

(14) Rondard, P.; Liu, J.; Huang, S.; Malhaire, F.; Vol, C.; Pinault, A.; Labesse, G.; Pin, J.P. Coupling of agonist binding to effector domain activation in metabotropic glutamate-like receptors. *J. Biol. Chem.* **2006**, *281*, 24653–24661.

(15) Sengmany, K.; Gregory, K.J. Metabotropic glutamate receptor subtype 5: molecular pharmacology, allosteric modulation and stimulus bias. *Br. J. Pharmacol.* **2016**, *173*, 3001–3017.

(16) Christopoulos, A. Advances in G protein-coupled receptor allostery: from function to structure. *Mol. Pharmacol.* **2014**, *86*, 463–478.

(17) Deleve, L.D. and Kaplowitz, N. Glutathione metabolism and its role in hepatotoxicity. *Pharmacol. Ther.* **1991**, *52*, 287–305.

(18) Shah, F.; Stepan, A.F.; O'Mahony, A.; Velichko, S.; Folias, A.E.; Houle, C., Mechanisms of skin toxicity associated with metabotropic glutamate receptor 5 negative allosteric modulators. *Cell Chem. Biol.* **2017**, *24*, 858–869.

(19) Jaeschke, G.; Kolczewski, S.; Spooren, W.; Vieira, E.; Bitter-Stoll, N.; Boissin, P.; Borroni, E.; Büttelmann, B.; Ceccarelli, S.; Clemann, N.; David, B.; Funk, C.; Guba, W.; Harrison, A.; Hartung, T.; Honer, M.; Huwyler, J.; Kuratli, M.; Niederhauser, U.; Pähler, A.; Peters, J-U.; Petersen, A.; Prinssen, E.; Ricci, A.; Rueher, D.; Rueher, M.; Schneider, M.; Spurr, P.; Stoll, T.; Tännler, D.; Wichmann, J.; Porter, R.H.; Wettstein, J.G.; Lindemann, L. Metabotropic glutamate receptor 5 negative allosteric modulators: Discovery of 2-Chloro-4-[1-(4-fluorophenyl)-2,5-dimethyl-1H-imidazol-4-ylethynyl]pyridine (Basimglurant, RO4917523), a promising novel medicine for psychiatric diseases. *J. Med. Chem.* **2015**, *58*, 1358−1371.

(20) Galambos, J.; Bielik, A.; Krasavin, M.; Orgován, Z.; Domány, G.; Nógrádi, K.; Wágner, G.; Balogh, G.T.; Béni, Z.; Kóti, J.; Szakács, Z.; Bobok, A.; Kolok, S.; Mikó-Bakk, M.L.; Vastag, M.; Sághy, K.; Laszy, J.; Halász, A.S.; Balázs, O.; Gál, K.; Greiner, I.; Szombathelyi, Z.; Keserű, G.M. Discovery and preclinical characterization of 3-((4-

(4-chlorophenyl)-7-fluoroquinoline-3-yl)sulfonyl)benzonitrile, a novel non-acetylenic metabotropic glutamate receptor 5 ($mGluR_5$) negative allosteric modulator for psychiatric indications. *J. Med. Chem.* **2017**, *60*, 2470–2484.

(21) Felts, A.S.; Rodriguez, A.L.; Blobaum, A.L.; Morrison, R.D.; Bates, B.S.; Gray, A.T.; Rook, J.M.; Tantawy, M.N.; Byers, F.W.; Chang, S.; Venable, D.F.; Luscombe, V.B.; Tamagnan, G.D.; Niswender, C.M.; Daniels, J.S.; Jones, C.K.; Conn, P.J.; Lindsley, C.W.; Emmitte, K.A. Discovery of N-(5-fluoropyridin-2-yl)-6-methyl-4-(pyrimidin-5-yloxy)picolinamide (VU0424238): A novel negative allosteric modulator of metabotropic glutamate receptor subtype 5 selected for clinical evaluation. *J. Med. Chem.* **2017**, *60*, 5072−5085.

(22) Berry-Kravis, E.; Des Portes, V.; Hagerman, R.; Jacquemont, S.; Charles, P.; Visootsak, J.; Brinkman, M.; Rerat, K.; Koumaras, B.; Zhu, L.; Barth, G.M.; Jaecklin, T.; Apostol G.; von Raison, F. Mavoglurant in fragile X syndrome: Results of two randomized, double-blind, placebo-controlled trials. *Sci. Transl. Med*. **2016**, *8*, 321ra5.

(23) Youssef, E.A.; Berry-Kravis, E.; Czech, C.; Hagerman, R.J.; Hessl, D.; Wong, C.Y.; Rabbia, M.; Deptula, D,; John, A.; Kinch, R.; Drewitt, P.; Lindemann, L.;

Marcinowski, M.; Langland, R.; Horn, C.; Fontoura, P.; Santarelli, L.; Quiroz, J.A. and FragXis Study Group, Effect of the mGluR5-NAM Basimglurant on behavior in adolescents and adults with fragile X syndrome in a randomized, double-blind, placebo-controlled trial: FragXis Phase 2 results. *Neuropsychopharmacology*, **2018**, *43*, 503–512.

(24) Stocchi, F.; Rascol, O.; Destee, A.; Hattori, N.; Hauser, R.A.; Lang, A.E.; Poewe, W.; Stacy, M.; Tolosa, E.; Gao, H.; Nagel, J.; Merschhemke, M.; Graf, A.; Kenney, C.; Trenkwalder, C.; AFQ056 in Parkinson patients with levodopa-induced dyskinesia: 13-week, randomized, dose-finding study. *Mov. Disorder*. **2013**, *28*, 1838–1846.

(25) Kumar, R.; Hauser, R.A.; Dronamraju, N.; Graf, A.; Merschhemke, M.; Kenney, C.; Mavoglurant (AFQ056) in combination with increased levodopa dosages in Parkinson's disease patients. *Inter. J. Neurosci.* **2016**, *126*, 20–24.

(26) Quiroz, J.A.; Tamburri, P.; Deptula, D.; Banken, L.; Beyer, U.; Rabbia, M.; Parkar, N.; Fontoura, P.; Santarelli, L. Efficacy and safety of basimglurant as adjunctive therapy for major depression - A randomized clinical trial, *JAMA Psychiatry.* **2016**, *73*, 675–684.

(27) Berry-Kravis, E.M.; Lindemann, L.; Jønch, A.E.; Apostol, G.M; Bear, F.; Carpenter, R.L.; Crawley, J.N.; Crie, A.; Des Portes, V.; Hossain, F.; Gasparini, F.; Gomez-Mancilla, B.; Hessl, D.; Loth, E.; Scharf, S.H.; Wang, P.P.; Von Raison, F.; Hagerman, R.; Spooren, W. and Jacquemont, S., Drug development for neurodevelopmental disorders: lessons learned from fragile X syndrome. *Nat. Rev. Drug Discov*. **2018**, *17*, 280–299.

(28) Nickols, H.H.; Yuh, J.P.; Gregory, K.J.; Morrison, R.D.; Bates, B.S.; Stauffer, S.R.; Emmitte, K.A.; Bubser, M.; Peng, W.; Nedelcovych, M.T.; Thompson, A.; Lv, X.; Xiang, Z.; Daniels, J.S.; Niswender, C.M.; Lindsley, C.W.; Jones, C.K. and Conn, P.J. VU0477573: Partial negative allosteric modulator of the subtype 5 metabotropic glutamate receptor with in vivo efficacy. *J. Pharmacol. Exp. Ther.* **2016**, *356*, 123–136.

(29) Stoppel, L.J.; Auerbach, B.D.; Senter, R.K.; Preza, A. R.; Lefkowitz, R.J.; Bear, M.F. β-arrestin2 couples metabotropic glutamate receptor 5 to neuronal protein synthesis and is a potential target to treat fragile X. *Cell Reports* **2017**, *18*, 2807–2814.

(30) Anighoro, A.; Graziani, D.; Bettinelli, I.; Cilia, A.; De Toma, C.; Longhi, M.; Mangiarotti, F.; Menegon, S.; Pirona, L.; Poggesi, E.; Riva, C.; Rastelli, G. Insights

into the interaction of negative allosteric modulators with the metabotropic glutamate receptor 5: Discovery and computational modeling of a new series of ligands with nano-molar affinity. *Bioorg. Med. Chem.* **2015**, *23*, 3040–3058.

(31) Leonardi, A.; Motta, G.; Riva, C.; Poggesi, E.; Graziani, D.; Longhi, M. Novel Heterocyclic Compounds as $mGlu_5$ Antagonists. International Patent Application WO2009015897, 2009, Recordati Ireland Limited.

(32) Van Summeren, R.P.; Feringa, B.L.; Minnaard, A.J. New approaches towards the synthesis of the side-chain of mycolactones A and B. *Org. Biomol. Chem*. **2005**, *3*, 2524–2533.

(33) Lavreysen, H.; Janssen, C.; Bischoff, F.; Langlois, X.; Leysen, J.E. and Lesage, A.S.J. [^{3}H]R214127: A novel high-affinity radioligand for the $mGlu_1$ receptor reveals a common binding site shared by multiple allosteric antagonists. *Mol. Pharmacol.* **2003**, *63*, 1082–1093.

(34) Bennett, K.A.; Doré, A.S.; Christopher, J.A.; Weiss, D.R. and Marshall F.H. Structures of mGluRs shed light on the challenges of drug development of allosteric modulators. *Curr. Opin. Pharmacol.* **2015**, *20*, 1–7.

(35) Emmitte, K.A.; Recent Advances in the design and development of novel negative allosteric modulators of $mGlu_5$. *ACS Chem. Neurosci.* **2011**, *2*, 411–432.

(36) Meanwell, N.A. Synopsis of some recent tactical application of bioisosteres in drug design. *J. Med. Chem.* **2011**, *54*, 2529–2591.

(37) Laurence, C.; Brameld, K.A.; Graton, J.; Le Questel, J.Y.; Renault, E. The pKBHX database: Toward a better understanding of hydrogen-bond basicity for medicinal chemists. *J. Med. Chem.* **2009**, *52*, 4073–4086.

(38) Green, M.D.; Jiang, X.; King, C.D. Inhibition of human hepatic CYP isoforms by $mGluR_5$ antagonists. *Life Sciences* **2004**, *75*, 947–953.

(39) Lewis, D.F.V.; Jacobs, M.N.; Dickins, M. Compound lipophilicity for substrate binding to human P450s in drug metabolism. *Drug Discov. Today* **2004**, 9, 530–537.

(40) Zhou, S.; Yang, L.; Zhou, Z.; Liu, Y.; Chan, E. Insights into the substrate specificity, inhibitors, regulation, and polymorphisms and the clinical impact of human cytochrome P450 1A2. *AAPS J.* **2009**, *11*, 481–494.

(41) Hitchcock, S. A. and Pennington L. D. Structure−Brain exposure relationships. *J. Med. Chem.* **2006**, *49*, 7559–7583.

(42) Mølck, C.; Harpsøe, K.; Gloriam, D.E.; Clausen, R.P.; Madsen, U.; Pedersen, L.Ø.; Jimenez, H.N.; Nielsen, S.M.; Mathiesen, J.M. and Bräuner-Osborne, H. Pharmacological characterization and modeling of the binding sites of novel 1,3-bis(pyridinylethynyl)benzenes as metabotropic glutamate receptor 5-selective negative allosteric modulators. *Mol. Pharmacol.* **2012**, *82*, 929–937.

(43) Gregory, K. J.; Nguyen, E. D.; Malosh, C.; Mendenhall, J. L.; Zic, J. Z.; Bates, B. S.; Noetzel, M. J.; Squire, E. F.; Turner, E. M.; Rook, J. M.; Emmitte, K. A.; Stauffer, S. R.; Lindsley, C. W.; Meiler, J.; Conn, P. J. Identification of specific ligand–receptor interactions that govern binding and cooperativity of diverse modulators to a common metabotropic glutamate receptor 5 allosteric site. *ACS Chem. Neurosci.* **2014**, *5*, 282–295.

(44) Pérez-Benito, L.; Doornbos, M.L.J.; Cordomì, A.; Peeters, L.; Lavreysen, H.; Pardo, L. and Tresadern, G. Molecular switches of allosteric modulation of the metabotropic glutamate 2 receptor. *Structure* **2017**, *25*, 1153–1162.

(45) Gregory, K. J.; Nguyen, E.D.; Reiff, S. D.; Squire, E. F.; Stauffer, S. R.; Lindsley, C. W.; Meiler, J. and Conn, P.J. Probing the metabotropic glutamate receptor 5

($mGlu_5$) positive allosteric modulator (PAM) binding pocket: Discovery of point mutations that engender a "molecular switch" in PAM pharmacology. *Mol. Pharmacol.* **2013**, *83*, 991–1006.

(46) Hopkins, A.H.; Keserü, G.M.; Leeson, P.D.; Rees, D.C.; Reynolds, C.H. The role of ligand efficiency metrics in drug discovery. *Nat. Rev. Drug Disc.* **2014**, *13*, 105–121.

(47) GALAS (Global, Adjusted Locally According to Similarity) Training set: 11,387 compounds; Internal validation: 4890 compounds. Source of experimental data-reference books (the Merck index, Therapeutic Drugs, Clarke's Isolation and Identification of Drugs), peer-reviewed scientific journals, and other public data sources such as handbooks and online databases. Provides a quantitative estimate of reliability of prediction through the Reliability Index (RI). This number, between 0 and 1, allows you to judge the relevance of the internal training set to the chemical space being investigated by looking for similar structures and evaluating how well the model performs in the local chemical environment of the compound (0=poor reliability, either nothing similar exists in the training set, or the model produces inconsistent predictions for similar compounds; 1=excellent reliability, several identical entries

present, and model predictions precisely match given experimental values). http://www.acdlabs.com/products/percepta/predictors/logp/. ACD/Labs 2016 Release (Build 2911, 12 July 2016).

(48) Shimizu, S.; Atsumi, R.; Nakazawa, T.; Fujimaki, Y.; Sudo, K. and Okazaki, O. Metabolism of ticlopidine in rats: Identification of the main biliary metabolite as a glutathione conjugate of ticlopidine S-oxide. *Drug. Metab. Dispos.* **2009**, *32*, 49–57.

(49) Colatsky, T.; Fermini, B.; Gintant, G.; Pierson, J.B.; Sager, P.; Sekino, Y.; Strauss, D.G.; Stockbridge, N. The comprehensive in vitro proarrhythmia assay (CiPA) initiative – Update on progress. *J. Pharmacol. Toxicol. Methods* **2016**, *81*, 15–20.

(50) Ward, K.W.; Hardy, L.B.; Kehler, J.R.; Azzarano, L.M.; Smith, B.R. Apparent absolute oral bioavailability in excess of 100% for a vitronectin receptor antagonist (SB-265123) in rat. II. Studies implicating transporter-mediated intestinal secretion. *Xenobiotica* **2004**, *34*, 367–377.

(51) Porter, R.H.P.; Jaeschke, G.; Spooren, W.; Ballard, T.M.; Buttelmann, B.; Kolczewski, S.; Peters, J-U.; Prinssen, E.; Wichmann, J.; Vieira, E.; Muhlemann, A.; Gatti, S.; Mutel, V.; and Malherbe, P. Fenobam: A clinically validated

nonbenzodiazepine anxiolytic is a potent, selective, and noncompetitive $mGlu_5$ receptor antagonist with inverse agonist activity, *J. Pharmacol. Exp. Ther.* **2005**, *315*, 711–721.

(52) Vogel, J.R.; Beer, B.; Clody, D.E. A simple and reliable conflict procedure for testing anti-anxiety agents. *Psychopharmacologia* **1971**, *21*, 1–7.

(53) Vranesic, I.; Ofner, S.; Flor, P.J.; Bilbe, G.; Bouhelal, R.; Enz, A.; Desrayaud, S.; McAllister, K.; Kuhn, R. and Gasparini, F.; AFQ056/mavoglurant, a novel clinically effective mGluR5 antagonist: Identification, SAR and pharmacological characterization. *Bioorg. Med. Chem.* **2014**, *22*, 5790–5803.

(54) Lindemann, L.; Porter, R.H.; Scharf, S.H.; Kuennecke, B.; Bruns, A.; von Kienlin, M.; Harrison, A.C.; Paehler, A.; Funk, C.; Gloge, A.; Schneider, M.; Parrott, N.J.; Polonchuk, L.; Niederhauser, U.; Morairty, S.R.; Kilduff, T.S.; Vieira, E.; Kolczewski, S.; Wichmann, J.; Hartung, T.; Honer, M.; Borroni, E.; Moreau, J-L.; Prinssen, E.; Spooren W.; Wettstein, J.G. and Jaeschke, G. Pharmacology of basimglurant (RO4917523, RG7090), a unique metabotropic glutamate receptor 5 negative

allosteric modulator in clinical development for depressions. *J. Pharmacol. Exp. Ther.* **2015**, *353*, 213–233.

(55) Bennett, G.J.; Xie, Y.K. A peripheral mononeuropathy in rat that produces disorders of pain sensation like those seen in man. *Pain* **1988**, *33*, 87–107.

(56) Lesage, A. S. J.; Role of Group 1 metabotropic glutamate receptors $mGlu_1$ and $mGlu_5$ in nociceptive signalling. *Curr. Neuropharmacol*. **2004**, *2*, 263–293.

(57) Guarneri, L.; Poggesi, E.; Angelico, P.; Farina, P.; Leonardi, A.; Clarke, D.E. and Testa R. Effect of selective antagonists of group I metabotropic glutamate receptors on the micturition reflex in rats. *BJU International* **2008**, *102*, 890–898.

(58) Baell, J.; Walters, M.A. Chemical con artists foil drug discovery. *Nature* **2014**, *513*, 481−483.

(59) Saubern, S.; Guha, R.; Baell, J.B. KNIME workflow to assess PAINS filters in SMARTS format. Comparison of RDKit and Indigo cheminformatics libraries. *Mol. Inform.* **2011**, *30*, 847–850.

(60) Madhavi Sastry, G.; Adzhigirey, M.; Day, T.; Annabhimoju, R.; Sherman, W. Protein and ligand preparation: Parameters, protocols, and influence on virtual screening enrichments. *J. Comput. Aided Mol. Des.* **2013**, *27*, 221–234.

(61) Maestro, version 10.3, Schrödinger, LLC, New York, NY, 2015.

(62) MacroModel, version 10.9, Schrödinger, LLC, New York, NY, 2015.

(63) LigPrep, version 3.5, Schrödinger, LLC, New York, NY, 2015.

(64) Banks, J.L.; Beard, H.S.; Cao, Y.; Cho, A.E.; Damm, W.; Farid, R.; Felts, A.K.; Halgren, T.A.; Mainz, D.T.; Maple, J.R.; Murphy, R.; Philipp, D.M.; Repasky, M.P.; Zhang, L.Y.; Berne, B.J.; Friesner, R.A.; Gallicchio, E.; Levy. R.M. Integrated modeling program, applied chemical theory (IMPACT). *J. Comp. Chem.* **2005**, *26*, 1752.

(65) Sherman, W.; Beard, H. S.; Farid, R. Use of an induced fit receptor structure in virtual screening. *Chem. Biol. Drug Des*. **2006**, *67*, 83–84.

(66) Induced fit docking protocol; Glide version 6.8, Schrödinger, LLC, New York, NY, 2015; Prime version 4.1, Schrödinger, LLC, New York, NY, 2015.

(67) Anderson, J.J.; Rao, S.P.; Rowe, B.; Giracello, D.R.; Holtz, G.; Chapman, D.F.; Tehrani, L.; Bradbury, M.J.; Cosford, N.D.; Varney, M.A. [3H]Methoxymethyl-3-[(2-

methyl-1,3-thiazol-4-yl)ethynyl]pyridine binding to metabotropic glutamate receptor subtype 5 in rodent brain: in vitro and in vivo characterization. *J. Pharmacol. Exp. Ther.* **2002**, *303,*1044–1051.

(68) Hargreaves, K.; Dubner, R.; Brown, F.; Flures, C. and Joris, J. A new and sensitive method for measuring thermal nociception in cutaneous hyperalgesia. *Pain* **1988**, 32, 77–88.

Figure legends

Figure 1. [^{3}H]MPEP displacement of compounds **12**, **32**, **49** and **55** on membranes of CHO cells stably transfected with human cloned $mGlu_5$ receptors. Data are plotted as percentage of total [^{3}H]MPEP specific binding and error bars represent ±SD.

Figure 2. Functional antagonism comparison for compounds **12**, **32**, **49** and **55** on quisqualate-evoked $[Ca^{2+}]_i$ for human cloned $mGlu_5$ receptors in CHO cells. The plots show the concentration-dependent inhibition, measured by intracellular Ca^{2+} mobilization, of compounds **12**, **32**, **49** and **55**. Data are expressed as normalized fluorescence of the maximal response to quisqualate.

Figure 3. LipE calculated for the different classes of molecules, using human $mGlu_5$ binding affinity and calculated $LogP_{GALAS}$ (ACD Labs). Carbamates showed the best LipE value and represent the larger pool of molecules with values higher than five (**12**, **14**, **15**, **16** and **24**). On the edge line of LipE equal to 5 fell a group of ureas compounds (**31**, **32** and **33**). Compound **49** is the only amide showing a LipE value higher than 5.

Figure 4. Superimposition of the different “in” (PDB code: 5CGD) and “out” (PDB code: 4OO9) conformations of Trp785 in the $mGlu_5$ receptor. 4OO9 and 5CGD are colored

in cyan and green, respectively. Image created with Pymol (The PyMOL Molecular Graphics System, Version 1.8 Schrödinger, LLC).

Figure 5. Close-up view of the docking binding modes observed for compound **46** in a $mGlu_5$ conformation with the "in" (panel *b*, PDB code: 5CGD) and "out" (panel *a*, PDB code: 4OO9) orientations of Trp785. In panel a, binding site residues and **46** compound are colored in green and cyan, respectively. In the panel b, binding site residues and **46** compound are colored in cyan and green, respectively. Image created with Pymol (The PyMOL Molecular Graphics System, Version 1.8 Schrödinger, LLC).

Figure 6. Effect of a single administration of **12** (0.3-3-30 mg/kg po) on Vogel Conflict Test in rats. The drug was administered 1 hour before testing. N = 10 animals per group. Mean values ± SEM ***p<0.001 vs vehicle rat (one-way ANOVA with Dunnett's post hoc test).

Figure 7. Effect of a single administration of **12** (10 mg/kg i.p.) on CCI-induced paw thermal hyperalgesia (A) and mechanical allodynia (B) in rats. The drug was administered seven days after nerve lesion and the effect evaluated after 1 hour. Heat

withdrawal latency and the mechanical threshold are respectively expressed in seconds and grams. N = 10 animals per group. Mean values ± SEM ***p<0.001, vs sham-operated/vehicle rat; °°°p<0.001vs CCI/vehicle mice (one-way ANOVA with Tukey's post hoc test).

Figure 8. Effect of iv administration of **12** in a DMF, Tween® 80 and water solution (8:8:84 respectively) at concentration of (0.01, 0.03 and 0.1 mg/kg) on isovolumic volume-induced voiding contractions in anaesthetized female rats. N = 7 animals per group. Mean values ± SEM **p<0.01 (paired t-test).

Figure 9. Effect of compound **12** on Bladder Volume Capacity (BVC) in conscious male rats. N = 7 animals per group. Data represent the percentage changes of BVC at different times, expressed in minutes, after oral administration of vehicle and 1 and 3 mg/kg of **12** in Methocel 0.5% solution. N = 8 animals per group. * P < 0.05, ** P < 0.01, and *** P < 0.001 vs basal values. Statistical significance was evaluated on the absolute data (one-way ANOVA with Dunnett's post hoc test).

Chart 1. Chemical structures of the $mGlu_5$ reference compounds **1**–**9**.

Chart 2. Chemical structures of carbamates 10–24.

Chart 3. Chemical structures of ureas 25–33.

Chart 4. Chemical structures of amides 34–49.

Chart 5. Chemical structures of sulfonamides 50–57.

Chart 6. Chemical structures of alkyl derivatives 58–61.

Scheme 1. Synthesis of compound 10, 11, 12, 13

[a]Reagents and conditions: (a) LHMDS, diethyl [3-(trimethylsilyl)prop-2-ynyl]phosphonate, THF, -70/-60°C 15 min, rt overnight. (b) 2-bromo-6-methylpyridine, $Pd(Ph_3P)_4$, NaOAc, TBAF, DMF, microwave oven 120°C, 10 min. (c) TFA, $CHCl_3$, rt or 0°C to reflux, 4h. (d) ethyl chloroformate TEA, DCM, rt.

Scheme 2. Synthesis of carbamates 14–16, 18–24 and intermediate 47b

[a]Reagents and conditions: (a) ethyl or methyl chloroformate, TEA, DCM, rt.(b) triphosgene, ROH, DIEA, DCM, 2.5h, rt then 14a, DIEA, DCM, rt, overnight. (c) LHMDS, diethyl [3-(trimethylsilyl)prop-2-ynyl]phosphonate, THF, -70/-60°C 15 min, rt, overnight. (d) aryl or heteroarylbromide(iodide) or 2-bromo-6-methylpyridine,

$Pd(Ph_3P)_4$, NaOAc, TBAF, DMF, microwave oven 120°C, 10 min. (e) TFA, $CHCl_3$, 0°C to reflux, 4h. **d**: triphosgene, ROH, DIEA, DCM. Yields for each compound are reported in Table S3 in Supporting Information.

Scheme 3. Synthesis of compounds **25–61**

[a]Reagents and conditions: (a): alkylisocyanate, TEA, DCM, rt (**25-27**) triphosgene, R^2R^3NH, DIEA, DCM, rt then **14a** or **12c**, rt, overnight (**28–31, 33**). (c) 3-methyl-1-[methyl(propan-2-yl)carbamoyl]-1H-imidazol-3-ium iodide, DCM, TEA, rt (**32**).(d) R^1COCl, TEA, DCM, rt (**34**, **40**, **48** and **49**).(e) R^1COOH, HOBt, EDC, DCM, rt (**35**, **36**, **39**, **41-43**, **46**).(f) R^1COOH, PS-DCC, DCM, rt (**37**, **38**, **44**, **45** and **47**). (g) R^1SO_2Cl, TEA, DCM, rt (**50-57**). (h) R_2CHO, $NaB(OAc)_3H$, DCM, rt (**58** and **59**). (i)2-chlorocyclopentanone, DIEA, DMA, rt (**60**); (j) (i)1-$BrCH_2COOH$, TEA, DMA, rt then PS-DCC, pyrrolidine, DCM, rt (**61**). Yields for each compounds are reported in Table S4 in Supporting Information.

Figure 1.

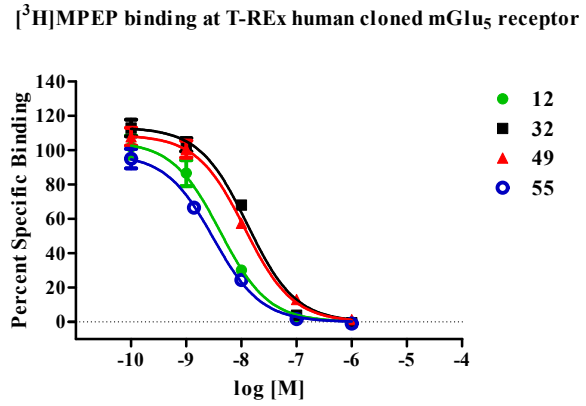

Figure 2.

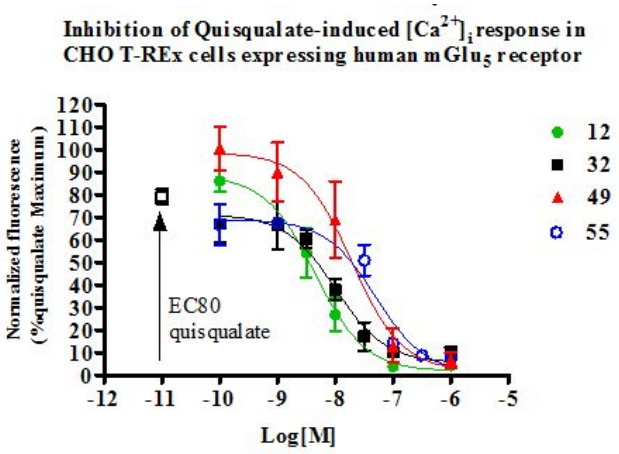

Figure 3.

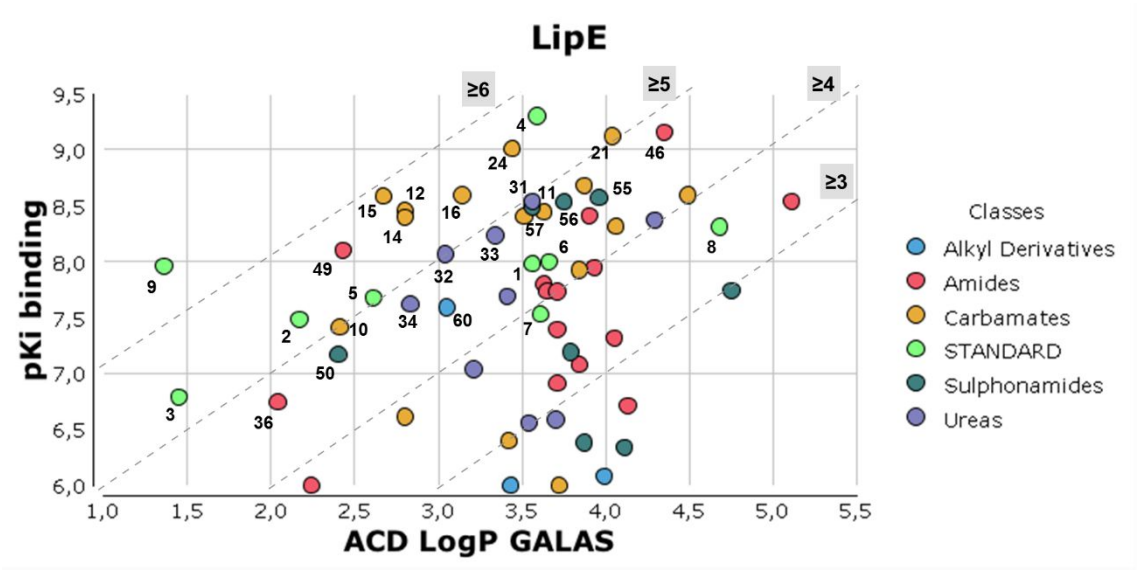
LipE
≥6
≥5
≥4
≥3
pKi binding
ACD LogP GALAS
Classes
Alkyl Derivatives
Amides
Carbamates
STANDARD
Sulphonamides
Ureas

Figure 4.

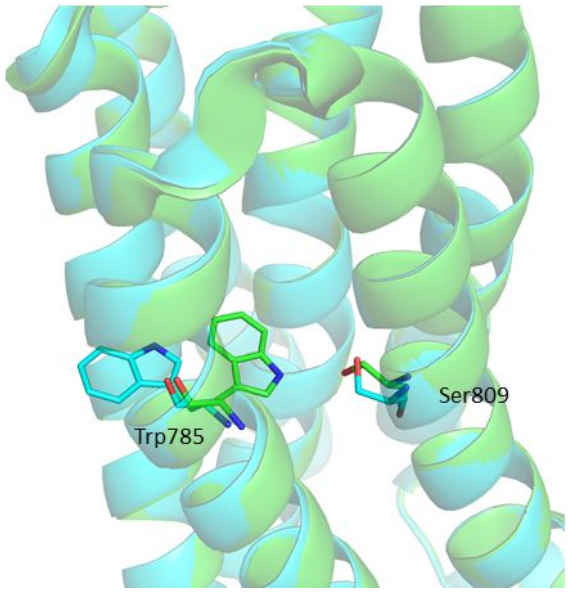

Figure 5.

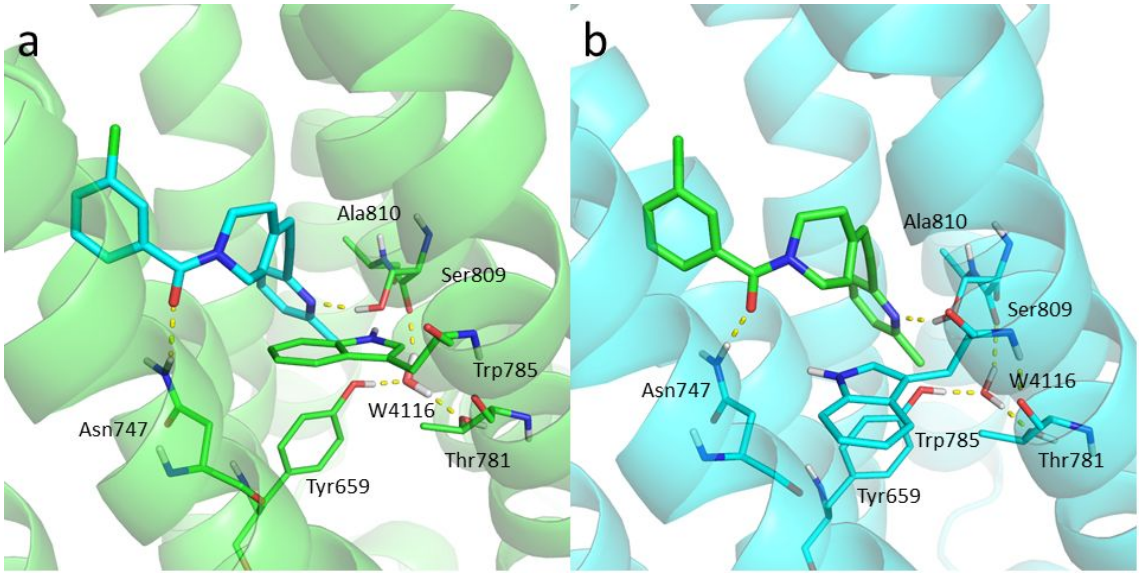

Figure 6.

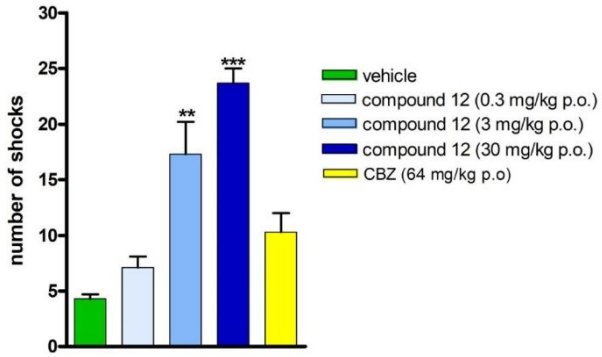

Figure 7.

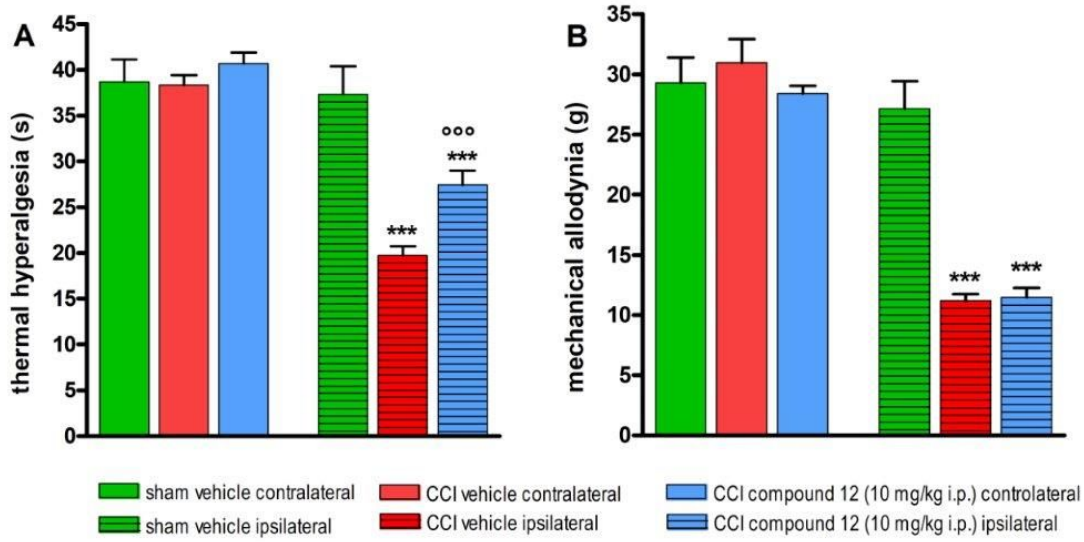

Figure 8.

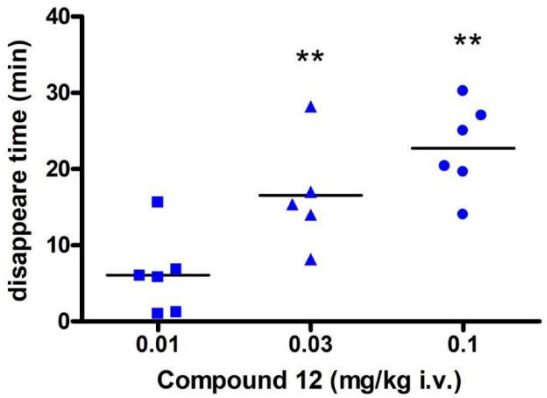
disappeare time (min)
40
30
20
10
0
**
**
0.01
0.03
0.1
Compound 12 (mg/kg i.v.)

Figure 9.

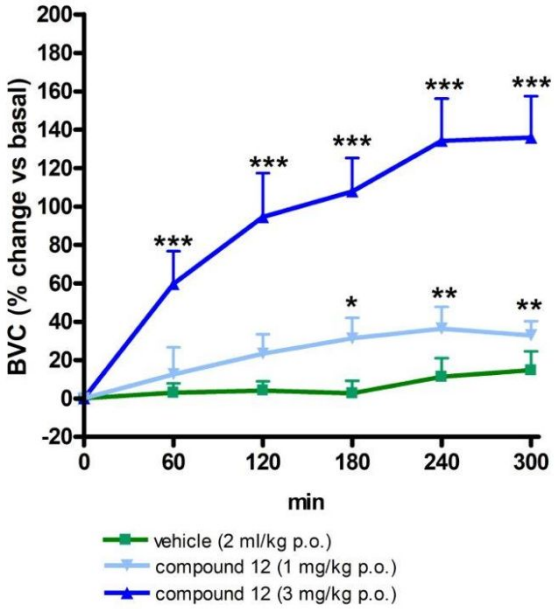
BVC (% change vs basal)
200
180
160
140
120
100
80
60
40
20
0
-20
0
60
120
180
240
300
min
***
***
***
***
***
*
**
**
vehicle (2 ml/kg p.o.)
compound 12 (1 mg/kg p.o.)
compound 12 (3 mg/kg p.o.)

Chart 1.

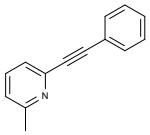

1 (MPEP)

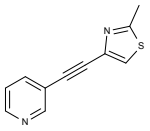

2 (MTEP)

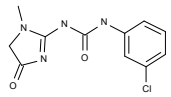

3 (Fenobam)

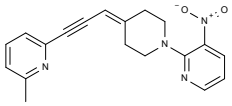

4

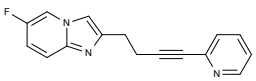

5 (ADX-48621)

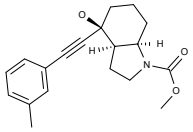

6 (AFQ-056)

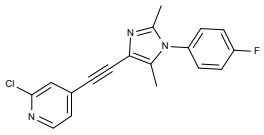

7 (RO-4917523)

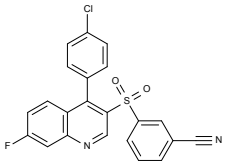

8 (RGH-618)

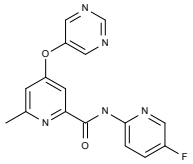

9 (VU0424238)

Chart 2.

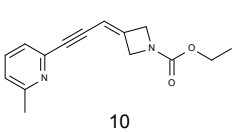

10

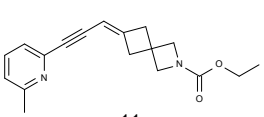

11

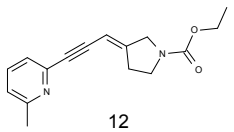

12

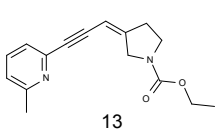

13

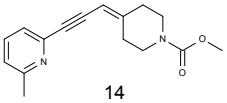

14

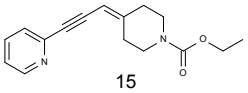

15

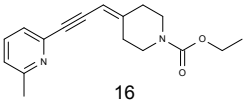

16

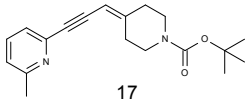

17

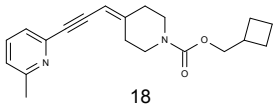

18

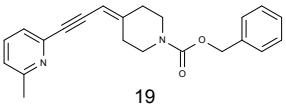

19

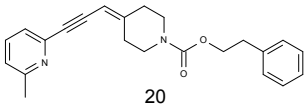

20

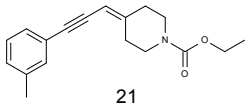

21

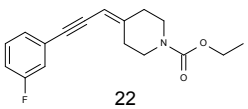

22

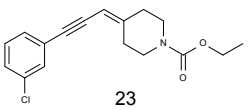

23

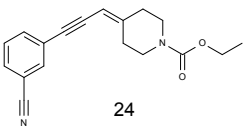

24

Chart 3.

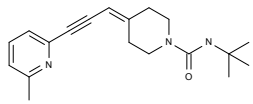
25

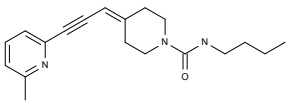
26

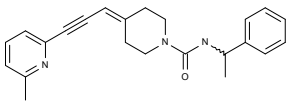
27

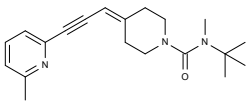
28

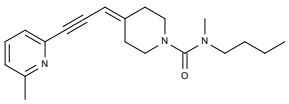
29

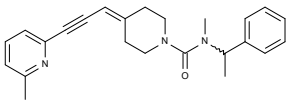
30

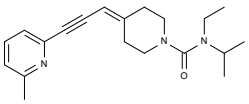
31

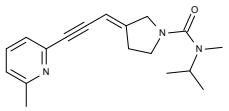
32

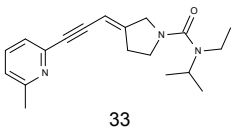
33

Chart 4.

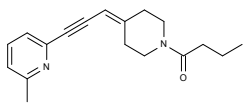
34

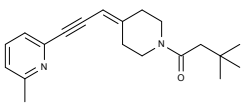
35

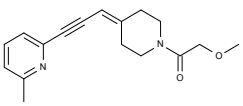
36

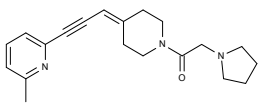
37

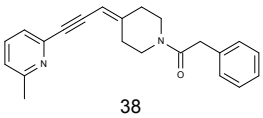
38

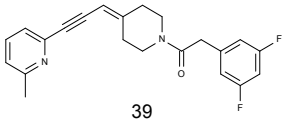
39

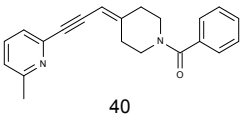
40

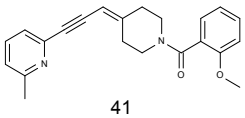
41

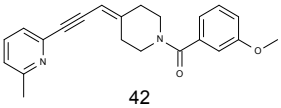
42

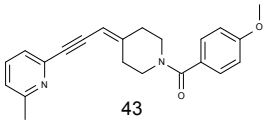
43

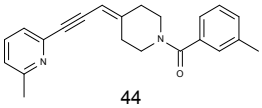
44

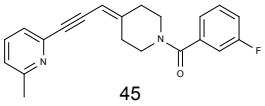
45

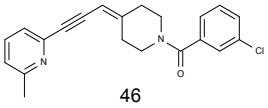
46

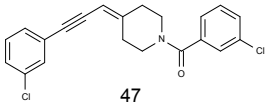
47

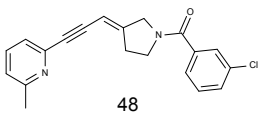
48

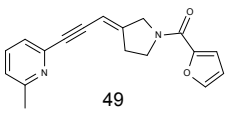
49

Chart 5.

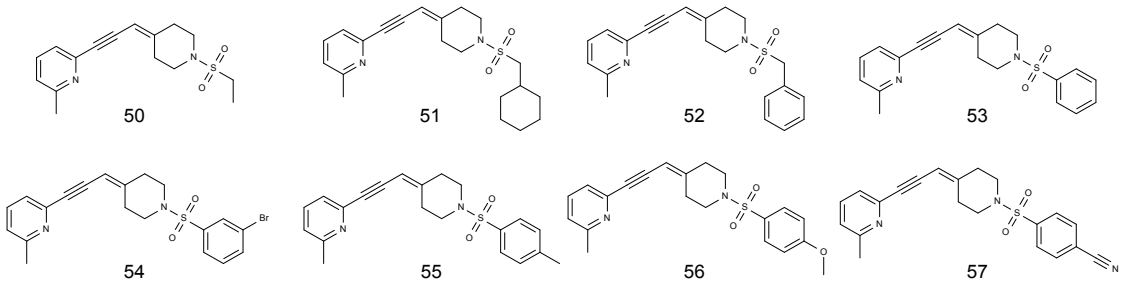

Chart 6.

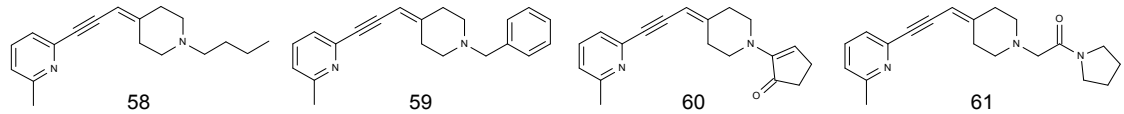

Scheme 1.

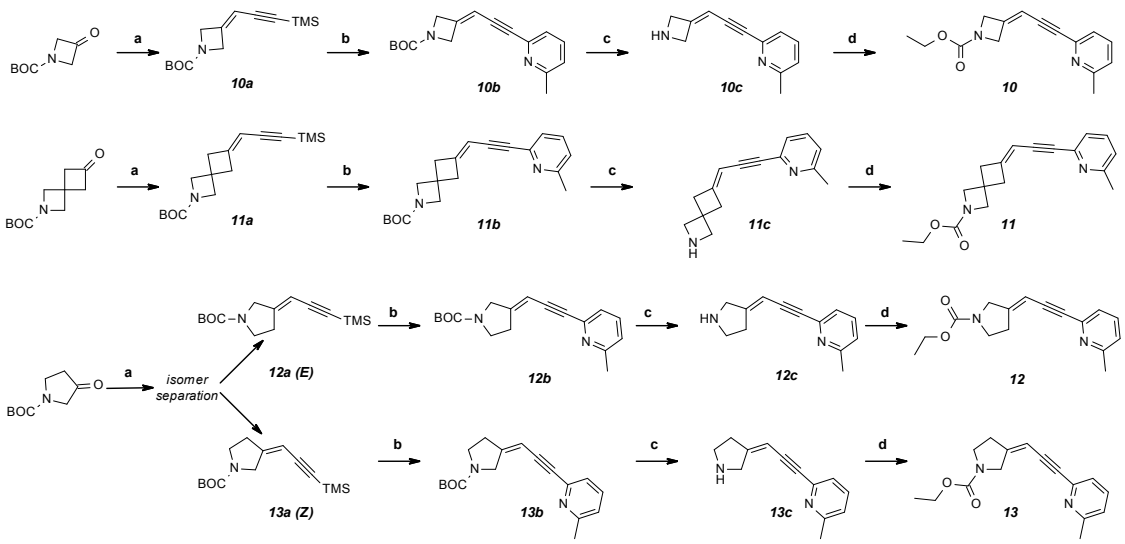

Scheme 2.

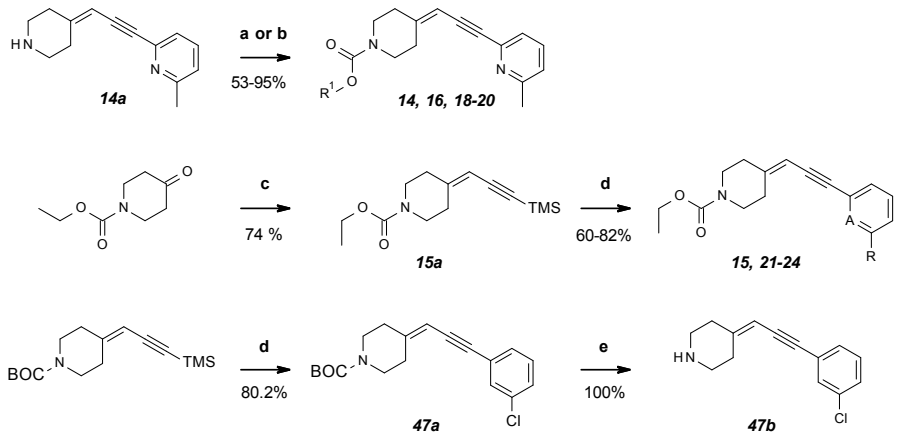

Scheme 3.

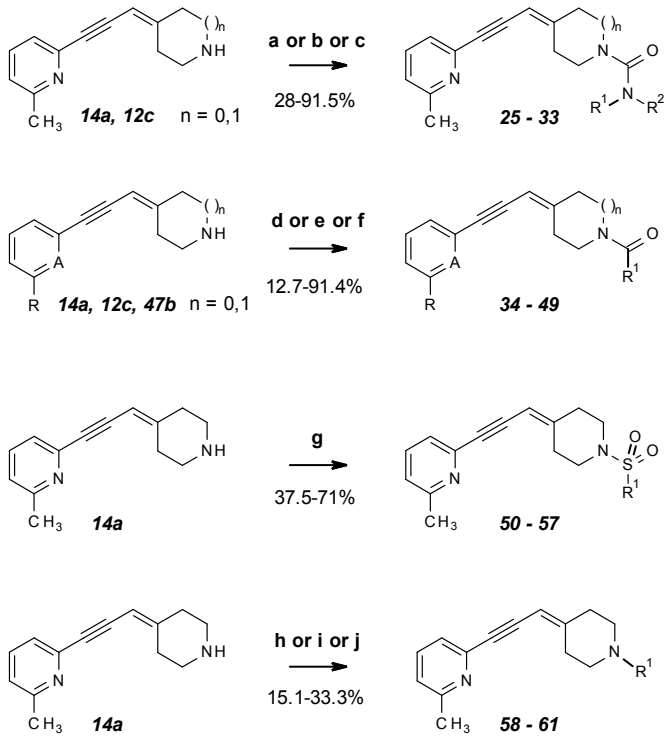
a or b or c
28-91.5%
14a, 12c n = 0,1
25 - 33
d or e or f
12.7-91.4%
14a, 12c, 47b n = 0,1
34 - 49
g
37.5-71%
14a
50 - 57
h or i or j
15.1-33.3%
14a
58 - 61

Table 1. Carbamates solubility, *in vitro* binding affinities (Ki, nM) for rat cloned $mGlu_1$ and human cloned $mGlu_5$, and *in vitro* Ca^{2+} functional mobilization assay activities (IC_{50}, nM) for rat cloned $mGlu_1$ and human cloned $mGlu_5$, cytochrome inhibition, rat and human percent remaining at 30 minutes and ligand efficiency

#	Sol.[a]	*h*-$mGlu_5$ Ki nM[b]	*h*-$mGlu_5$ Ca^{2+} IC50 nM[b]	*r*-$mGlu_1$ Ki nM[c]	$CYP1A_2$ IC50 μM	$CYP2D_6$ IC50 μM	$CYP3A_4$ IC50 μM	rat % rem[d]	hum % rem[d]	LE
1		10.4 ± 1.8	11.2 ± 1.3	>10000	e	>100	>100			0.73
2		32.7 ± 1.1	47.3 ± 3.6	>10000	e	60.7	>100			0.73
3		162.2 ± 3.3	36.3 ± 7.2							0.52
4	28	0.5 ± 0.06	0.8 ± 0.2	184.2 ± 35.6	<0.7	>20	4.5	3.4	63	0.51
10	939	38.3 ± 2.5	117 ± 24	>1000	1.85	>20	>20	6	93	0.50
11	872	3.6 ± 0.1	23.1 ± 1.0	>1000	10.4	>20	17.2	80	>95	0.53
12	768	3.5 ± 0.7	4.1 ± 1.1	>1000	4.5	>20	>20	35	>95	0.58
13	853	243 ± 14		>1000	<0.7	>20	9.7	17	1	0.45
14	799	4.0 ± 0.2	6.0 ± 3.0	>1000	4.0	>20	>20	23	73	0.58
15	54	2.6 ± 0.3	6.5 ± 2.6	>1000	<0.7	>20	>20	20	94	0.59
16	600	2.5 ± 0.7	3.3 ± 2.0	>1000	5.0	>20	>20	2	79	0.56

17		11.9 ± 1.5	34 ± 17	>1000		>2	>2	1	90	0.47
18	12	>1000								
19		4.8 ± 0.6	248 ± 96	>1000	4.4	>20	7.7	3	65	0.44
20	31	2.5 ± 0.3	52.5 ± 1.4	413 ± 48	4.7	>20	3.7	2	19	0.44
21	4	2 ± 0.1	5.1 ± 1.1	>1000	2	>20	5.4	64	71	0.57
22	829	4 ± 0.4	18.7 ± 2.9	>1000	<0.7	>20	4.2	29	>95	0.55
23	15	0.7 ± 0.1	2.5 ± 0.4	>1000	<0.7	>20	12.8	58	>95	0.59
24	544	0.98 ± 0.03	*	>1000	0.9	>20	>20	32	76	0.56

Binding and functional results were obtained by three independent experiments and each assay point was determined at least as duplicate. [a] Solubility is expressed as μM concentration at pH 7.4 in TRIS HCl buffer solution; [b] CHO human cloned $mGlu_5$ receptor; [c] CHO rat cloned $mGlu_1$ receptor; [d] per cent remaining after 30 minutes of tested compound in rat and human microsomes; [e] **1** and **2** were moderate competitive inhibitors of recombinant human CYP1A2 (Ki, 0.5-1 μM).[34] * compound was interfering with the assay and it was impossible to define the value.

Table 2. Ureas solubility, *in vitro* binding affinities (Ki, nM) for rat cloned $mGlu_1$ and human cloned $mGlu_5$, and *in vitro* Ca^{2+} functional mobilization assay activities (IC_{50},

nM) for rat cloned $mGlu_1$ and human cloned $mGlu_5$, cytochrome inhibition, rat and human percent remaining at 30 minutes and ligand efficiency.

#	Sol.[a]	*h*-$mGlu_5$ Ki nM[b]	*h*-$mGlu_5$ Ca^{2+} IC_{50} nM[b]	*r*-$mGlu_1$ Ki nM[c]	*CYP1A2* IC_{50} µM	*CYP2D6* IC_{50} µM	*CYP3A4* IC_{50} µM	*rat % rem*[d]	*hum % rem*[d]	*LE*
25		399 ± 15		>1000						0.38
26		92 ± 12		>1000						0.42
27		276 ± 48		>1000						0.33
28		258 ± 24		>1000						0.38
29		20.4 ± 1.3		>1000		>20	13.4			0.44
30		4.3 ± 0.3		>1000		>20	4.0	<1	<1	0.41
31		2.9 ± 0.4	133 ± 17	>1000	3.4	>20	15.4	<1	<1	0.49
32	962	8.6 ± 0.2	15.1 ± 3.9	>1000	>20	>20	>20	57	93	0.50
33	927	5.8 ± 1.4	29.1 ± 4.1	>1000	>20	>20	>20	20	11	0.49

Binding and functional results were obtained by three independent experiments and each assay point was determined at least as duplicate. [a] Solubility is expressed as µM concentration at pH 7.4 in TRIS HCl buffer solution; [b] CHO human cloned $mGlu_5$ receptor; [c] CHO rat cloned $mGlu_1$ receptor; [d] per cent remaining after 30 minutes of tested compound in rat and human microsomes.

Table 3. Amides solubility, *in vitro* binding affinities (Ki, nM) for rat cloned $mGlu_1$ and human cloned $mGlu_5$, and *in vitro* Ca^{2+} functional mobilization assay activities (IC_{50}, nM) for rat cloned $mGlu_1$ and human cloned $mGlu_5$, cytochrome inhibition, rat and human percent remaining at 30 minutes and ligand efficiency.

#	Sol.[a]	*h*-$mGlu_5$ Ki nM[b]	*h*-$mGlu_5$ Ca^{2+} IC_{50} nM[b]	*r*-$mGlu_1$ Ki nM[c]	*CYP1A2* IC_{50} µM	*CYP2D6* IC_{50} µM	*CYP3A4* IC_{50} µM	*rat % rem*[d]	*hum % rem*[d]	*LE*
34		24 ± 1.2		>1000	6.1	>20	>20	1	>90	0.5
35	243	48.2 ± 6.3		>1000						0.44
36		178 ± 5.7		>1000						0.44
37		>1000								
38		83 ± 3.6		>1000						0.39
39		194 ± 2.3		>1000						0.34
40		18.4 ± 1.4	67.3 ± 21.2	>1000	>20	>20	>20	<1	62	0.44
41	468	40 ± 1.9		>1000		>20	13.8	<1	3.3	0.39
42	386	18.5 ± 0.1	88.4 ± 18.8	>1000	>20	>20	4.6	<1	3.9	0.41
43		122 ± 23.6		>1000						0.36
44		11.3 ± 1.9	1383 ± 58	>1000	>20	>20	6.1			0.44
45		15.8 ± 0.9	50.1 ± 10.2	>1000	>20	>20	>20	0.2	42	0.43

46	58	0.7 ± 0.4	49.2 ± 12.4	>1000	>20	>20	>20	0.2	18.6	0.50
47	1.0	2.9 ± 0.2	287 ± 10	>1000	1.4	12.7	2.3	64	>95	0.47
48	157	3.9 ± 0.4	27 ± 7.1		5.9	>20	12.9	55	84	0.48
49	420	7.9 ± 0.5	6.4 ± 3.8		9.6	>20	>20	77	94	0.5

Binding and functional results were obtained by three independent experiments and each assay point was determined at least as duplicate. [a] Solubility is expressed as μM concentration at pH 7.4 in TRIS HCl buffer solution; [b] CHO human cloned $mGlu_5$ receptor; [c] CHO rat cloned $mGlu_1$ receptor; [d] per cent remaining after 30 minutes of tested compound in rat and human microsomes.

Table 4. Sulfonamides solubility, *in vitro* binding affinities (Ki, nM) for rat cloned $mGlu_1$ and human cloned $mGlu_5$, and *in vitro* Ca^{2+} functional mobilization assay activities (IC_{50}, nM) for rat cloned $mGlu_1$ and human cloned $mGlu_5$, cytochrome inhibition, rat and human percent remaining at 30 minutes and ligand efficiency.

#	Sol.[a]	*h*-$mGlu_5$ Ki nM[b]	*h*-$mGlu_5$ Ca^{2+} IC_{50} nM[b]	*r*-$mGlu_1$ Ki nM[c]	*CYP1A2* IC_{50} µM	*CYP2D6* IC_{50} µM	*CYP3A4* IC_{50} µM	*rat % rem*[d]	*hum % rem*[d]	*LE*
50		67.3 ± 5.1		>1000		>20	17.2	21	86	0.47
51	49	456 ± 65		>1000						0.33
52	0.5	415 ± 61		>1000						0.34
53		64.2 ± 13		>1000						0.39
54	1	18.2 ± 2.2	89.9 ± 8.3	>1000		>20	3.3			0.41
55		2.7 ± 0.1	43.8 ± 3.5	>1000	>20	>20	1.9	<1	39.3	0.45
56		2.9 ± 0.4	95.2 ± 4.1	>1000	>20	>20	1.9	<1	37.8	0.43
57	1	3.3 ± 0.3	163 ± 3	>1000	>20	>20	5.0	1.1	13.7	0.43

Binding and functional results were obtained by three independent experiments and each assay point was determined at least as duplicate. [a] Solubility is expressed as µM concentration at pH 7.4 in TRIS HCl buffer solution; [b] CHO human cloned $mGlu_5$ receptor; [c] CHO rat cloned $mGlu_1$ receptor; [d] per cent remaining after 30 minutes of tested compound in rat and human microsomes.

Table 5. *In vitro* human microsome and CYP3A4 %remaining after 30 minutes of incubation for compounds **16**, **31**, **32**, **41** and **47**.

#	hum % rem	
	microsomes	*CYP3A4*
16	79	72
31	<1	1
32	93	69
41	3	13
47	>95	55

Table 6. *In vitro* characterization of compound **12**.

P450 inhibition assay		
P450	*Control*[a]	*IC_{50} (μM)*
CYP3A4	Ketoconazole	>20
CYP2D6	Quinidine	>20
CYP2C9	Sulfaphenazole	>20
CYP2C19	Tranylcypromine	>20
CYP2C8	Quercetin	>20
CYP2B6	Tranylcypromine	>20
CYP1A2	Furafylline	4.52
Stability in human microsomes		
Intrinsic clearance (CL_{INT})	0.39 (mL/min/Kg)	
Half-life ($t_{1/2}$)	770 (min)	

Predicted hepatic clearance (CL_{HEP})	0.45 (μL/min/mg protein)
In vitro GSH conjugates	
GSH adduct formation	negative
Cardiac safety panel	
hERG (IC_{50})	>30 μM
Nav 1.5 (IC_{50})	12.29 μM
Cav 1.2 (IC_{50})	16.23 μM
MiniAmes test	
TA98	TA100
negative	negative
Cytotoxicity test	
Cell viability (inhibition at 10μM)	5%
Transporter inhibition	
P-gP inhibition in Caco Cells at 10μM conc.	25%

[a] Selective positive inhibitor control for each specific isoform.

Table 7. Preliminary rat and dog pharmacokinetic plasma characterization of compound **12** following iv and oral administration.

Specie	*Route*	*Dose*	T_{MAX}	C_{MAX}	*AUC*	*T1/2*	*Vss*	*Cl*	*F*
		(mg/kg)	*(h)*	*(ng/mL)*	*H*ng/mL*	*(h)*	*L/Kg*	*mL/min/Kg*	*(%)*
rat	iv	1	0.08	1617	1386	0.47	0.45	12	
	po	3	1	552	2123	2.22			51
dog	iv	1	0.08	423	228	0.91	3.1	88	
	po	3	0.25	584	1094	2.02			>100

Table of Contents Graphics

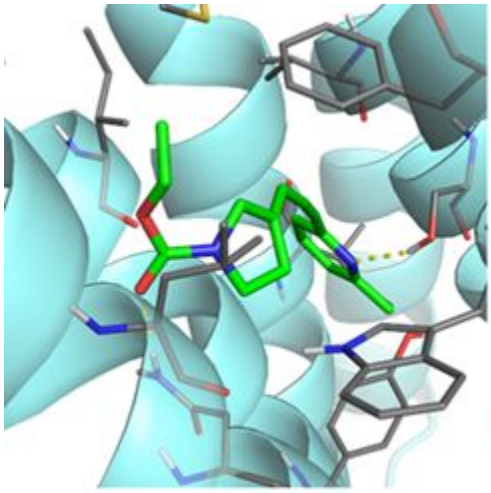

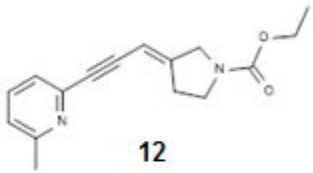

12

Compound 12

IC_{50} mGlu5 = 4.1 nM

IC_{50} CYP (3A4, 2D6, 2B6, 2C8, 2C9, 2C19 and 2E1) > 20 μM